ISBN 978-82-471-1708-8 (printed ver.)
ISBN 978-82-471-1709-5 (electronic ver.)
ISSN 1503-8181

Doctoral theses at NTNU, 2009:158

Efren Ayala-Uraga

Reliability-based Assessment of Deteriorating Ship-shaped Offshore Structures

Efren Ayala-Uraga

Doctoral Thesis

NTNU
Norwegian University of
Science and Technology

NTNU
Norwegian University of
Science and Technology
Thesis for the degree of
doktor ingeniør
Faculty of Engineering Science and Technology
Department of Marine Technology

Doctoral theses at NTNU, 2009:158

NTNU

NTNU
Norwegian University of
Science and Technology

Efren Ayala-Uraga

Reliability-based Assessment of Deteriorating Ship-shaped Offshore Structures

Thesis for the degree of doktor ingeniør

Trondheim, November 2009

Norwegian University of
Science and Technology
Faculty of Engineering Science and Technology
Department of Marine Technology

NTNU
Norwegian University of
Science and Technology

NTNU
Norwegian University of Science and Technology

Thesis for the degree of doktor ingeniør

Faculty of Engineering Science and Technology
Department of Marine Technology

ISBN 978-82-471-1708-8 (printed ver.)
ISBN 978-82-471-1709-5 (electronic ver.)
ISSN 1503-8181

Doctoral Theses at NTNU, 2009:158

Printed by Tapir Uttrykk

Reliability-based Assessment of Deteriorating Ship-shaped Offshore Structures

A thesis submitted in partial fulfilment of the
requirements for the degree of

Doktor Ingeniør

by

Efrén Ayala Uraga

Department of Marine Technology
Faculty of Engineering Science and Technology
Norwegian University of Science and Technology

Trondheim, June 2009

Abstract

Floating production, storage and offloading ships, referred to as FPSOs, are hybrid structures in the sense that these vessels are ships being operated as offshore facilities. Production ships or FPSOs constitute an efficient solution for remote oil field locations due to their storage capacity of crude oil. Production ships are either tanker conversions or purpose-built vessels. Most of the applications of production ships are converted ocean-going oil tankers, of different ages, to operate in relatively benign environmental areas.

Keeping in mind that merchant ships are usually dry-docked every fifth year for inspection, maintenance and repair (IMR) tasks, they are designed according to a more relaxed safety criteria compared to those normally applied for permanent offshore structures, in which the required IMR activities need to be carried out in-situ as they cannot be easily dry-docked. Moreover, ocean on-going ships may in principle avoid heavy weather conditions, whereas FPSOs are moored to a fixed location and could be exposed to harsher extreme conditions. Additionally, FPSOs are exposed to continuously varying still-water load effects, due to the permanent loading-offloading operations. These fundamental differences are even more important to recognize as most of the existing FPSOs around the globe are built based on converted hulls of oil tankers that have already operated during some years. This issue is particularly relevant for vessels whose service life need to be extended, as the deteriorating agents such as fatigue cracking and corrosion become more important.

During the initial design of ship structures, the effects of fatigue and corrosion are accounted for separately. However, as the structure ages, the interaction between these two degrading agents increases, and thus such an interaction needs to be accounted for. Moreover, as the number of cracks in a hull structure increases with time, the likelihood of fracture occurrence in main structural components rises accordingly. Therefore, it is indispensable for FPSO operators to assess the safety of existing vessels with proper consideration of the uncertainties involved.

The aim of this dissertation is to discuss the safety assessment of an existing ship-shaped offshore structure subjected to deterioration, where the interaction among different deteriorating phenomena such as fatigue, corrosion and fracture, are explicitly accounted for in a systematic and consistent manner. The format of this thesis report consists of an extended summary intended to emphasize the main contributions achieved and the relevant issues dealt with during this research work,

which resulted in the production of three articles that have already been published, annexed at the end of the report.

The first article, referred to as *Article 1* throughout this report, was published in the International Journal of Fatigue (2007). This article deals with the treatment of uncertainties related to the fatigue crack growth of surface cracks on plated connections and compares different reliability-based limit state formulations including a bi-linear crack growth law that is recommended by the British Standard BS-7910 (1999). Calibration of the bi-linear fracture mechanics formulation is performed with respect to design SN curves considering the parameters with largest uncertainties.

The second article, *Article 2*, published in Reliability Engineering and System Safety (2008) describes a procedure based on reliability techniques to assess the safety level on a welded connection of an aging FPSO with respect fatigue failure, taking into account in the crack growth estimation the effect of the vessel being exposed to various climate conditions throughout the service life. This means that the fatigue damage accumulated under previous operational conditions of the vessel, e.g. as tanker before conversion, is explicitly accounted for in the failure function. Thus, the uncertainties are also explicitly considered for each environmental condition the vessel has been or is being exposed to. In this study, the combined effect of corrosion and fatigue is used to evaluate the failure probability i.e. explicit interaction between fatigue and corrosion is accounted for. Moreover, reliability updating with inspection results is carried out by defining relevant inspection events, emphasizing the implications of inspection quality. The procedure can be used to assess service life extension.

Finally, *Article 3* of this dissertation, which was published in the Journal of Offshore Mechanics and Arctic Engineering (2007), deals with the assessment of fracture likelihood of a cracked stiffened panel on an FPSO hull girder when exposed to extreme environmental conditions. The proposed methodology includes a procedure to quantify the random propagation of a long crack in a stiffened panel, i.e. through-thickness cracks. Further, the procedure takes into account the mean stress effects induced by the continuously varying still-water loading, which relates to the loading-offloading operation of the offshore vessel. Moreover, an efficient time-variant reliability based procedure is established to estimate the probability of fragile fracture failure of a stiffened panel with an abnormal transverse crack, detected by leak at the bottom plating/deck structure of an FPSO. The master curve approach is utilized to determine the decreasing fracture resistance threshold, induced by the long crack random propagation in the panel, in order to perform the up-crossing rate estimation of the loading process. The failure probability is determined by means of Monte Carlo simulation based on a time-invariant procedure proposed by Marley and Moan (1994).

Acknowledgements

There are several people I have to thank. Firstly, I would like to acknowledge the support, advice and encouragement received over all these years from Professor Torgeir Moan. His always open and positive attitude is very much appreciated. Even when I went back to Mexico without having concluded the thesis, I always received Torgeir's support and encouragement.

During the years of my stay in Trondheim I had the opportunity of meeting friendly and talented people, from each of whom I have learnt something valuable. Thanks go to fruitful discussions with Dr. Sverre Haver from Statoil and professor at NTNU, Dr. Zhen Gao, from CeSOS, and Dr. Hadi Amlashi from Dept. of Marine Technology.

All the competent professors (Amdahl, Berge, Faltinsen, Larsen, Leira, Moan, Vinnem), administrative staff and colleagues at the Department of Marine Technology who have made a nice work environment during these years in Trondheim: Drs. Marilena Greco, Rune Yttervik, Paul Thomassen, Gaute Storhaug, Bin Zhang, Sebastian Fouques, Mateusz Graczyk, Kamran Koushan, Kjetil Skaugset, Martin Murillo, Fabio Celani, Svein Ersdal, Wenbo Huang, Csaba Pakozdi, Cesare Rizzo. All these people from different countries and backgrounds have made the most enriching experience to me. To all the staff members at the Department of Marine Technology (Institutt for Marin Teknikk, in Norwegian) who have been quite supportive from the very beginning, special thanks go to Sigrid B. Wold, Marianne Kjølaas, Bjørn Tore, Mustafa Jalali.

To all those "Norwegian-Latin" people who after some time became like our "relatives" in Norway: Bety and Vidar, Vanessa and Arve, Branda and Agustin, Conny and Boris. Those discussions about Mexico and Norway I had with Dr. Mario Polanco are very much appreciated.

Finally, the biggest of my appreciations goes to my family: my wife Alfa, who besides all the support and encouragement she has provided me, she has been taking care of our children and my refuge in difficult days. To my children Nallely, Hannah and Erick who have always been there to remind me what the most important things in life are. To my mother Sara whose words have been a balsam when things seem difficult, to my brother Gerardo and sisters Claudia and Ana, and to all other relatives in Mexico who have been very important to us.

The opportunity to pursue post-graduate studies and the financial support received at the beginning of my doctoral studies from Instituto Mexicano del Petróleo is acknowledged. There are several people I received support from and who trusted me when I decided to come to Norway to study. I specially thank Dr. Efraín Rodriguez and Mr. Roberto Ortega for their support. Further financial support received during the last years of my stay in Norway from NTNU's Department of Marine Technology, partly through projects sponsored by the American Bureau of Shipping, is also deeply appreciated. It is also acknowledged the support I received from the NTNU to attend some of the international conferences in which part of the research work carried out during these years was presented.

Contents

CHAPTER 1

Introduction

1.1. Background

A common practice in the offshore industry is to operate floating production structures (FPS) during a certain period of time in a given location to later be deployed to a different location, most likely in different climate conditions. The most common FPS's for deep-water applications are semi-submersibles and ship-shaped vessels. Semi-submersibles have been preferred as production facilities due to their good motion characteristics and large layout capacity. On the other hand, production ships constitute an efficient solution for remote oil field locations due to their storage capacity of crude oil. Production ships are either tanker conversions or purpose-built vessels. The former are often used in many deepwater developments due to their relatively short time execution compared to new-built ones. Most of the applications of production ships are converted ocean-going oil tankers, of different ages, to operate in relatively benign environmental areas such as Southeast Asia, West Africa and Offshore Brazil near the Equator. In the coming years, the use of double hull production ships in the Gulf of Mexico will be as well a reality.

Floating production, storage and offloading ships, referred to as FPSOs, are hybrid structures as these vessels are ships being operated as offshore facilities. This feature is particularly challenging for converted FPSOs considering that the safety management and inspection, maintenance and repair (IMR) activities are different in the shipping and offshore industries. Keeping in mind that merchant ships are usually dry-docked every fifth year for IMR tasks, it leads to a more relaxed design and safety criteria compared to those normally applied for offshore structures, in which the required IMR activities need to be carried out in-situ as they cannot be easily dry-docked. Moreover, on-going ships may in principle avoid heavy weather conditions, whereas FPSOs are moored to a fixed location and could be exposed to harsher extreme conditions. Additionally, FPSOs are exposed to continuously varying still-water load effects, due to the permanent loading-offloading operations. These fundamental differences take even more relevance as most of the existing FPSOs around the

globe are built based on converted hulls of oil tankers that have already operated during some years.

Hence, one of the main concerns of operators of FPSOs around the globe is to keep an adequate balance between maintenance costs and safety levels throughout the service life of the vessel. This issue is particularly more relevant for vessels whose service life need to be extended, as the deteriorating agents such as fatigue cracking and corrosion become more important.

Cracks in ship hull structures have always been an important concern for regulators and operators, as shown by the service experiences reported by Sucharski (1997). Until recently, fatigue of trading vessels was implicitly covered by allowable stress (section modulus) requirements to wave loading. Its treatment as design criterion in offshore structures obeys to the fact that fatigue damage is very dependent on local wave conditions.

Fatigue cracking problems occurred in semi-submersibles in the late 60s led to explicit fatigue design requirements implemented in codes of FPSs and other offshore structures. For the early rigs fatigue design checks were not even done, implying as low mean fatigue lives as 4 years. Some rigs were structurally modified to accommodate more buoyancy components and to improve fatigue life (Moan, 2005). Contrary to ships, the most fatigue-prone and critical areas of a semi-submersible are much more focused and specific. Nevertheless, there are several similar structural details in ships and semi-submersibles.

The overall safety of the FPSO hull structure with respect to fatigue failure is to be guaranteed throughout the service life by maintaining acceptable safety levels of the structural components with adequate application of in-service inspection, maintenance and repair measures. The information relating to inspection, maintenance and repair (IMR) history is therefore crucial in this context.

During the initial design of ship structures, the effects of fatigue and corrosion are accounted for separately. However, as the structure ages, the interaction between these two degrading agents increases, and thus such an interaction needs to be accounted for. Moreover, as the number of cracks in a hull structure increases with time, the likelihood of fracture occurrence in main structural components rises accordingly. Therefore, it is indispensable for FPSO operators to assess the safety of the vessels with proper consideration of the uncertainties involved.

1.2. Motivation for the present work

Great part of the offshore infrastructure around the world has already completed the initially intended service life and the economical restrictions in the industry have led owners to operate them beyond this term. Terms such as service life extension and requalification are often used to describe the process to assess the safety levels on existing facilities. Updated operating conditions and eventual damage accumulated on the structure is taken into account in addition to the experience gained during its operation in terms of resistance behaviour and load effects eventually recorded. In this connection, the effects of degradation produced by fatigue and corrosion being accumulated on the structure are of primary importance, though their uncertain effects are often difficult to be quantified. The use of reliability-based methods has consolidated in the offshore industry as the proper approach to deal with assessment of existing infrastructure, taking due account of the uncertainties involved in resistance and

load/load effects, as well as the actual operational conditions of the structure, in a systematic manner.

Fatigue and corrosion effects on the structural strength are dealt with by design, as well as inspection, maintenance and repair during operation. Such degradation becomes particularly more important in connection with service life extension. Due to the significant uncertainties inherent in the degradation process and the uncertainties in the inspection and repair, a reliability model is preferable to obtain a measure of safety.

During design, the effects of deteriorating phenomena, i.e. fatigue and corrosion, are considered independently one another in the estimation of their effects on the structures. An important interacting effect between fatigue and corrosion occurs. This interaction is explained as an increase of the fatigue damage introduced by the effect of corrosion in two manners, namely: 1) an increase of the stress ranges induced by the material loss and 2) the crack growth rate is accelerated by the corrosion-fatigue phenomenon. Both effects are of random nature and change with time, thus, they are difficult to be characterized. Further, the uncertainty level of the crack propagation process is necessarily increased by the interaction with the effect of corrosion. The best design practice considers an increase in the stress levels due to material loss by assuming a deterministic reduction of the scantlings based on a corrosion rate. Fatigue cracks are still found in hull structures of FPSOs designed with the best practices, just after few years in operation (OLF, 2002). Hence, the interaction between both deteriorating agents becomes more important and more uncertain as the structure ages. Additionally, corrosion increases as well the likelihood of other failure modes such as buckling and fracture.

Figure 1.1 exemplifies the non-desirable combined effects of degradation produced by the development of fatigue cracks and corrosion which led to fracture of a tanker's deck under normal operational conditions (ABS, 2001). This fact may be of relevance for offshore ships as two thirds of the fleet of FPSOs in operation around the world are converted tankers, and more than half are single-hulled vessels (Offshore, 2005).

Another aspect worth of being highlighted is the difference in attitude towards the treatment of cracks in the shipping and offshore industries. In merchant ships, it is quite common that cracks are detected with visual inspection when they are long enough to be found, i.e. when they have already grown through the plate thickness. In offshore structures the use of non-destructive techniques (NDT) is a common practice and, in general, the structural safety management is less tolerant to the presence of cracks. The difficult and costly in-site repairs of permanently moored FPSOs are therefore non-desirable tasks and need to be avoided.

The use of reliability-based methods results attractive for assessing the safety management of deteriorating structures. The effect of inspection may be introduced and hence the reliability level of the components can then be updated using Bayesian methods based on additional information (e.g. Madsen et al, 1986).

Figure 1.1. Very long crack at deck of tanker Castor, (from ABS, 2001)

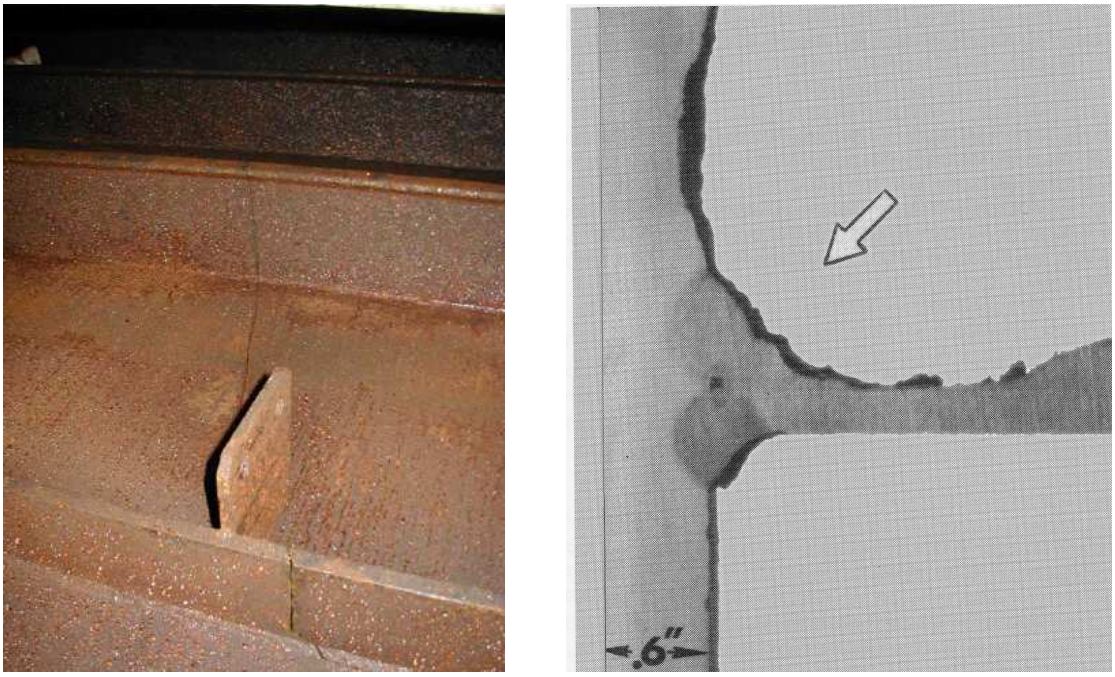

a) b)

Figure 1.2. Typical deterioration findings in structural details of tankers: a) crack of more than 1.8 m long in a tanker, (from Bjørheim et al, 2004), b) necking effect in welds (from TSCF, 1997)

1.3. Discussion of previous work

Safety assessment of deteriorating ships and offshore structures has been studied by different researchers, applying reliability-based techniques, with the aim of developing efficient tools for decision-making purposes. Efforts have been devoted to study fatigue failure on structural elements as an isolated phenomenon, e.g. the interaction with other deteriorating agents such as corrosion is normally disregarded. However, such an interaction becomes more important as the structure ages, as it is the case of marine structures. Recently, it is more commonly observed in structural reliability assessment models of aging structures to incorporate, in the study of certain failure modes such as buckling and fracture, the simultaneous effect of fatigue and corrosion.

1.3.1. Fatigue-corrosion interaction

Overall safety assessment of degraded ships was studied by Akpan et al (2002) who propose a reliability-based assessment procedure of hull structures accounting for the simultaneous aging effect of both fatigue and corrosion on the ultimate longitudinal hull girder strength. Akpan and collaborators' model does consider the interaction that may exist between fatigue and corrosion in terms of a corrosion-enhanced crack growth rate factor. Additionally, the reduction of the transverse section modulus due to the presence of both through-thickness cracks and corrosion-induced thickness loss in structural components is considered. In this research work, time-variant reliability of the primary hull is estimated with the use of the hazard rate concept in reliability theory, which takes into account the previous survival of the structure in determining its safety as function of time.

Zhang & Mahadevan (2001) have investigated the raising effect of pitting corrosion on fatigue crack growth of aircraft fuselages. They propose a model that explicitly accounts for both the surface and through-thickness crack growth lives in the estimate of failure probabilities. The initiation of the surface crack is supposed to be accelerated by the pitting corrosion damage on the surface of the plate.

Guedes Soares & Garbatov (1998a) proposed a reliability-based approach used to ensure the maintainability of ship hull structures subjected to the effects of fatigue cracking and corrosion-induced material loss. Their procedure enables to assess the safety of the longitudinal hull girder strength of deteriorating vessels by means of a time-dependent reliability model, in which the effects of repair may be accounted for in terms of reliability updating. In this research, fatigue and corrosion are considered independent to each other, i.e. the crack growth rate is not increased by the effect of corrosion. Further, Guedes Soares & Garbatov (1998b, 1999) consider other aspects that also affect the time-variant failure probability estimation of the hull structure, such as the effect of different loading combinations as well as the inclusion of an improved corrosion prediction model that accounts for the randomness in the time for the corrosion protection system to fail.

Paik et al (2003b) presented an approach to evaluate the safety of an aging ship structure as function of time, taking into account different deteriorating items that are present in vessels, namely general and pitting corrosion, fatigue cracking and denting. The time-dependent failure probabilities are determined assuming that the different deteriorating agents act independently on the structure.

Efforts have been devoted to reduce the negative effects and undesirable costs of corrosion on ships, (e.g. SSC, 1995b, 1997; TSCF, 1997; Sucharski, 1997) . Despite corrosion is not considered a failure mode, it needs especial attention on assessing the safety of aging

structures in order to properly account for its effects. Thus, data on corrosion rates are important income for the reliability engineer to perform such a task. Melchers (2002a, 2002b) performed a comprehensive study to propose a probabilistic model of corrosion wastage rates for reliability applications. Paik et al (2003a) developed a non-linear model to describe corrosion wastage on FPO and FPSO vessels. Recently, Garbatov et al (2007) developed a nonlinear model to describe corrosion rates on plating of cargo and ballast tanks of tankers. Wang et al (2003) studied the wastage rates from a large database collected from historical information on ship surveys.

1.3.2. Fatigue crack growth analysis

Steel plated connections in ship structures are mainly dealt with in this study as they are present in all the joints of hulls. Many of these joints are formed by long welds that, in terms of fatigue damage, are sources of defects found along the weld toes which are potential cracks initiation points.

Design of welded connections against fatigue failure in ship structures is normally required to fulfil a fatigue life of 20 years, as merchant vessels are dry-docked every fifth year for inspection and repair, as required, (e.g. DNV, 1995; Mansour et al, 1997; DNV, 2001; Moan, 2005). Converted hull structures to be used as FPSOs represent a challenge for owners and designers to achieve a balance between safety and maintenance and repair costs in the extended service life. Thus, reliability-based methods are necessary in order to extend the fatigue service life of welded joints of FPSOs, and still keep adequate safety levels in the extended period, (e.g. Moan, 2005). Cracking problems are still a concern for designers as reported in the experiences collected from FPSO operators in the Northern North Sea, (OLF, 2002). Even with the best design practices being applied, cracking cases are still being recorded.

Reliability-based models have been proposed to assess the safety of welded structures by means of fracture mechanics formulations, where explicit consideration of the different uncertainties involved is introduced. Such formulations also allow for additional information, e.g. inspection results, to be considered. Various researchers have contributed with improvements to the fracture mechanics formulations utilized in the reliability-based models, (SSC, 1995a, 1995c; Bouchard et al, 1991; Ma et al, 1995; Bowness & Lee, 1999; Fujimoto et al, 1997; Lotsberg & Sigurdsson, 2005). Significant efforts have been done to improve inspection techniques and their reliability levels (e.g. Visser, 2000; Moan et al, 2000).

Stiffened panels are the main longitudinal resisting components in hull ship structures. These components are normally exposed to: a) longitudinal tension and compression as consequence of the wave-induced hull girder bending, b) transverse loading due to in-plane pressure or local lateral pressure. These all dynamic loading effects induce cyclic stresses that make several structural details prone for fatigue cracking. Cracking in main structural components are of concern as their failure may lead to loss of life or damage to environment, but cracking initiated in secondary components may also lead to crack propagation on major components. Long welds as those joining together a stiffened panel with a transverse frame or bulkhead are usually subjected to highly correlated loading between panels on the same location along the ship. Moreover, along the weld in the span between two contiguous longitudinals there may be crack initiation in different points along such a connection, which when merging, may lead to a long crack propagation. Presence of long crack in a hull ship may be the cause of a major fracture of a main component during extreme loading conditions.

Long crack propagation in complex structures has been investigated by Nussbaumer et al (1999), performing experiments in a welded box beam subjected to cyclic bending. One of the main remarks from the study was that long crack propagation is heavily dependent upon the residual stress on which it grows. Hence, proper modelling of the residual stress field as well as its effect on the stress intensity factor calculation is necessary.

Dexter and collaborators (Dexter & Pilarski, 2000; Dexter et al, 2003; Dexter & Mahmoud, 2004) have studied the propagation of long cracks on stiffened panels. Based on systematic testing of stiffened panels, they developed an analytical model with the use of linear-elastic fracture mechanics. In the stress intensity factor computation different effects are considered by superposition, such as the compressive residual stress fields in the vicinity of the stiffeners. One of the main conclusions drawn from their experiments is that the stiffeners substantially reduce the crack propagation rate compared to a plate without stiffeners. This reduction is due to: 1) the compressive residual stresses, and 2) the restrain of the stiffeners.

Recently, Bjørheim (2006) performed a comprehensive testing program in full scale specimens for investigating the fatigue propagation of long cracks in ship hull structures. The main finding of this study is that stable propagation of long cracks is expected, i.e. no unstable fracture has been experienced in his test program.

On the other hand, the British Standard Institute recommends in its BS 7910 (1999) the use of a bi-linear crack growth propagation law for assessing fatigue lives by means of a fracture mechanics approach. This recommendation is based on the study reported by King (1998) who analized a collection of crack growth rate data from a number of investigations of different researchers. The bi-linear crack growth approach has been studied by few researchers under a reliability framework point of view. Righiniotis & Chryssanthopoulos (2004) implemented a probabilistic fracture mechanics approach applying the bi-linear crack growth law to predict fatigue life of bridge structures under random loading. Additionally, the model includes a fracture criterion based on the failure assessment diagram as recommended in the BS 7910 (1999).

1.3.3. Fatigue-induced fracture

Likelihood of fatigue-induced fracture on marine infrastructure gains more relevance in aging structures, as the frequency of crack occurrence increases significantly with time. Catastrophic failure cases have been registered in the history on both the maritime and offshore industries where loss of entire vessels (under certain operational conditions) have been initiated from relatively small cracks, often undetected, that have led to sudden fracture of main structural components when subjected to extreme loading conditions. Beck & Melchers (2004a) propose an approach to calculate overload failure probability of a structural component subjected to random loading and a stochastic crack growth propagation model. Their approach requires the determination of the transition distributions of crack size and fracture resistance in order to characterize the structure's resistance degradation as a random process of time. Then, the failure probability is based on the evaluation of crossing rates of the loading process over a scalar barrier. Beck & Melchers (2004b) propose the ensemble up-crossing rate (EUR) formulation to solve the up-crossing rate problem as long as the barrier is high. However, in cases where the barrier is too low or the resistance variability is larger that that of the loading, e.g. in highly degraded structures, the number of crossing are more likely to occur. In this case, the EUR is a too conservative solution and a correction needs to be applied, as suggested in Beck & Melchers (2005).

An alternative practical solution of the ensemble crossing rates calculation was proposed by Hagen & Tvedt (1991), where the up-crossing rates over a random barrier are evaluated by means of a parallel systems sensitivity approach, which may be solved with first order reliability methods.

Wen & Chen (1987, 1989) proposed an efficient approach to perform time-variant reliability estimates of structural systems exposed to extreme loading conditions. This approach consists in performing the integration of the multidimensional distribution problem in cases where the distributions of any variables are changing with time.

Marley (1991) and Marley & Moan (1994) proposed a simplified approach for estimation of a long-term up-crossing rate approximation which, as they demonstrated with use of Monte Carlo simulation, is an efficient and yet conservative method to calculate time-variant reliability of offshore structures exposed to extreme environmental conditions and subjected to fatigue cracking as deteriorating agent.

Jiao (1992) proposed a stochastic model for fracture analysis of Gaussian response processes as combinations of narrow-banded processes of different different frequencies. Time-dependent fracture reliability is assessed considering the first-passage of the load process upcrossing the strength threshold, where the resistance of the structure is deteriorated due to crack propagation. CTOD fracture criterion is applied to consider both brittle and plastic fracture likelihood.

Kent et al (2002), Sumpter & Kent (2004), Kent & Sumpter (2004) explored, under a probabilistic approach, the likelihood of fracture failure of ship structures with the presence of fatigue cracks. Their approach is based on the variability of the fracture toughness properties of the material as the cracks propagate with time. Thus, they assess the failure probability by means of a time-variant reliability method with the use of the hazard rate concept. One of the main findings of these studies is that ship structures are tolerant to fatigue cracking, and hence in some cases, cracks may be left unrepaired until certain size, without compromising its safety.

1.4. Purpose of the research

The utmost aim of this work is to establish an applicable procedure to provide the engineer a tool during the decision making process, to be able to assess the safety of an existing ship-shaped offshore structure subjected to deterioration, where the interaction among different deteriorating phenomena such as fatigue, corrosion and fracture, are explicitly accounted for in a systematic and consistent manner.

The levels of uncertainties inherent in FPSOs with respect to fatigue failure differ from those normally assumed in either ships or other offshore structures. Such differences are determined by the especial operational features implicit in production ships. The thesis includes reliability-based formulations of fatigue crack growth of welded joints that allow considering different relevant aspects. Structural safety of structural details of vessels exposed to various climate conditions throughout the service life is efficiently estimated with a series of failure functions. Corrosion-enhanced crack growth modelling is included to estimate fatigue reliability of components. Mean stress effects on fatigue damage are also included as this is a relevant aspect due to the randomness introduced by the continuously varying still-water loading in offshore ships. Further, a bi-linear fracture mechanics formulation for crack growth analysis is proposed and a calibration of parameters with largest uncertainties is

performed with respect to design SN curves. Reliability updating with inspection results is carried out by defining relevant inspection events, emphasizing the implications of inspection quality. Additionally, a methodology of fatigue crack growth in stiffened panels of FPSO hull girders is proposed, taking into account mean stress effects induced by the randomness of still-water loading.

Finally, a time-variant reliability based procedure is established to estimate the probability of fragile fracture failure of a stiffened panel with an abnormal transverse crack, detected at the bottom plating/deck structure of an FPSO, where the resistance reduction against fracture is driven by the combined deteriorating action of random fatigue cracking and corrosion. Figure 1.3 depicts the interaction between the topics dealt with in the research work and the manner they are included on each of the annexed articles.

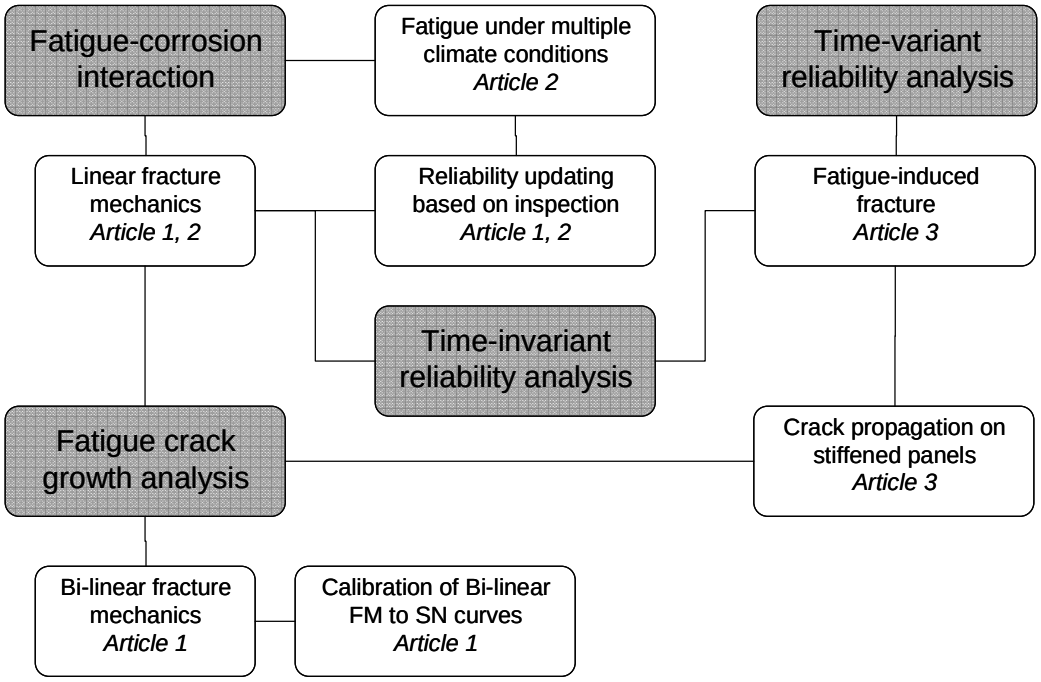

Figure 1.3. Interaction between topics and Articles in the dissertation

1.5. Articles and contributions of the thesis

The research work reported in this dissertation is based on articles already published in different refereed journals. The articles, which are annexed at the end of this report, are related to reliability-based assessment of ship-shaped offshore structural components subjected to fatigue cracking, corrosion-enhanced fatigue and fracture failure. The articles presented in this dissertation are:

Article 1:

Ayala-Uraga, E. and Moan, T., "Fatigue reliability-based assessment of welded joints applying consistent fracture mechanics formulations", *International Journal of Fatigue*, Vol. 29 No. 3, pages 444-456, 2007.

Article 2:

Moan, T. and Ayala-Uraga, E., "Reliability-based assessment of deteriorating ship structures operating in multiple sea loading climates", *Reliability Engineering and System Safety*, Vol. 93(3) pp. 433-446, 2008.

Article 3:

Ayala-Uraga, E. and Moan, T., "Time-variant reliability assessment of FPSO hull girder with long cracks", *Journal of Offshore Mechanics and Arctic Engineering*, Vol. 129 No. 2, pp. 81-89, 2007.

With respect to the authorship of these three articles and my contributions, I have been the first author of *Articles* 1 and 3, for which I was responsible for establishing the models, performing the calculations, providing the results and writing the papers under the supervision of Prof. Torgeir Moan. Regarding *Article 2*, even though I appear as second author, I was also responsible to performing all the calculations, providing results and writing the article, all under direction of my supervisor.

The body of the thesis report is organized into five chapters, each of which draws and highlights the main contributions and the relevant issues dealt with on the different topics touched upon during this research work. After the introductory remarks presented in the present chapter, the second chapter describes the basic concepts on structural reliability analysis being applied throughout this research work. Chapter three deals with the models related to crack growth on structural components of existing offshore infrastructure, emphasizing on the interaction between fatigue and corrosion. Surface and through-thickness cracks propagation in stiffened panels are discussed. A methodology based on reliability methods is presented by defining failure functions that enable to parameterize the uncertainties involved in both random processes. The use of a bi-linear fracture mechanics formulation is introduced and some of the parameters are calibrated with respect to SN curves. In Chapter four, fatigue reliability issues concerning to operational peculiarities of FPSO hull structures are dealt with. Additionally, this chapter deals with the methodology for reliability updating, describing the safety margins and inspection events corresponding to fatigue cracking and corrosion interaction, the effect of changing climate conditions and the characterization of the different inspection techniques that are relevant for ship structures. Aspects such as inspection planning and service life extension are also treated.

Chapter five deals with a methodology based on time-variant reliability analysis to assess the likelihood of fatigue-induced fracture of stiffened panels in an FPSO, e.g. in locations at the deck or bottom plating. The methodology is based on time-variant reliability theory to estimate the probability of overload fracture of a stiffened panel with an existing crack whose growth rate is also affected by the continuously-varying mean stress level introduced by the still-water bending moment of the production ship.

1.6. Additional articles

Additional articles were published during the development of the doctoral studies of the author which are not included as part of the present dissertation, since some of them discuss topics that are either overlapped with those articles listed above or not directly related to the

main topic contained in this thesis. Such additional articles were presented in international conferences or published in refereed journals, namely:

1. **Ayala-Uraga, E. and Moan, T. (2002)**, "System Reliability Issues of Offshore Structures Considering Fatigue Failure and Updating Based on Inspection", In: Proc. of 1st International ASRANet Colloquium, Glasgow, Scotland, UK.

2. **Moan, T. and Ayala-Uraga, E.**, **Wang, X. (2004)**, "Reliability-based service life assessment of FPSO structures". Transactions of the Society of Naval Architects and Marine Engineers, Vol. 112, pp. 314-342.

3. **Moan, T., Gao, Z., Ayala-Uraga, E. (2005)**, "Uncertainty of wave-induced response of marine structures due to long-term variation of extratropical wave conditions". Marine Structures Vol. 18(4) pp. 359-382.

4. **Ayala-Uraga, E., Moan, T., (2005)**, "Time-variant reliability assessment of FPSO hull girder with long cracks". In: Proc. 24th International Conference of Offshore Mechanics and Arctic Engineering, Halkidiki, Greece.

5. **Ayala-Uraga, E., Moan, T., (2005)**, "Reliability-based assessment of welded joints using alternative fatigue failure functions". In: Proc of International Conference on Structural Safety and Reliability, ICOSSAR'05, Rome, Italy.

CHAPTER 2

Structural reliability analysis

2.1. Background on structural reliability

2.1.1. Basic concepts

In the most general sense, the *reliability* of a structure is its ability to fulfil its design purpose for a certain time and under specified conditions. In a mathematical sense it is the *probability* that a structure will not attain each specified limit state (ultimate or serviceability) during a specified *reference period*.

In this context the focus will be on structural reliability in the narrow sense, as the complementary quantity to *failure probability,* P_f defined by

$$P_f = P\left[R \le S\right] \tag{2.1}$$

where R is the resistance and S represents the load effect.

Depending upon how R and S are related to time, the failure probability also will be defined with respect to a reference time period, say year or service life time. Strictly speaking, both R and S in a marine structure, an in any other kind of infrastructure, vary with time, thus the reliability of such a structure also varies with time. Nevertheless, often both resistance and loading are characterized as time-independent variables for a certain time span, e.g. one year, 20 years. These problems are solved by means of the so called time-invariant reliability analysis, in which the safety of a structure is estimated for a certain instant of time but it is valid for the period of time assumed in the characterization of the variables. On the other hand, some reliability problems may require considering that either the resistance or loading effects or both need to be modelled as time-dependent variables. Such cases are regarded as time-variant reliability problems. Both time-invariant and time-variant reliability

analysis methods to assess the safety of structures are briefly discussed in the following sections as these techniques are used in research work presented in this dissertation.

2.1.2. Time-invariant reliability

The failure probability can generally be written as:

$$P_f = \Phi(-\beta); \tag{2.2}$$

where

$$\Phi(u) = \int_{-\infty}^{u} \phi(t)\,dt = \int_{-\infty}^{u} \frac{1}{\sqrt{2\pi}} \exp\left[-\frac{1}{2}t^2\right] dt \tag{2.3}$$

and $\phi(t)$ is the probability density of a normal variable with mean value $\mu = 0$ and standard deviation $\sigma = 1$. Hence, the *reliability index* β is uniquely related to the *failure probability*, P_f.

The notion of failure probability has so far been introduced with reference to a resistance R and an action effect S. Explicit expressions have been given for some special cases of R and S. P_f in this case may be expressed by a two-dimensional integral. This two-dimensional formulation may be generalized by considering multiple variables to describe the problem.

In general the failure probability for a time-invariant reliability problem, may be formulated as

$$P_f = P\left[g(\mathbf{x}) \le 0\right] \equiv \iint_{g(\mathbf{x})\le 0} f_{\mathbf{x}}(\mathbf{x})\,d\mathbf{x} \tag{2.4}$$

where $\mathbf{X}$ is the set of n random variables used to formulate the problem. $f_{\underline{\mathbf{x}}}(\mathbf{x})$ in the joint probability density of function $\mathbf{X}$. The n-dimensional integral is taken over the region in where: $g(\mathbf{x}) \le 0$, corresponding to failure.

An important class of limit states are those for which all the variables are treated as time independent, either by neglecting time variations in cases where this is considered acceptable or by transforming time dependent processes into time invariant variables (e.g. by using extreme value distributions). The integral of Eq. (2.4) may be calculated by direct integration, simulation or FORM/SORM methods as described in, e.g., textbooks (e.g. Ang and Tang, 1984; Madsen et al., 1986; Melchers, 1999). In this section the basics of structural reliability analysis is briefly outlined.

2.1.3. FORM/SORM

The basic steps in the reliability analysis by the First Order Reliability Method (FORM) comprises

- definition of failure function, $g(x_1, ..., x_n)$ and the random variables accounted for
- establish uncertainty measures and distributions for the various variables

- transform the possibly dependent variables in the **X**-space into a **U**-space of independent standard normal variables according to a probability preserving transformation, (e.g. Melchers, 1999)

$$\mathbf{X} = T(\mathbf{U}) \tag{2.5}$$

and correspondingly transform g(**X**) into g'(**U**).

- calculation of the failure probability, P_f

$$P_f = P\left[g'(\mathbf{u}) \le 0\right] \tag{2.6}$$

Hence, e.g. according to Madsen et al (1986):

$$P_f = \iint\limits_{g'(\mathbf{u})\le 0} ..\int f_{\mathbf{u}}(\mathbf{u})\, d\mathbf{u} = \iint\limits_{g'(\mathbf{u})\le 0} ..\int \phi(u_1)\cdot\phi(u_2)\,..du_1 du_2 = \Phi(-\beta) \tag{2.7}$$

where β is the shortest distance from the origin to the surface g'(**u**)=0.

The FORM method can be improved by a second order reliability method (e.g. Madsen et. al, 1986; Melchers, 1999). The SORM is based on a quadratic approximation of the limit state surface at the design point. Nevertheless, experience has shown that the FORM result is sufficient for many structural engineering problems. When using the FORM, the computation of reliability (or equivalently of the probability of failure) is transformed into a geometric problem, than of finding the shortest distance from the origin to the limit state surface in standard normal space.

In general it should be noted that FORM and SORM are approximate analytical methods. The advantage of the analytical methods is that they are fast. FORM and SORM have proved to be useful tools for evaluating reliability of marine structures.

2.1.4. Simulation methods

In this approach, random sampling is employed to simulate a large number of (usually numerical) experiments and to observe the results. In the context of structural reliability, this means, in the simplest approach, sampling the random vector **X** to obtain a set of sample values. The limit state function is then evaluated to ascertain whether, for this set, failure (i.e. $g(\mathbf{x}) \le 0$) has occurred. The experiment is repeated many times and the probability of failure, P_f, is estimated from the fraction of trials leading to failure divided by the total number of trials. This so-called Direct or Crude Monte Carlo method is not likely to be of use in practical problems because of the large number of trials required in order to estimate with a certain degree of confidence the failure probability. Note that the number of trials increases as the failure probability decreases.

More advanced simulation methods are currently used for reliability evaluation whose aim is to reduce the variance of the estimate of P_f. Such methods can be divided into two categories, namely indicator function methods (such as Importance Sampling) and conditional expectation methods (such as Directional Simulation). Simulation methods are also described in a number of textbooks (e.g. Ang and Tang, 1984; Melchers, 1999).

Reliability estimates by simulation methods are considered verified if a sufficient number of simulations are carried out. Simulations by basic Monte Carlo and importance sampling

methods should be carried out with a number of simulation samples not less than $100/P_f$ where P_f denotes the failure probability. Simulations by other methods should be carried out such that the estimate of P_f is positive and the coefficient of variation of the simulations is less than 10%.

2.1.5. Time-variant reliability assessment

So far, the failure probability has been expressed by two random variables, R and S. In general, R and S are functions of the time. For instance, the ultimate resistance may be a slowly decreasing function with time due to crack growth (fatigue) or corrosion. Load effects due to waves clearly vary with time, and a stochastic process model is required to describe these phenomena. However, good approximations for the reliability analysis may be established also in the case of time-dependent resistances and load effects. This is especially the case if the time-dependence of the resistance can be neglected or is very slowly varying, and the action process is e.g. a stationary process. Both $f_R(r|t)$ and $f_S(s|t)$ may then be modeled as time-independent functions. In particular, the action process is replaced by the extreme value distribution, as shown in Figure 2.1.

The probability of failure in t_L may be determined by:

$$P_f\left(\underline{t_L}\right) = P\left[R \le \underline{S_{\max}}\left(\underline{t_L}\right)\right] \tag{2.8}$$

where $S_{max}(t_L)$ is max S in the period t_L. This implies that the mean load effect is calculated by the expected maximum value in the reference period for the failure probability, e.g. the annual maximum if the annual P_f is to be calculated. The scatter of this expected maximum is combined with model uncertainties.

Time-dependent reliability is used to determine the likelihood in time of an excursion of the random vector X(t) out of a safe domain **D** defined by **G**(X)**>0**. The first-passage probability may be equivalent to the probability $pf(t)$ of structural failure during a certain period [0,T], e.g. Melchers (1999).

$$p_f(t) = 1 - P\left[N(t) = 0 \mid X(0) \in D\right] P\left[X(0) \in D\right] \tag{2.9}$$

where $X(0) \in D$ signifies that the process $X(t)$ starts in the safe domain ***D*** at zero time and $N(t)$ is the number of outcrossings in the time interval $[0,t]$.

The general solution of (2.11) is rather difficult to obtain owing to the need to account for the complete history of the process $\boldsymbol{X}(t)$ in the interval $[0,t]$. Usually the solution will depend on the nature of the process **X(**t). For reliability problems, outcrossings usually occur so rarely that often it is satisfactory for the individual outcrossings to be assumed independent events, and therefore independent of the probability of any earlier outcrossings, including one at t=0. The probability of no outcrossings in $[0,t]$ may then be approximated using the Poisson distribution.

Obviously, the outcrossing rate υ depends on the barrier that separates the safe from the failure domain. For a scalar stochastic process, such as the wave-induced stress history over a resistance barrier, the up-crossing rate is of interest. In problems of deteriorating resistance,

i.e. depending on time, the up-crossing rate may be represented by the average up-crossing rate $\upsilon t = \int_0^T \upsilon^+(r,t)\,dt$

Then, then failure probability reads:

$$P_f(t) \approx 1 - \exp\left(-\int_o^T \upsilon^+(r,t)\,dt\right) \tag{2.10}$$

This approximation is good for rare out-crossings, i.e. the out-crossings are independent events, but it is not good choice for cases where the barrier is low or close to the origin, which implies that the assumption of independent crossings is not completely valid.

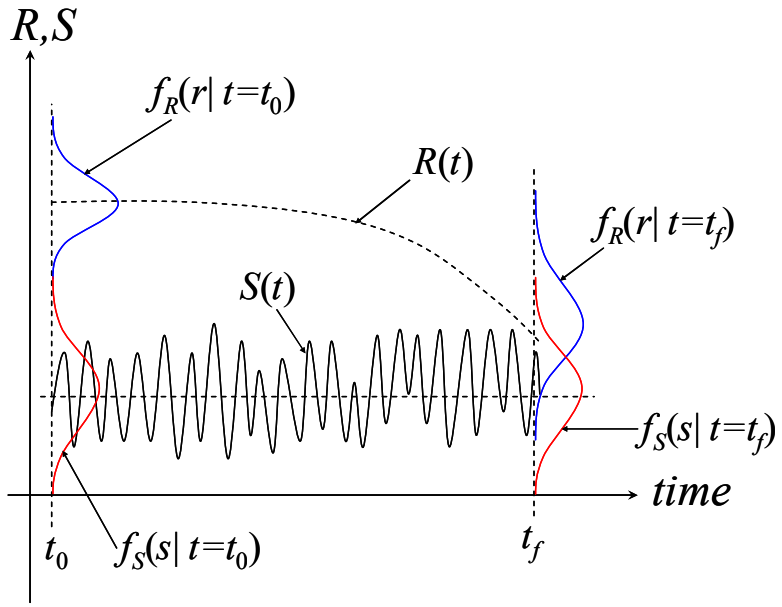

Figure 2.1. Time-dependent reliability problem.

2.1.6. Hazard rate

Reliability analysis is a decision tool. Hence, calculated P_f's are compared with an acceptable failure probability, P_{ft}, i.e. the target level for P_f. The target level may be expressed by the annual or service life value. The annual value may conveniently be expressed by the (annual) hazard rate. However, since most fatigue requirements have not been consistently calibrated, the implied failure probability in relevant codes may vary and the target level would have to be based on a weighed mean of implied safety levels.

The hazard rate $h(t)$ is defined as $h(t) = f(t)/(1-F(t))$ where $F(t)$ is the distribution function of the time-to-failure of a random variable T, and $f(t)$ is its probability density function. This expression represents the probability that the structure of age t will fail in the interval $t+\Delta t$, given it has survived up to time t, namely (see e.g. Mann et al, 1974; Melchers, 1999)

$$h(t) = P\left[T \le (t+\Delta t) | T > t\right] = \frac{P\left[t \le T \le t+\Delta t\right]}{\Delta t \cdot \left(1 - P\left[T \le t\right]\right)} = \frac{dP_F(t)/dt}{1 - P_F(t)} \tag{2.11}$$

For instance, the implicit service life failure probability of a structural component designed against fatigue failure with a cumulative fatigue damage of D=1, would be of the order of 10^{-1}. However, the corresponding maximum hazard rate (in the last year of service) is 10^{-2}.

Fatigue failure probabilities are naturally referred to the cumulative damage during the service life. However, an alternative is to use annual hazard rates as discussed in *Article 2* on Appendix A.

2.1.7. Uncertainty measures

Uncertainties in structural engineering systems may be classified into three types, namely inherent uncertainties, statistical uncertainties and model uncertainties.

- Inherent uncertainty is usually associated with physical randomness that, from a practical point of view, is not possible to predict. Inherent uncertainty exists in the description of the environment the ship is exposed to over the lifetime due to, e.g., inherent randomness in the encountered sea states and wave directions, wave heights, spectral shape, wind speed, etc.
- Model uncertainty originates from simplifications and ignorance in the theoretical model being applied to describe a physical phenomenon. These uncertainties can be of both a systematic (e.g., systematic underestimation) or random nature. Some sources of this uncertainty include our imperfect knowledge of, for instance, a failure mechanism or a wave load effect on a structure.
- Statistical uncertainty is defined as uncertainty in the parameter modelling due to lack of statistical information. Characterization of metocean conditions depend upon the amount of data collected about wave heights and periods, wind speed, current direction, etc, from a certain location, but in all the cases such data will be of limited size.

The estimation of uncertainties is a crucial task in performing reliability analysis of structural systems. In connection to safety assessment of existing marine structures, it is important to define the magnitude of the uncertainties and the relative importance of both the load and load effects, as well as the resistance uncertainties. Furthermore, uncertainties related to resistance may vary with time due to degradation effects such as fatigue and corrosion which are inherently random.

The uncertainties used in reliability analysis should include all imponderables which may affect the reliability. These would include “inherent” statistical variability in the basic strength or action parameter. Additional sources of uncertainty arise due to modelling and prediction errors and incomplete information; included in these “modelling uncertainties” would be errors in estimating the parameters of the distribution function, idealizations of the actual action process in space and time, uncertainties in calculation, and deviations in the application of standard and material specification from the idealized cases considered in their development. The key test in differentiating between the “inherent” and “modelling” uncertainties is in whether the acquisition of additional information would materially reduce their estimated magnitude. If the variability is intrinsic to the problem, additional sampling is not likely to reduce its magnitude, although the confidence interval on the estimate would contract. In contrast, uncertainties due to “modelling” should decrease as improved models and additional data become available.

For structures with time-variant loads and resistances it is necessary to define the failure probability with reference to a time period, say, one year or service life. For a single (stationary) load process this can be achieved by considering the (time variant) extreme value in the given period as the random load variable. If several time variant loads are dealt with, the combination of these loads may be represented by a set of time variant loads, e.g. wave-induced and still-water bending moments in the hull girder.

For the purpose of quantifying uncertainties and for subsequent reliability analysis, it is necessary to define a set of *basic variables*. The basic variables are described by probability density functions or distributions. Alternatively the statistical moments, e.g. mean value, variance (square of standard deviation) may be applied. Reference is made to textbooks, e.g. Madsen et al (1986); Melchers, (1999). In many cases, important variations exist over time (and sometimes space), which have to be taken into account in specifying basic variables. In probabilistic terms, this may lead to a random process rather than random variable models for some of the basic variables. However, simplifications might be acceptable, thus allowing the use of random variables whose parameters are derived for specified reference period (or spatial domain). The values of the uncertainties are crucial to the estimates of the reliability.

Chapter 3 of this report discussed aspects related to the uncertainties involved in fatigue damage estimations of both surface cracks, as well as long crack propagation in stiffened panels. Additionally, the uncertainties on the corrosion phenomenon description vary with time, as discussed by Melchers (2003a, 2003b). Moreover, aging structures may experience resistance reduction in terms of fatigue and ultimate strength induced by the effect of corrosion, thus the interaction of corrosion with fatigue and ultimate strength introduce additional time-variant uncertainties.

To determine the statistical description for extreme (maximum) values of the variable loads in a specified time interval, it is necessary to transform the distributions of the basic data collected. For wave loads, for example, it is convenient to use such statistics as the long-term variation of sea states in terms of scatter diagrams or some joint probability distribution. The load effects are obtained by a frequency domain for a linear problem or a time domain analysis when important nonlinearities affect the load effects. For instance, Weibull distribution is found to well describe different types of long-term load effects for structures in extra-tropical climate. Extreme values corresponding to one year or 100 year periods can then be readily established based on extreme value theory. Annual variability of extreme wave height may, however, be of importance especially if the reliability estimation is referred to annual values. Moan et al (2005) assessed the year-to-year variability of extreme values of wave heights with data collected over 29 years in a site of the North Sea.

CHAPTER 3

Probabilistic fatigue and corrosion models

3.1. General

Marine structures are subject, throughout their service lives, to the dynamic action of waves, wind and current. In early 80's fatigue design of merchant vessels was implicitly covered by allowable stress (section modulus) requirements to wave loading. Use of high tensile steel and particularly local dynamic loads (e.g. wave pressure variations around mean water level) has meant fatigue a crucial design criterion. Design of offshore and ship structures includes fatigue limit state (FLS) requirements, which is often a predominant criterion in the design of this kind of structures. Offshore Class Rules generally require that a permanent offshore structure meet a fatigue life which is at least three times the intended service life of the platform. Areas of a platform which are not accessible for inspection must meet a fatigue life of ten times the service life. Ship-shaped FPSO vessels are hybrid structures as they are structurally similar to typical merchant ships, e.g. tankers or VLCC, but anchored to a fixed location and operated as an offshore facility. Moreover, most of FPSO vessels in operation around the world are based on converted tanker structures formerly designed for sailing under harsh conditions, as those for North-Atlantic routes, and being operated under benign weather conditions (Moan et al, 2004b). The challenge is therefore to operate these kinds of vessels safely and cost-effectively, by taking advantage on experiences gained over the years on operation of oil tankers and adequate them into the framework defined by the safety and economic requirements proper of the offshore industry.

Design criteria against fatigue failure are based upon SN data, obtained from tests on typical structural details. The use of the SN curve approach for design has proved to be practical, though it provides no idea on the magnitude of the uncertainties involved in both the resistance and loading components. There is evidence of cracks appearing after few years in

operation, even after having applied the best design practices in recently installed FPSOs (OLF, 2002). The increasing need of assessing ageing structures makes it necessary to properly account for these uncertainties in a systematic and consistent manner. Good design practices also imply the use of in-service inspection, maintenance and repair (IMR), to keep adequate structural safety and system integrity. The introduction and development of Fracture Mechanics and reliability-based methods for crack growth assessment, e.g. in the offshore industry, has signified substantial benefit and understanding of the different parameters and corresponding uncertainties involved in the fatigue damage process. The combined use of these disciplines has become a very important tool to support decision making activities concerning to inspection planning and service life extension of fatigue sensitive structures.

Design of welded structures for fatigue limit state is normally carried out by means of either single- or two-sloped SN curves. To properly assess the effect of an inspection and repair strategy of structures degrading due to crack growth, fracture mechanics (FM) models need to be applied to describe crack propagation. To provide a proper tool for making decisions regarding the balance between design criteria and an optimal plan for inspection and repair in view of the inherent uncertainties, reliability methods should be applied. In this section alternative SN and FM formulations of fatigue are investigated. They include a crack growth formulation based on bi-linear crack growth law, considering both segments of the crack growth law as correlated and non-correlated in the failure probability calculation.

SN curves combined with the hypothesis of linear cumulative damage are applied to carry out the fatigue design check under variable amplitude loading, e.g. NORSOK (1998). Besides adequate design against fatigue failure, inspection and repair can be used to increase the reliability in view of crack growth. In order to guarantee the effect of inspection more details about the crack growth than provided by SN-data are required. Fracture mechanics then represents a potential tool to describe the gradual development of crack and hence account for the effect of inspection and possible repair at the different stages of crack growth. Due to the inherent uncertainties of the crack growth method and data, as well as those in the inspection procedure, reliability methods can be used to support the decisions regarding the balance between design, inspection and repair plan, e.g. Moan (2005). Recently, the use of an FM-based bi-linear crack growth law for fatigue analysis has been introduced (BS7910, 1999), which reduces the excessive conservatism believed to be implicit in the single slope Paris' law approach.

3.2. Fatigue failure

3.2.1. SN-based failure functions

Recalling from Miner's rule the number of cycles contributing to fatigue damage N, i.e. $N=KS^{-m}$, where K is a constant defined under constant amplitude loading, S is the stress range and $-m$ is the slope of the curve. New design approaches based on the SN curves, e.g. NORSOK (1998), include bi-linear curves to account for the effect of variable amplitude loading. Gurney (1976) first proposed using a detailed fracture mechanics model of fatigue crack initiation and growth in joints with fillet and butt welds. Haibach (1970) proposed an integrated approach, also using fracture mechanics, and derived a bi-linear SN curve. The first segment extends until a limit of constant amplitude validity, whereas the second segment was found to have a slope equal to $1/(2m-1)$, with m being the slope of the first segment.

The fatigue damage with a two-sloped SN curve may be expressed as:

$$D = \frac{N}{K_1} A^{m_1} \left\{ \Gamma\left[1 + \frac{m_1}{B}; \left(\frac{S_0}{A}\right)^B\right] + \left(\frac{S_0}{A}\right)^{m_1 - m_2} \gamma\left[1 + \frac{m_2}{B}; \left(\frac{S_0}{A}\right)^B\right] \right\} \tag{3.1}$$

where $f_S(s)$ is probability density of the of the long-term stress range s, assumed to be Weibull distributed (e.g. Guedes and Moan, 1991). m_1 and m_2 are the corresponding slopes of the curve, long-term stress range s, A and B are, respectively, the scale and shape parameters of the long-term stress range Weibull distribution, S_0 is the stress range at the knuckle of the slopes and the constant K_2 for the second slope is determined by $K_2 = K_1 S_0^{m_2 - m_1}$. This implies that the uncertainty corresponding to the first slope (i.e. CoV of K_1) is the same for the second slope. In principle, the uncertainty for the latter fatigue life is larger as this corresponds to long fatigue endurances, for which there are limited data. This uncertainty is also reflected in the debate about which value of slope should be applied for the lower segment.

The safety margin is expressed as:

$$M(t) = \Delta - D \leq 0 \tag{3.2}$$

where Δ is the fatigue damage at failure. The fatigue design criteria can be expressed by $D_c \leq \Delta_d$, where D_c is the characteristic damage value determined in a long term period, and depends on the characteristic value of K (mean minus two standard deviations). Further, a common design practice in the shipping industry is to consider a cumulative fatigue damage of Δ_d=1 in a 20-year service life. In the offshore industry structures are designed against fatigue degradation considering fatigue damage ranging from Δ_d equal to 0.1 to 1.0, depending upon the consequences of failure and accessibility of inspection (e.g. NORSOK, 1998).

Article 1 presents results of reliability calculations using safety margins corresponding to a single- (margin 1 slope) and two-slope (margin 2-slope) SN models for curve F according to BS 7608 (1993). The design SN curve F corresponds to a T-butt welded joint. As discussed in *Article 1*, at a low stress level corresponding to Δ_d =0.1 the difference is large. This implies that at low stress levels the effect of the second slope has, as expected, a significant effect. See *Article 1* in Appendix A for details about the input data.

3.2.2. Fatigue analysis based on fracture mechanics

The application of fracture mechanics and reliability analysis in the recent decades has enabled to develop decision-making tools that have ensured safety in infrastructure of different industries such as nuclear, aerospace and offshore, among others.

Fatigue analysis and updating formulation, as treated in *Article 1*, is based on the fracture mechanics approach defined by the Paris' crack propagation law, which reads

$$\frac{da}{dN} = \begin{cases} C(\Delta K)^m & for \quad \Delta K > \Delta K_{th} \\ 0 & for \quad \Delta K \leq \Delta K_{th} \end{cases} \tag{3.3}$$

where a is crack depth, N is number of cycles, C is crack growth parameter, m is the inverse slope of the SN curve, and ΔK_{th} is a threshold of the stress intensity factor range ΔK given as a function of the crack size a as

$$\Delta K = Y(a) \cdot S\sqrt{\pi a} \ = \left(Y_m S_m + Y_b S_b\right)\sqrt{\pi a} \tag{3.4}$$

S is the stress range and the sub-indices m and b refer to membrane and bending stress, $Y(a)$ is the geometry function, which is dependent upon the crack size and shape. The geometry function may be defined as $Y(a) = Y_{plate}(a)$ x $M_k(a)$, where $Y_{plate}(a)$ is the geometry function corresponding to a semi-elliptical surface crack as proposed by Newman and Raju (1981) from finite element analysis in flat plates subjected to axial and bending remote stresses. $M_k(a)$ is a magnification factor which depends on the local weld geometry and accounts for the crack size and loading, as recommended the BS 7910 (1999). Often, a model uncertainty γ_{geom} is introduced for the geometry function in the reliability analysis. Thus, the failure function for fatigue as function of time can be written as $M(t) = a_f - a(t) \le 0$ (e.g. Madsen et al, 1986), or

$$M(t) = \int_{a_0}^{a_f} \frac{da}{G(a)\left[Y(a)\sqrt{\pi a}\ \right]^m} \ - \ C \cdot v_0 \cdot A^m \Gamma\left(1 + \frac{m}{B}\right) \cdot t \le 0 \tag{3.5}$$

Here a_0 and a_f are initial and final crack depths, respectively. It may be expressed in terms of the number of cycles N as the product of time t, and the average stress cycle frequency, v_0. In case of through thickness crack, a_f = plate thickness. G(a) is an auxiliary function that helps account for the threshold of stress intensity range ΔK_{th}, and it is defined analytically based on the two-parameter Weibull distribution of stress range, see *Article 1*. The failure probability is calculated as:

$$P_f = P\left[M(t) \le 0\right] \tag{3.6}$$

3.3. Bi-linear model based on Fracture Mechanics (FM)

The fatigue reliability and updating formulation often used is based on a fracture mechanics approach given by the Paris' crack propagation law (e.g. Madsen et al, 1986; Moan et al, 1993; Lotsberg and Sigurdsson, 2005). In general, the Paris' law may be used in a multi-segmented one-dimensional crack growth as follows

$$\frac{da}{dN} = \begin{cases} 0 & for \quad \Delta K \le \Delta K_{th} \\ C_1 (\Delta K)^{m_1} & for \quad \Delta K_{th} < \Delta K \le \Delta K_1 \\ \vdots & \\ C_{n+1} (\Delta K)^{m_{n+1}} & for \quad \Delta K > \Delta K_n \end{cases} \tag{3.7}$$

where a is crack depth, N is number of cycles, C_i is the crack growth parameter for segment i in the, m_i is the corresponding the slope of the segment, and ΔK_i is the point of intersection of two consecutive segments.

The British Standard BS7910 (1999) recommends the use of a bi-linear crack growth law for fatigue assessment of welded structures, which is based on the study carried out by King (1998), see Figure 3.1. The uncertainties reported for both segments of the crack growth are different, with the largest CoV in the lower segment. However, there is no information on the

correlation level between the two segments. Righiniotis and Chryssanthopoulos (2004) assumed that the two segments of the crack growth law were uncorrelated. The effect of correlation in failure probability is investigated in *Article 1*.

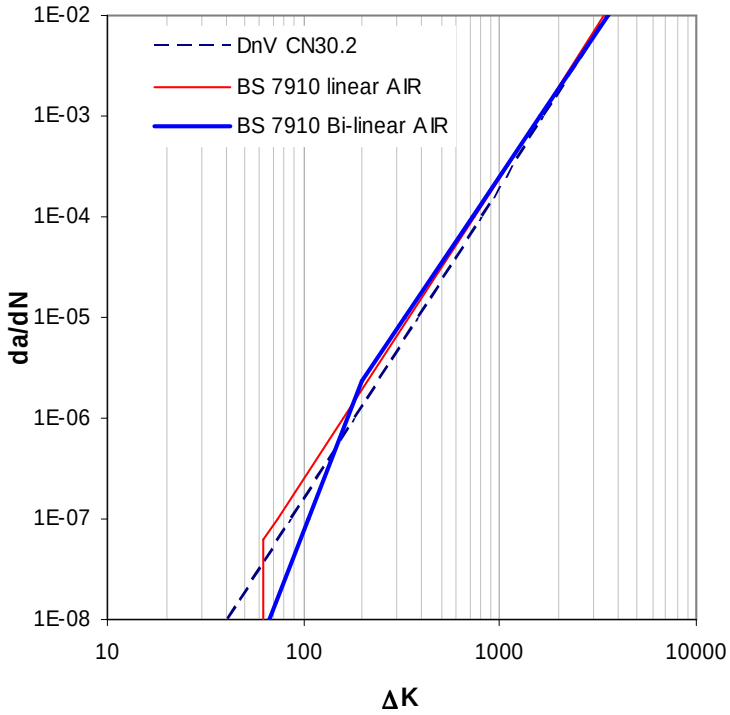

Figure 3.1. Mean values of crack growth laws according to BS 7910 (1999) and DNV (1984) data.

Following Paris' law, a weighed (averaged) crack growth rate may be estimated based on the multi-segmented crack growth law implied by Eq. (3.7). Then, the crack growth rate for the bi-linear model may be expressed as (e.g. Kam and Dover, 1989)

$$\frac{da}{dN} = C_1 \left(\Delta K\right)^{m_1} + C_2 \left(\Delta K\right)^{m_2} \tag{3.8}$$

The intersecting point of the two slopes of the crack growth law, ΔK_0, corresponds to a value given by:

$$\Delta K_0 = \exp\left(\frac{\ln C_1 - \ln C_2}{m_2 - m_1}\right) \tag{3.9}$$

From Eq. (3.7) and with the assumption of Weibull distributed long-term stress range, a closed-form solution for a bi-linear crack growth law may be obtained, as described in *Article 1*. From the integration of Eq. (3.8) the failure function at time t for the bi-linear FM model may be given by

$$M(t) = \int_{a_0}^{a_f} \left(\frac{da}{dN} \right)^{-1} da \quad - \quad v_0 (t - t_0) \leq 0 \tag{3.10}$$

where t_0 is the initiation time and da/dN is given by

$$\begin{aligned} \frac{da}{dN} &= C_1 A^{m_1} \left(Y(a)\sqrt{\pi a} \right)^{m_1} \cdot G_1(a) \\ &+ C_2 A^{m_2} \left(Y(a)\sqrt{\pi a} \right)^{m_2} \cdot G_2(a) \end{aligned} \tag{3.11}$$

The auxiliary functions of Eq. (3.11) $G_1(a)$ and $G_2(a)$ are defined in *Article 1*.

3.3.1. Validity of FM bi-linear models

In general, according to the data provided in the BS7910 (1999) and King (1998) the uncertainties of the material parameter C corresponding to the lower segment is larger than that of the upper segment. This also implies that the near-threshold crack growth rates have an influence, due to both the inherent uncertainty of very small crack growth behavior and due to the difficulty of measuring such rates in the tests. In addition, there is lack of information regarding the degree of correlation existing between both segments, which has an implication in the reliability calculations. In *Article 1* of this dissertation a verification study was performed in order to determine the implication of correlation on the reliability level. The recommendation is to assume high correlation between lower and upper segments when performing crack growth calculations with a bi-linear fracture mechanics model. The non-correlated model may introduce unrealistic negative values of ΔK_0, i.e. lower shadowed area shown in Figure 3.2, that lead to spurious higher reliability estimates.

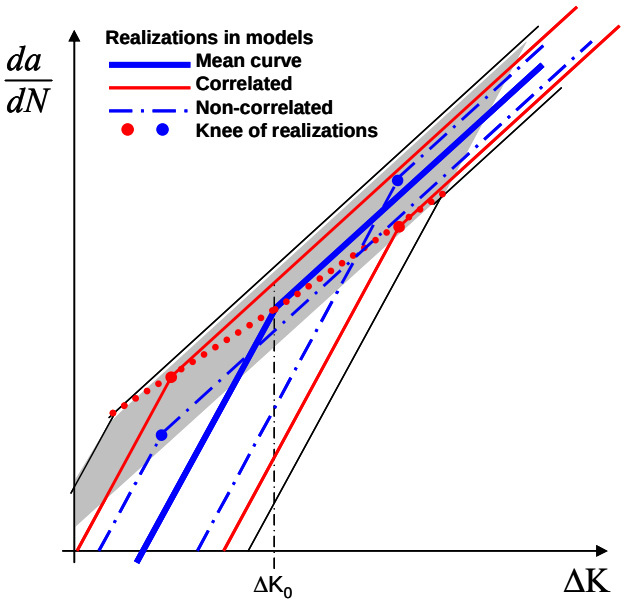

Figure 3.2. Schematic representation of correlation effect in realizations of ΔK_0 in bi-linear crack growth model. Larger uncertainty in lower segment assumed.

3.4. Calibration of FM bi-linear model

Article 1 presents a sensitivity study that includes the effect on reliability calculations of the initial crack size, crack aspect ratio development and the threshold of stress intensity factor range, ΔK, for a flush-welded joint (joint C) and a fillet-welded joint (joint F). The study includes calculations based on both linear and bi-linear fracture mechanics formulations, and compared to calculations obtained with an SN-based model. One of the main findings of these studies is that the linear FM models may be fitted to the SN models, whereas the bi-linear ones seem to have a very different slope, which makes it difficult to calibrate this model.

3.4.1. Initial crack size

According to Bokalrud and Karlsen (1981), the initial crack size obtained from actual welded details in ship hull structures was found to follow an exponential distribution with a mean value of 0.11 mm, and a rate of 16 cracks per m. In SN tests, however, small specimens are normally used. Then, assuming 2 independent initial cracks in a specimen as the type described above, the expected largest value would be of 0.17 mm, characterized by a Gamma distribution with standard deviation equal to 0.12 mm. Carrying out fatigue tests on small specimens, Otegui et al (1989) reported an average of 8.8 initiation sites per 25 mm of weld toe. Their findings also indicate that for specimens under relatively high stress ranges up to 13 initiation sites were reported from undercut defects, whereas only 1 site was found in a specimen subjected to 2.5 times lower stress range. This is an indication of the large scatter on the initial crack sizes and spatial distribution along a weld, even in small specimens. This implies that higher uncertainties on these parameters may be found in actual long welds as those in ship structures.

3.4.2. Crack aspect ratio development

In long fillet welds subjected to uniform stresses, e.g. welded joint of a bulkhead to the bottom plating of a hull structure, the local weld geometry increases the likelihood of coalescence of single surface cracks, which leads to longer cracks (i.e. low aspect ratio), and hence shorter fatigue lives. The crack aspect ratio a/c varies as the crack propagates through the thickness, depending on the stress pattern and the effect of the local weld geometry, e.g. Burns et al (1987). The use of forcing functions to describe the aspect ratio development is attractive for being used in a reliability framework, though their results are based on finite width specimens under specific loading conditions, which are sometimes difficult to generalize. Multiple initial crack and coalescence models have been suggested, e.g. Vosikovsky et al (1985), Eide and Berge (1987), Otegui et al (1991), Frise & Bell (1992) and Rodriguez-Sanchez et al (1998). With exception to Vosikovsky et al (1985), all the other references report an aspect ratio development describing a humped shape before coalescence. This means that initial defects are rather long with a low a/c ratio which increases to around 0.4-0.6 and then decrease before coalesce into a single crack. It was also found that the larger the stress level being applied the larger the frequency of crack initiation sites, which leads to earlier crack coalescence (i.e. low aspect ratio) and hence faster crack growth..

In general, the reliability analyses results showed that only the aspect ratio development taking place in the very few millimeters (e.g. les than 5 mm) are the most influential in the results, meaning that the single crack shape, after coalescence takes place, may be assigned a fixed value. The study presented in *Article 1* demonstrates that Vosikovsky's model is more conservative than Eide & Berge's, indicating that as most of the fatigue life is spent in the initial stages the larger aspect ratio of the former model results in larger reliability levels.

However, neither of the curves seems to fit the reliability index curve obtained with SN curve F.

3.4.3. Threshold of ΔK

According to the data review by King (1998) the threshold of the stress intensity factor range (SIF) depends on the stress ratio R. For ferritic steels with yield stress less than 60 MPa the threshold increases as R reduces. According to the findings reported in *Article 1* of Appendix A, the safety of the joint, in terms of reliability index, is more sensitive for the linear FM model to the effect of SIF threshold than for the bi-linear FM model. It is recommended to disregard SIF threshold for the calculations based on the bi-linear FM model, which is also reflected in reduced computational effort for reliability of joints under low stress level, when applying FORM/SORM.

3.4.4. Calibration of bi-linear FM curves

As mentioned above, the reliability index curves corresponding to the bi-linear FM model is difficult to be calibrated (fitted) to an SN-based reliability curve by utilizing a single parameter in the fitting procedure, as it is possible for the linear FM model. This means that a different strategy needs to be applied. For instance, Figure 3.3 shows calibrated bi-linear curves with respect to the corresponding SN-curve for C- and F joints. For both cases 3 parameters were used in the calibration procedure, namely initial crack size, aspect ratio and initiation time. It is observed that in order for the curve corresponding to joint *C* an initiation time of 2 years was utilized compared to 1 year for joint F, which agrees with the fact that the initiation time for the latter is shorter.

3.5. Interaction effects between fatigue and corrosion

3.5.1. Corrosion phenomenon

The most common causes and mechanisms of hull corrosion are galvanic corrosion, direct chemical attack, and anaerobic corrosion. Pitting in ballast tanks can start through the latter mechanism and then accelerate through differential aeration, a type of local galvanic attack caused by differences in oxygen levels at the surface of the steel.

Melchers (2001, 2003a) has reviewed the models used to statistically describe corrosion rates in immersed marine structures. A non-linear behaviour of corrosion wastage in the marine environment is suggested by Melchers (2003b). Guedes Soares and Garbatov (1999) also suggest a non-linear model to characterize the material loss on time, but instead of an anaerobic phase they suggest that the anodic-controlled and diffusion control stages may be repeated when the metal is exposed to the corrosive environment if the rust is removed or cracked due to normal operation of the structure.

In principle, the main types of corrosion patterns are general corrosion, pitting corrosion, grooving corrosion and weld metal corrosion. All of them may have an enhancing affect on fatigue damage on welded connections. The effect of general corrosion in terms of the amount of material loss is accounted for in the fatigue reliability formulation proposed and discussed in *Article 2* of this dissertation.

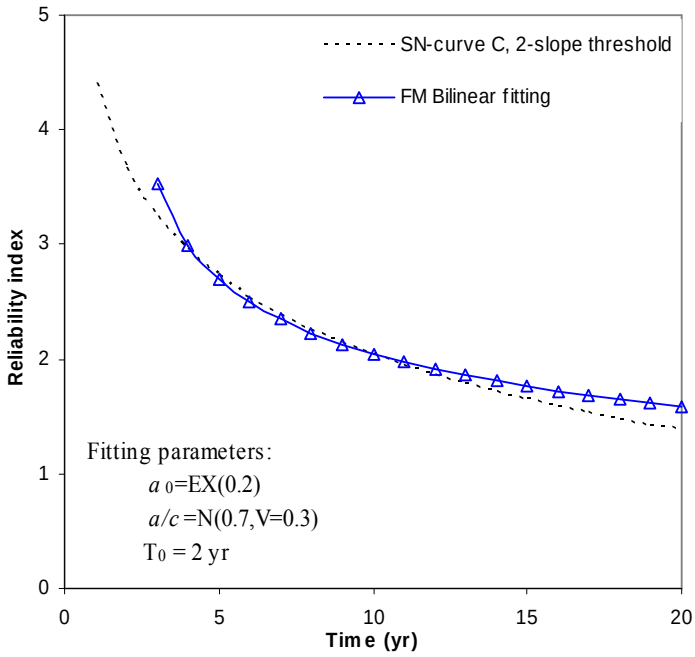

a)

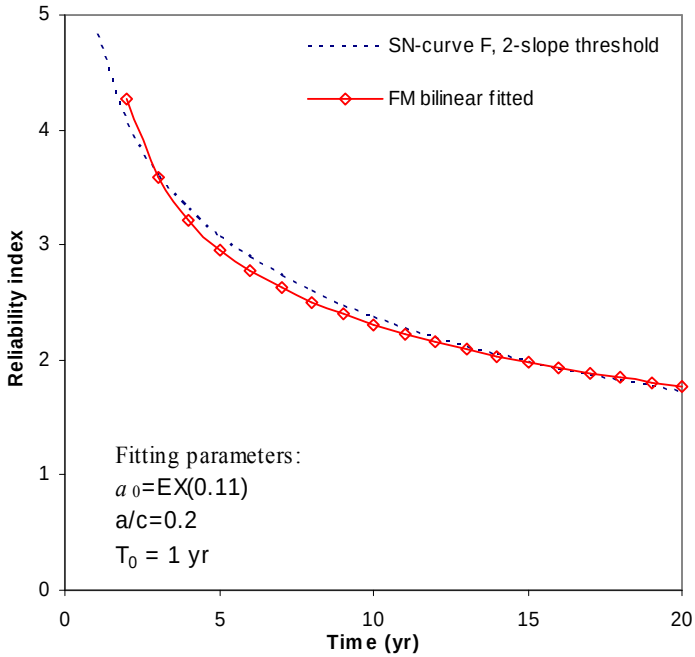

b)

Figure 3.3. Calibration of bi-linear FM model for C-joint (a) and F-joint (b)

3.5.2. Corrosion rates

Studies based on empirical models in ships have suggested that the general corrosion rate for steel in seawater is about 0.1 mm/year. The corrosion rates in ballast spaces are potentially much greater and can become the controlling factor in determining a ship's life. If a compartment is not protected by coatings or sacrificial anodes, the time in ballast represents the most corrosive condition. As a result, the International Association of Classification Societies (IACS) now requires that all ballast spaces with one or more boundaries on the hull envelope must have a protective coating.

Different studies (Wang et al, 2003; TSCF, 1997) have shown a large variability of existing data on corrosion rates in ship structures. Melchers (2003a, 2003b) describes statistically and physically the corrosion phenomenon in marine environments. Additionally, Rauta et al (2004) indicate that corrosion rates in double-hull tankers are much higher than initially estimated in design. Corrosion rates are influenced by many factors such as the type and service of the vessel, position throughout the structure, environmental conditions, and even the geographical location. The latter means that different rates are believed to occur in vessels located in North Sea, as compared to those in West Africa or Gulf of Mexico. However this aspect has not been quantified.

The uncertainty in the corrosion rate is accounted for by assuming it as a random variable. Guedes Soares and Garbatov (1998a) assumed a corrosion rate normally distributed with an even coefficient of variation (CoV) of 0.1 for all the members. Akpan et al (2002) utilized mean values recommended in the TSCF (1997) and assumed a Weibull distribution with CoV between 0.1 and 0.5. Paik et al (2003a) carried out a comprehensive study for determining corrosion rate wastages based on data obtained from single- and double-hull trade tankers and FPSO/FSO vessels. They propose corrosion rates for 34 different structural member groups by type and location. According to Paik et al the corrosion rate follows a Weibull distribution with rather large scatter, e.g. CoV around 0.9 in many cases. The mean values of corrosion rates and uncertainties may be larger in double-hull tankers due to the higher temperatures kept in the hold tanks, leading to enhanced bio-chemical corrosion (Rauta et al, 2004). Wang et al (2003) presented results of an extensive database with thickness measurements of 140 tankers, where the mean corrosion rates varied between 0.02 and 0.06 mm/yr, but with a very large scatter, as well large spatial variation. Maximum corrosion rates of 0.55 mm/yr were also reported for bottom plating and deck longitudinals. Melchers (2001) suggests that the coefficient of variation of the corrosion rate increases with time exposure.

3.5.3. Corrosion-enhanced fatigue

In ships and offshore structures the use of coatings is a common means of protection against corrosion, however, these coats have a limited life. In general, the areas of major material loss due to corrosion coincide with those of high stress concentration, e.g. at the toe of welded connections. The formulation proposed in *Article 2* to account for the fatigue-corrosion interaction in terms of an accelerated crack growth rate is to be considered into two ways:

1) The corrosion fatigue phenomenon will be accounted for by introducing a correction factor to the material parameter C, e.g. C_{corr}. This correction factor is equal to 1 before failure of the coating, and greater than 1 after no corrosion protection exists. The crack growth rate under free corrosion conditions may correspond to a factor C_{corr} of around 3, (e.g. DnV, 2001; BS 7910, 1999; Almar-Næss, 1985).

2) The increased fatigue crack growth rate that is due to the corrosion wastage (plate thinning) is induced by an increment of the long-term stress ranges in the corroded plate. A probabilistic model to account for this effect is described in the following.

3.5.4. Probabilistic corrosion model

A basic issue to be taken into account to define a probabilistic model for corrosion is the time of the corrosion protection system to fail, e.g. coating. The life of the coating is the average time the coating system is effectively protecting the structure against corrosion. The time for the coating protection to fail has a large scatter, since it may fluctuate between 5 to 15 years, see e.g. CN 30.7 (DNV, 2001), depending upon the type and quality of the coating. This parameter is properly taken into account in *Article 2*, and treated as a random variable. Once the corrosion protection fails the metal starts to corrode with a certain corrosion wastage rate, which is dependent upon the location within the ship structure and geometry of the component. The effect of pitting/grooving corrosion may be relevant in certain particular cases, but it is not modelled in the formulation discussed in this dissertation.

3.5.5. Plate thinning due to material loss

Assuming a fixed annual thickness reduction rate due to corrosion throughout the service life of a certain component, the long term stress range may be defined as function of a fixed corrosion rate R_{corr}. Considering that the long-term stress range is Weibull distributed, thus a time varying scale parameter A is defined in *Article 2*. Thus, a time-dependent scale parameter is derived as follows (*Article 2*):

$$A(t) = \begin{cases} A_0 & ; \quad for \quad t \le t_0 \\ \gamma A_0 \left[\dfrac{t_0}{t} + \dfrac{\left(kt_0 - kt + 1\right)^{1-m} - 1}{k(m-1)t} \right]^{\frac{1}{m}} & ; \quad for \quad t > t_0 \end{cases} \tag{3.12}$$

where $k=\alpha\ R_{corr}\ /h_0$; here h_0 is the initial value of wall thickness; A_0 is the initial scale parameter i.e. in intact conditions; α is a factor equal to 1 or 2 depending whether the corrosion is one-sided or two-sided, respectively; t_0 is the coating protection time, which is a random variable; γ is a model uncertainty introduced to account for the uncertainty in the global redistribution of stresses due to spatial variation of the corrosion rates throughout the hull structure. This means that the neutral axis of the hull cross section remains insensitive to the spatial variability of the corrosion rates, i.e. the stress level of interest would depend upon an average thickness reduction.

Interaction between fatigue and corrosion is therefore, obtained by applying the time varying scale parameter $A(t)$ from Eq. (3.12) into the safety function defined in Sections 3.2 and 3.3.

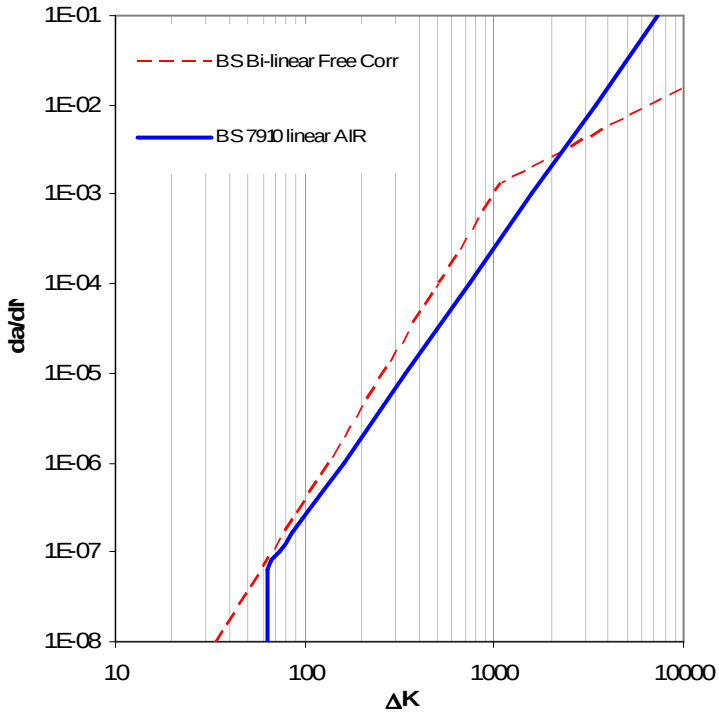

Figure 3.4. Fatigue crack growth rate for steel under free corrosion and under cathodic protection, from data of BS 7910 (1999)

3.5.6. Crack growth rates in corrosive environment

The effect of corrosion on crack growth of welded connection has been referred to as corrosion fatigue in the literature, (see e.g. Almar-Næss, 1985, Kam, 1990), and recently studied in high strength steels in the offshore industry, e.g. Lindley and Rudd (2001), Dover et at (2002). Factors considered in defining SN curve parameters for corrosion fatigue include cathodic protection level, weld profile, corrosive sea water environment, hydrogen embrittlement, etc. The crack growth rate is increased by the effect of corrosion as it is suggested by the BS 7910 (1999), see Figure 3.4.

Under corrosive conditions the initiation period for fatigue cracking is greatly reduced compared to the in-air conditions. Additionally, any possible mechanical improvement to the weld profile is less effective for joints exposed to sea water. Intermittent immersion of specimens on sea water gives approximately the same fatigue life than those under continuous immersion, (Almar-Næss, 1985). The former case could be applied to connections located into a ballast tank of a hull structure.

3.6. Fatigue crack growth in stiffened panels

The fatigue crack growth models discussed so far deal with surface cracks only. The crack growth in a stiffened panel can be roughly divided into four stages, namely: 1) surface crack growth, 2) propagation of through-thickness crack, 3) crack propagation in the stiffener and 4) further propagation in the plate beyond the stiffener. Zhang and Moan (2005) performed analysis of the crack propagation for all these stages by means of finite element models.

Nussbaumer et al (1999) describe similar definition of crack propagation stages based on experiments performed on a cellular box beam, under variable amplitude loading tests.

3.6.1. Residual stress fields

During fabrication of ship structures, residual stresses are introduced in the components, due to cutting, straightening, fitting, welding, etc. Complex welded structures like stiffened panels have rather complicated residual stress fields. Many parameters are involved in the definition of the magnitude and shape of welding-induced residual stresses in typical structural details; they include the local geometry of the detail, welding method and assembly sequence. Fatigue crack growth calculation is based on the so-called stress range approach where the main assumption is that the residual stresses are at yield strength magnitude, implying that the stress range is always applied under tensile stresses. In reality, the residual stresses may be even compressive in some cases, which may lead to a reduction in the crack growth.

According to the Rules for fatigue assessment of ships by DnV (DnV, 2001), the fatigue analysis is based on a reduction in the stress range in order to account for the mean stress effect. The calculated stress range is reduced by a factor f_m depending on whether the mean applied cyclic stresses are tensile or compressive as shown in Figure 3.5.

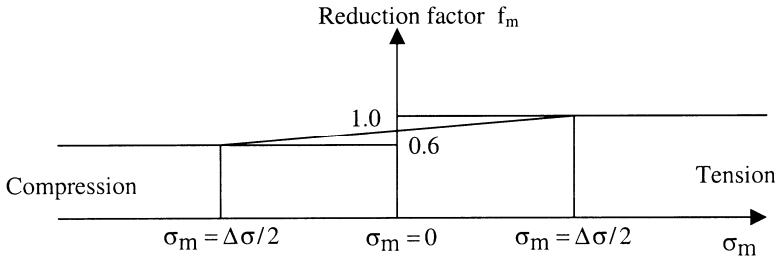

Figure 3.5. Stress range reduction factor for SN-curves (DnV, 2001)

Dexter et al (2000, 2004) carried out fatigue crack propagation tests of through-thickness cracks in stiffened panels with residual stress fields. One of the main conclusions drawn from their study is that stiffened panels are fatigue tolerant to long cracks. Dexter's resulting formulation from the study does not consider the effect of load shedding/redundancy nor does it include the residual stress redistribution as the crack grows.

For a panel with various stiffeners the simplest model of residual stress fields is assumed with a triangular form in the tensile part and a constant compressive stress, as shown in Figure 3.6 (e.g. Faulkner simple model). The width of the tensile region was found to be 7 times the plate thickness based on test results (Dexter and Pilarski, 2000).

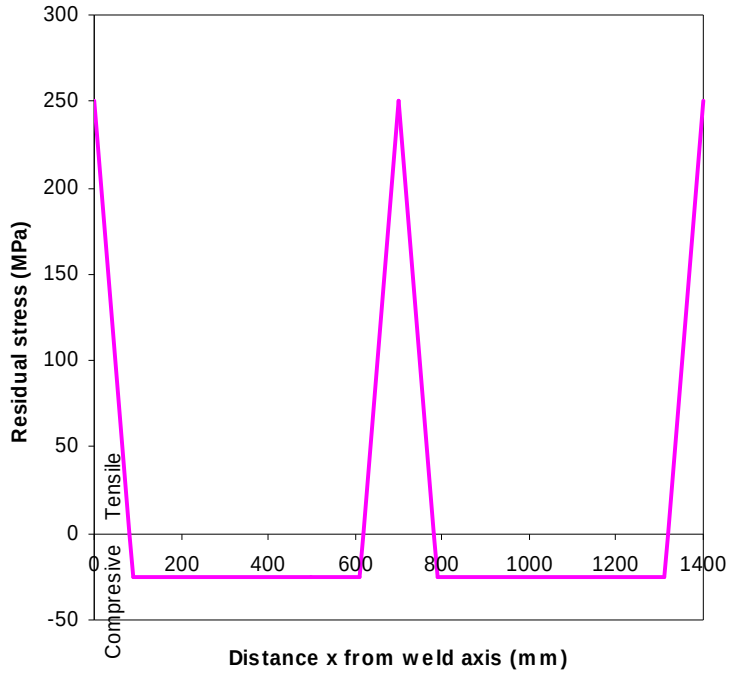

Figure 3.6. Residual stress field due to welded stiffener

On the other hand, it is also known that as the long crack propagates the residual stress field redistributes. Additionally, overloads will induce shakedown effect that tends to remove the peaks of the residual stress fields. These two effects imply that, in principle, a relaxation of the residual stress field will take place during the service life which leads to an overestimation of the fatigue damage if the stress range approach is used.

3.6.2. Crack growth calculation in stiffened panels

In ship structures it is not rare to observe through-thickness cracks since cracks are normally detected by close visual inspection, i.e. when they are already long enough to be seen. Recently, Nussbaumer et al (1999) and Dexter and Pilarski (2000), Dexter et al (2004) have reviewed the crack propagation properties of long cracks in stiffened panels, which is affected by the presence of welded stiffeners, complex residual stress fields and structural redundancy. Their main conclusion is that stiffened panels are fatigue tolerant to long cracks.

So far, propagation of surface cracks has been considered in most of studies related to fatigue cracking, where the main assumption is that the crack growth depends directly on the stress range, regardless of the stress ratio, R. However, for long cracks the effect of mean stress matters, especially in complex structures such as stiffened panels. For instance, a long crack in a stiffened plate propagating perpendicularly to the longitudinal stiffeners, will most likely propagate under compressive residual stress fields in some part of the span between stiffeners. These compressive stresses, depending on the applied stress range level, may lead to crack closure and hence reduced fatigue crack growth. For this reason it is important to explicitly consider the mean stress level in a stiffened panel subjected to cyclic stresses in terms of an effective stress intensity range, ΔK_{eff}.

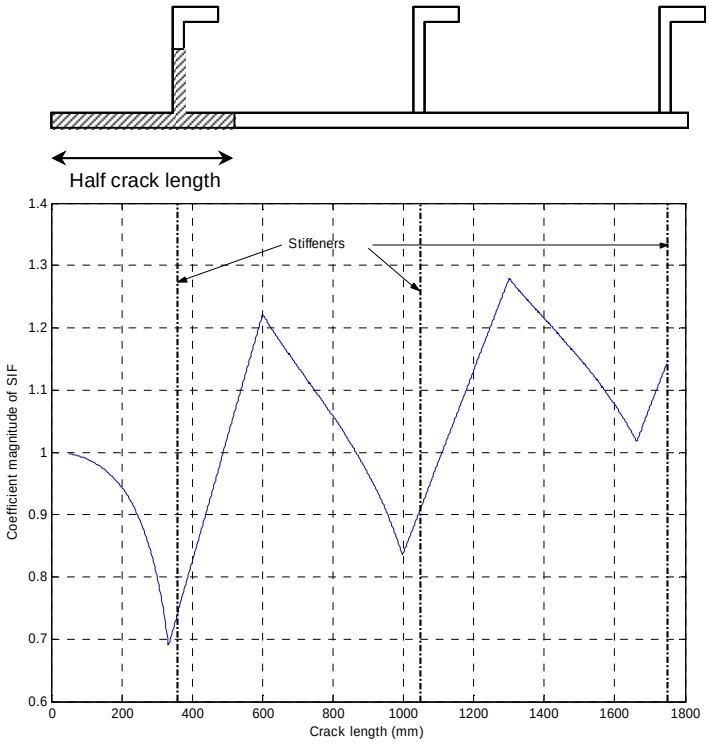

a)

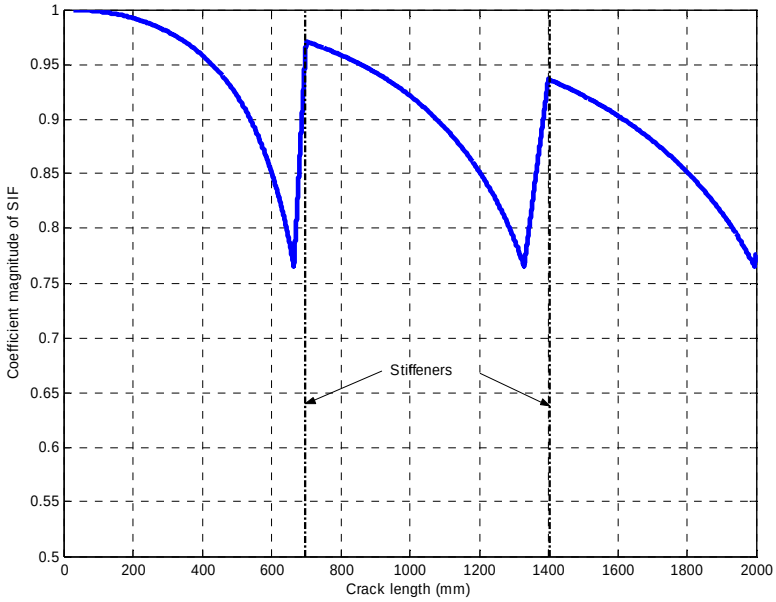

b)

Figure 3.7. Stress intensity factor solution for a stiffened panel with through-thickness cracks, a) initial central crack including stiffener severance and b) initial crack at toe of rat-hole detail with intact stiffeners. In this example, the stiffener spacing is S_{st}=700 mm, plate thickness Th=15mm, stiffeners of size = 250x90x10/15 mm, and A_{st}=3850mm^2

In addition, FPSOs are subjected to continuous load-offloading operation which implies a continuous variation on the still-water (SW) load effects and hence a continuous variation of the mean stress level, i.e. in principle variable amplitude loading approach is necessary to use for computing crack growth under these variable mean stress conditions.

One implication of the use of a variable amplitude loading approach, as employed herein, is that it also requires consideration of adequate values for material parameters C and m which depend upon the stress ratio R. An alternative is to utilize those values of C and m parameters corresponding to a high value of R (e.g. > 0.5) which implies that the full stress range is effective in the fatigue damage. Then, an equivalent stress range is determined (as shown below) where SW-induced stresses and residual stresses are explicitly accounted for.

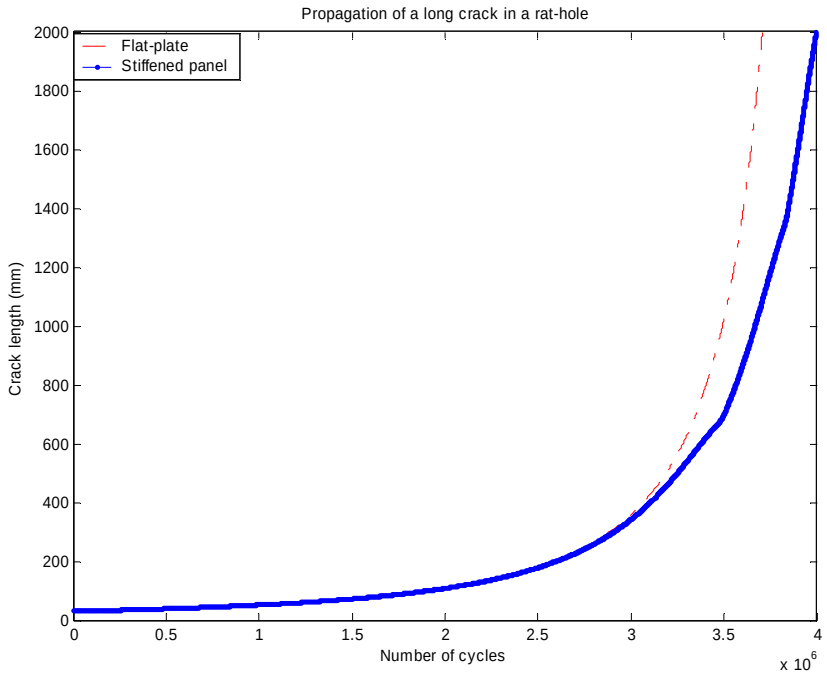

Figure 3.8. Through-thickness crack growth in an infinite flat plate compared to that on a stiffened panel with the correcting functions due to the stiffeners as shown in Figure 3.7.

The applied stress intensity factor (SIF) in a stiffened panel with a symmetric crack located in the center between two stiffeners, as proposed by Dexter and Pilarski (2000), are based on the models initially proposed by Isida (1973). The model and crack growth calculations for the stiffened panel used in *Article 3* of this dissertation are adapted from the analytical solution proposed by Dexter and Pilarski. The model is based on the assumption that a symmetric through-thickness crack in a stiffened panel initiates at a rat-hole detail. It has been found that the presence of the stiffeners on the crack propagation has a limited effect as compared to the case of an infinite plane plate, as long as the stiffeners remain intact. This assumption is non-conservative if the stiffeners begin to crack. The model of Dexter and Pilarski for the effect of stiffener severance seems to be too conservative according to the FE results obtained by Zhang and Moan (2005).

Based on the formulation proposed by Dexter and Pilarski (2000) and by assuming that the stiffener remains intact, the results in Figure 3.8 are obtained. This figure shows the

propagation curves of a long crack in a flat plate in comparison with that predicted in a stiffened plate, whose SIF solution is given by Figure 3.7.

3.6.3. Mean stress effect in crack growth

Crack growth calculation for a stiffened panel of an FPSO is performed with due account of the mean stress level. The residual stresses in combination with the continuously varying still-water loading conditions of the vessel have a crucial effect in the propagation rate of long cracks in stiffened panels. Proper modelling of these effects is therefore decisive in the estimation of failure probability of panels under brittle/ductile facture mode.

The mean level of the imposed cycling loading is known to be determining factor in the crack growth propagation in engineering structures. However, it is well accepted to design welded structures utilizing the so-called stress range approach, in which the maximum stress level is supposed to be high enough, e.g. close to yield strength of the material, to make the whole stress range fully effective in the fatigue damage accumulation.

The stress level induced by the still-water bending moment (SWBM) in both hogging and sagging mode at a certain structural detail, e.g. at bottom plating, represents the mean stress level that serves as reference for the fluctuating stress range induced by the wave effects. In addition, the actual magnitude of residual stress that locally affects a welded joint is combined with the mean stresses due to SWBM. Depending on the location of the structural detail and on the magnitude residual stress, in some cases the wave-induced stress reversals are no fully effective or could even not produce any fatigue damage at all.

The mean stress level induced by the still-water loading, though continuously varying, compared to the wave-induced stress process may be considered as being constant during a certain period of time, i.e. constant mean stress level. Therefore, mean stress level induced by the random still-water loading process consists of a discretization of the stress process into various mean stress levels, which implies that the fatigue damage accumulated in the detail will be different for each SW loading level. The fatigue damage introduced in the structure by the wave-load effects is calculated for each mean stress level defined by each still-water-induced stress level, $\sigma_{SW,i}$, in addition to the residual stress field, σ_{res}, which varies as the crack propagates along the stiffened panel. However, it has to be emphasized that even though the residual stress level varies as the crack grows, it is considered as a constant value compared to the wave induced stresses. Therefore, the i-th mean stress level reads

$$\sigma_{m,i} = f(\sigma_{SW,i}; \sigma_{res}) \tag{3.13}$$

Depending on the magnitude of a given mean stress level $\sigma_{m,i}$, the wave stress reversals may cross the zero-stress level, below of which in principle there is no fatigue damage contribution. Nevertheless, there is a fraction of the remote compressive stress part that still contributes to fatigue damage, herein referred to as σ_{th} or stress threshold. Roughly speaking, this may be explained as follows: when a loading reversal goes below the zero stress level, compressive stresses are exerted at the crack tip front. These compressive stresses relieve the residual (compressive) stresses introduced by the tensile-induced plastic zone at the crack tip, which leads to an accelerating effect of the crack growth; see e.g. Schijve (2001). Hence, the threshold value may vary depending on the magnitude of each stress cycle, but a constant value is considered herein for simplicity. In addition, the plasticity-induced crack closure is disregarded in this model. The effect of the stress threshold in the stress range definition is

schematically represented in Figure 3.9. The threshold needs to be determined by comparison with experimental evidence as discussed in *Article 3*.

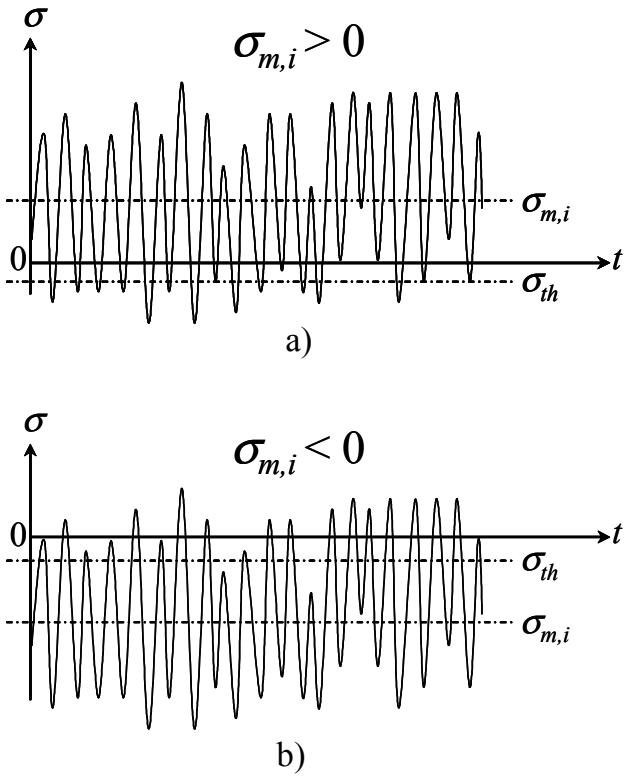

Figure 3.9. Mean stress effect in fatigue

The total fatigue damage is given by the sum of the weighed contribution of each mean stress level *i* implied by Eq. (3.13). Hence, a total equivalent stress range may be determined as the weighed sum of equivalent stress ranges corresponding to each mean stress level *i* defined in Eq. (3.14), namely

$$\overline{S}_{eq}^{m} = \sum_{i=1}^{n} w_i \cdot \overline{S}_{eq,i}^{m} \tag{3.14}$$

where w_i is the weight corresponding to the average time the vessel operates under a given SWL level, i.e. mean stress level $\sigma_{m,i}$. Further details are given in *Article 3*. The equivalent stress range *i* is given by

$$\overline{S}_{eq,i}^{m} = \int_{0}^{2\sigma_{m,i}} s^m f_S(s) ds + \int_{2\sigma_{m,i}}^{\infty} (s/2 + \sigma_{m,i} - \sigma_{th})^m f_S(s) ds \tag{3.15}$$

if $\sigma_{m,i} \geq 0$, and

$$\overline{S}_{eq,i}^{m} = \int_{0}^{\infty} (s/2 + \sigma_{m_i} - \sigma_{th})^{m} f_S(s) ds \tag{3.16}$$

if $\sigma_{m,i} < 0$, see Figure 3.9. Here, s is the wave-induced stress range, $f_s(s)$ is the distribution of the stress range assumed Weibull.

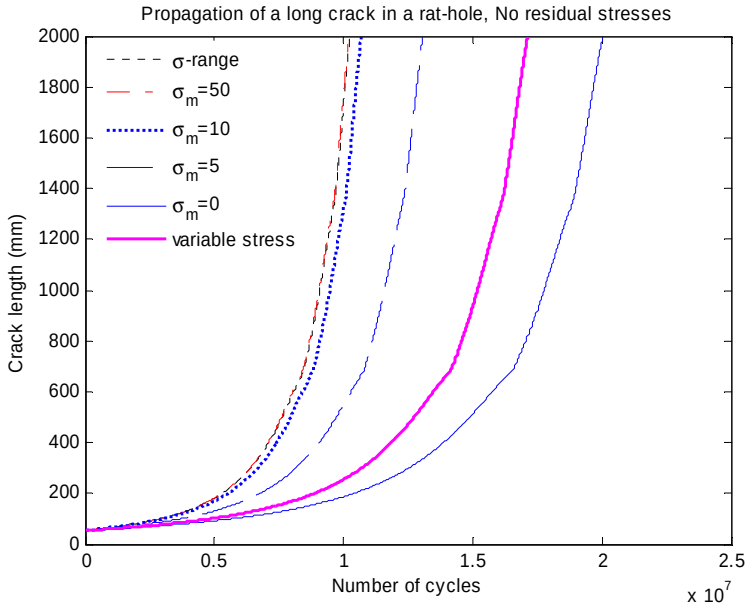

Figure 3.10. Crack growth in a stiffened panel for different mean stress levels.

Figure 3.10 shows the effect of mean stress levels in the crack growth behavior of a stiffened panel with the formulation discussed above (see *Article 3* for details on the assumptions). Various mean stress levels are considered for the crack growth calculation, spanning from σ_m=0 to σ_m=50 MPa, in addition to crack growth calculations made with the full stress range approach. The case "variable stress" is determined with the weighed combination of five mean stress levels, namely =-30, -10, 20, 50, 85 MPa, and considering the weight values indicated in Section 5 of *Article 3*, c.f. Eq. (3.14).

Figure 3.11 depicts the effect of the residual stress field on the crack growth. This figure also shows the crack growth using the stress range approach (s-range) for reference. In this case the residual stress field is considered as not being redistributed as the crack propagates. In reality, the maximum tensile residual stress is also reduced by the shake-down effect besides of the propagation of the crack. This redistribution implies a reduction in the magnitude of the compressive stresses for the section to keep equilibrium. It is therefore non-conservative to utilize a fixed residual compressive stress field.

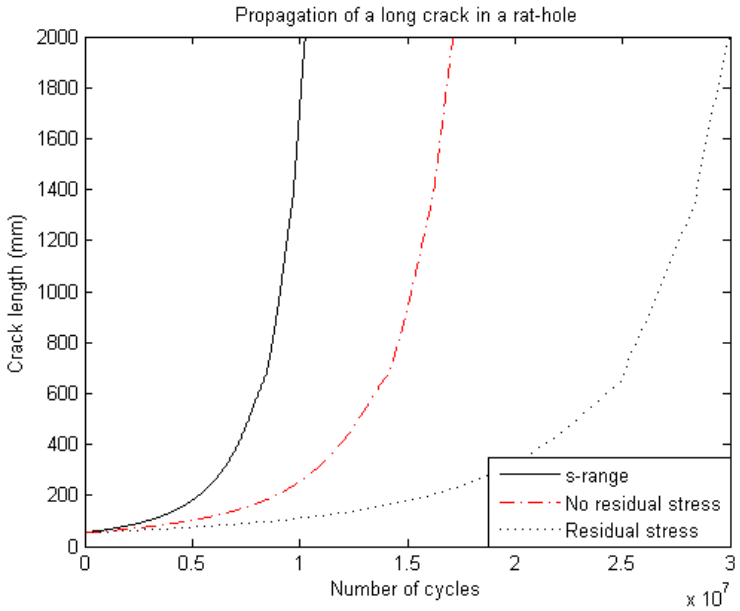

Figure 3.11. Long crack propagation in a stiffened panel, considering residual stresses and mean stress effect.

CHAPTER 4

Fatigue reliability of FPSO hull structures

4.1. Overview of crack control in ship-shaped offshore structures

Ship-shaped production vessels have a series of operational features that make them different from other offshore facilities and hence, make crack control particularly challenging. One of the fundamental differences between design practices of the shipping and offshore industries concerned with the fact that ships are dry-docked periodically, e.g. every fifth year, whereas offshore structures are often designed to operate permanently for a period of twenty years. In this connection it is worth mentioning that most of ship-shaped production vessels currently under operation are based on tanker conversions, which in many cases imply the utilization of existing ships originally designed to fulfil requirements of merchant vessels, to be installed as offshore structures in either benign or harsh conditions. Moreover, FPSO units cannot avoid heavy weather conditions whereas merchant tankers are in principle able to do it. Merchant ships are exposed to wave-induced resistance due to forward speed, while FPSOs are stationary. Another operational difference is given by the still-water loading which is a time-varying process for offshore ships.

The storage capability of FPSOs introduces an additional source of uncertainty to be accounted for with respect to the global and local load effects. The continuous load-offloading process on the vessel implies that still-water loading, which is also a human-dependent process, varies randomly in time. The time-variant cargo filling level and its spatial distribution along the vessel have a direct implication in the ultimate capacity and fatigue damage accumulation. In contrast, on-going tankers are exposed primarily to only two still-water loading conditions, namely: laden and ballast.

Crack control in offshore structures has been based on experiences initiated and developed in the aircraft industry regarding crack growth analysis under a structural reliability

framework. The main aim has been to optimize the amount of costly underwater inspection of tubular joints on jacket platforms, see e.g. Dover et al (1995). Underwater non-destructive techniques (NDT) have been developed specifically for offshore applications. Techniques such as Alternate Current Potential Drop (ACPD) or Alternate Current Field Measurement (ACFM) are now commonly used in the industry. These NDTs provide high probability values of detection and sizing, see Visser et al (1996) and Visser (2000). In the shipping industry the use of reliability methods for design and assessment was introduced more recently, e.g. Mansour (1997). Optimal in-service inspection and maintenance scheduling in terms of the best balance between cost and safety level in offshore structures has always been an aim among operators.

The shipping industry has a different approach in the treatment of crack control of hull structures. It is assumed that a major part of the cracks will never have the potential to threaten the integrity of the vessel. Nonetheless, crack phenomena in ship structures have always been an important concern for regulators and operators all over the world in terms of maintenance costs, and efforts have been devoted in order to keep cracking problem as low as possible. According to Sucharski (1997), the spatial distribution of cracks in typical tankers obtained from more the 60 ship years of service, indicates that the largest incidence of cracks is observed in the midship region and close to the bottom plate and in the side shell longitudinals. Cracks in secondary structural elements are usually regarded as less severe than cracks in the shell plating, as long as there is no immediate risk for the crack to grow into the primary structure.

The consequences of failure are significantly larger for FPSOs than for merchant ships. One day of lost production will generally be far more expensive than one day of delayed departure for a merchant ship. Moreover, FPSOs cannot easily be dry-docked as it is periodically done for an on-going ship. Similarly, economical consequences in case of total loss are much larger for the case of an FPSO. According to actual experiences with FPSOs operated on the Norwegian Continental shelf there have been occurrences of internal cracks between tanks which were detected through minor leaks. No leakage has occurred outside the hull in the three FPSOs where these cracks have appeared (OLF, 2002). In each case a program of inspection and repair has been initiated. This involves taking the affected tanks and adjacent tanks out of service, making a manned entry and after cleaning, fitting appropriate stiffeners. This is a clear example of undesirable situations which, although for a trading tanker may represent routine repair activities, for FPSO operators it results in extremely costly and operationally impractical offshore repairs. Further, this kind of leaks from cargo tanks may represent a hazardous accumulation of hydrocarbons gases in ballast tanks that could lead to catastrophic consequences. This also indicates that conventional hull design and basic fatigue analysis has been unable to eliminate FPSO hull cracking in service.

Aging offshore structures are not just exposed to fatigue cracking deterioration, but also to corrosion. Corrosion damage is not considered as a design criterion, even though its undesirable presence in offshore and ship structures increases the likelihood of occurrence of other failure modes, such as fatigue, e.g. Guedes Soares and Garbatov (1998a), Akpan et al (2002), Paik et al (2003b), Moan et al (2004b). This chapter deals with the reliability-based models for fatigue as well as its interaction with corrosion phenomena, i.e. corrosion-induced fatigue crack propagation. As subsequently discussed, the presence of corrosion in a marine structure increases the crack growth rate in two manners. Firstly, the material loss provoked by the effect of corrosion induces consequently a stress increase in the remaining material, and secondly, the corrosive environment increases the crack growth rate once the corrosion protection system fails.

4.2. Reliability updating through inspection of cracks

4.2.1. Basic formulations

The updating methodology is useful in connection with extension of service life for structures with joints governed by the fatigue criterion. In such cases, the design fatigue life is in principle exhausted at the end of the planned service life. However, if no cracks have been detected during inspections, a remaining fatigue life can be demonstrated. Nevertheless, it is not possible to bring the structure back to its initial condition by inspection only, then repairs are needed.

The margin event $M(t)$ as defined in Sections 3.2 and 3.3 for evaluating failure probability in fatigue of joint i is updated based on the definition of conditional probability as

$$P_{f_i,UP} = P\left[\left(M(t) \le 0\right) \middle| IE_j\right] = \frac{P\left[\left(M(t) \le 0\right) \cap IE_j\right]}{P\left[IE_j\right]} \tag{4.1}$$

where the inspection event IE may represent either *"no crack detection"* or *"crack detection"*. The inspection event for *no crack detection* at time T_j, is in general defined as (e.g Madsen et al, 1986)

$$\begin{aligned} &I_{ND}(T_j) = a_D - a(T_j) > 0 \\ &or \\ &I_{ND}(T_j) = \int_{a_0}^{a_D} \frac{da}{\left[Y(a)\sqrt{\pi a}\right]^m \cdot G(a)} - C \cdot A^m \Gamma\left(\frac{1}{B}+1\right) v_0 \cdot T_j > 0 \end{aligned} \tag{4.2}$$

The distribution function of the detectable crack size aD is equal to the probability of *detection* (POD) curve, as discussed below. For the linear FM model the inspection event $I_{ND}(t)$ is equivalent to the failure function defined in Eq. (3.5) where the upper limit of the integral is substituted by a_D. Similarly, for the bi-linear FM model, the event $I_{ND}(t)$ is equivalent to Eq. (3.10) substituting the upper limit of the integral by a_D as well. If several inspections are carried out, the random variables a_D are mutually independent. The inspection event of *crack detection* is complementary to that expressed in Eq. (4.2), i.e. $I_D(T_j) = a_D - a(T_j) < 0$. If the detected crack is measured at inspection T_j the inspection event margin reads as an equality of Eq. (4.2), i.e. $I_{MS}(T_j) = a_m - a(T_j) = 0$, where a_m is a random variable representing uncertainties inherent to the crack measurement, e.g. Madsen et al (1986).

The safety margin of a joint may be updated when n inspection events are considered, e.g. *no detection* I_{ND}, *detection,* I_D and crack *measured* I_{MS} event margins., as follows

$$P_{f,UP} = P\left(M(t) \le 0 \mid I_{ND,1} > 0 \cap I_{ND,2} > 0 \cap \cdots \cap I_{D,j} \le 0 \cap I_{MS,k} = 0\right) \tag{4.3}$$

As the number of inspection outcomes increases, the calculation of Eq. (4.3) becomes more difficult to perform. However, conservatively only the last inspection result may be

considered if the previous inspection outcome history is no detection, see e.g. Ayala-Uraga and Moan (2002).

The bi-linear model represents a challenge, as discussed in *Article 1*, to calculate updated reliabilities to account for inspection results. This is due to the difficulty of evaluating the intersection of the non-linear event margins, i.e. failure function and inspection event. The use of either FORM or SORM gives non-conservative results as compared to the results from Monte Carlo simulation. The latter is carried out by mean of axis-orthogonal simulation, which is an improved importance sampling technique, (DNV, 1996).

4.2.2. Quality of inspection of cracks (POD)

Periodic updating of the fatigue reliability level of a connection in a vessel depends upon how likely is that a crack is detected during an inspection. Much effort has been devoted in different industries to evaluate the quality of Non-Destructive Techniques (NDT) for inspection of cracks in metals. The likelihood that a crack is detected is expressed by the probability of detection (POD) curve corresponding to every NDT used. POD curves for various applications of NDT obtained from different industrial projects have been compiled by Visser (2000). Fujimoto et al (1996; 1997) show POD curves for Close Visual Inspection (CVI) of ships (cf. Table 4.1). This procedure is commonly used as initial inspection procedure, followed by an NDT inspection in areas more prone to cracking.

Table 4.1. Mean detectable crack size through visual inspection (within 0.5m distance) on trading vessels, depending upon access to crack site (Fujimoto et al, 1996; 1997)

Access	Length	Depth (based on a/c=0.2)	Depth (based on a/c=0.83)
Easy	40 mm	4 mm	16.6 mm
Moderate	70 mm	7 mm	29.1 mm*
Difficult	100 mm	10 mm	41.5 mm*

* Normally through-thickness crack

4.2.3. Reliability updating as a function of the FDF

The likelihood that a crack is detected is expressed by the probability of detection (POD) curve corresponding to every NDT used. The reliability level of a welded joint may be updated based on inspection results. Two different inspection methods are assumed here, namely Close Visual Inspection (CVI) and Non-destructive techniques (NDT). Their effect on updated reliabilities are studied for two stress levels determined as function of the Fatigue Design Factor (FDF), i.e. FDF=1 and FDF=10. Based on POD curves defined by Fujimoto et al (1996) for Close Visual Inspection on ships the POD assumed herein is exponentially distributed with mean value of 16.6 mm, (see Table 4.1). For the NDT used in the present calculation, a POD exponentially distributed with mean value of 2.0 mm is assumed.

Figure 4.1 shows the effect of FDF on updating on a T-butt joint applying two different inspection methods, i.e. two POD curves. Two inspections are performed at T=10 and 20 years with no crack found. It is observed that at high stress levels (FDF=1.0) there is still a

considerable gain in reliability even when applying close visual inspection, if no crack is found. That data for the calculations is found in *Article 1*.

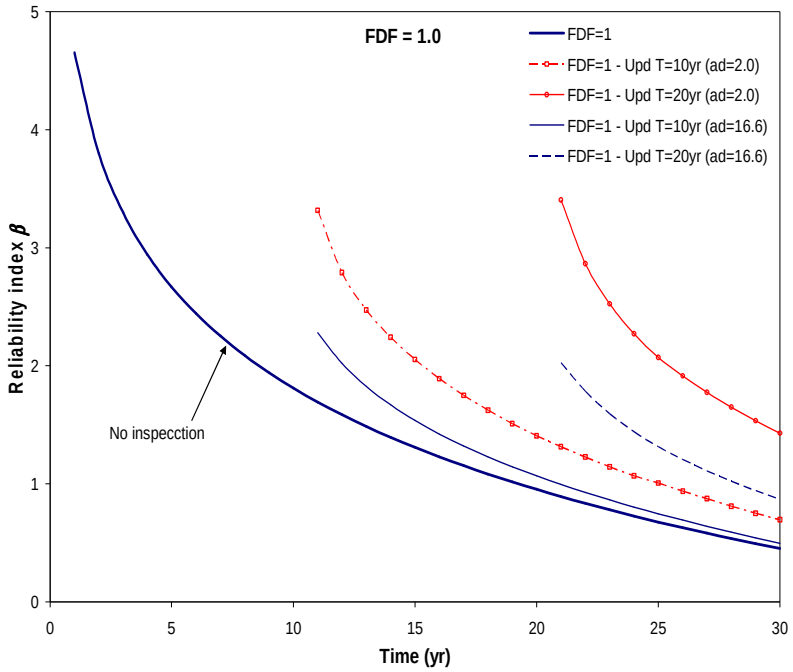

a)

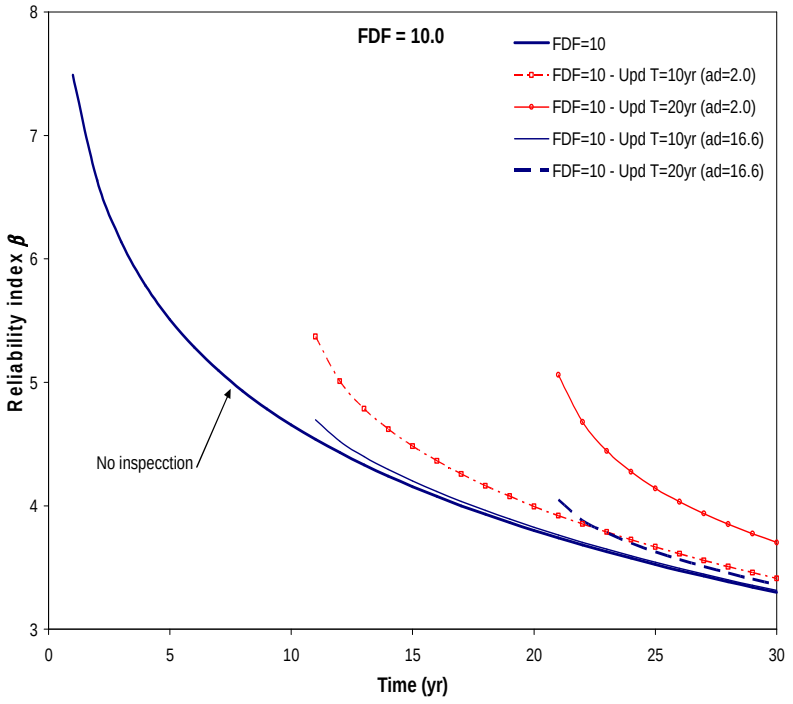

b)

Figure 4.1. Reliability index for a T-butt welded joint design, considering two different inspection qualities and no crack detection, performed at T=10yr and T=20yr: a) FDF=1.0; b) FDF=10.0

4.3. Fatigue reliability in sequentially different environments

A reliability measure of the fatigue damage in welded connections of FPSOs that have formerly sailed as merchant ships is presented in *Article 2*. The reliability model accounts for the fact that the FPSO may be subjected to two different environmental conditions during its service life. The cumulative fatigue damage is accordingly divided into two stages. Interacting model for fatigue crack growth and corrosion as described above is also included in the formulation. The fatigue crack growth in a plated joint being initially subjected to environmental conditions *j*, and then moved to a different location with climate conditions *k*, i.e. $a_{j\to k}$, may be expressed by the following safety margin (*Article 2*),

$$M_{j\to k}(t) = \int_{a_0}^{a_f} \frac{da}{\left[Y(a)\cdot\sqrt{a\pi}\right]^m} - C\cdot v_{0,j}\cdot A_j^m\cdot\Gamma(1+m/B_j)T_{change} - C\cdot v_{0,k}\cdot A_k^m\cdot\Gamma(1+m/B_k)(t-T_{change})\le 0 \tag{4.4}$$

Eq. (4.4) is valid for $t > T_{change}$. The derivation of this expression is described in *Article 2* (see Appendix A). In general, Eq. (4.4) may be expressed for a welded joint subjected to *n* sequentially different climate conditions as (*Article 2*),

$$M_{j\to k}(t) = \int_{a_0}^{a_f} \frac{da}{\left[Y(a)\cdot\sqrt{a\pi}\right]^m} - C\cdot v_{0,j}\cdot A_j^m\cdot\Gamma(1+m/B_j)T_{change(j)} - C\cdot v_{0,k}\cdot A_k^m\cdot\Gamma(1+m/B_k)(t-T_{change(j)}) - \cdots \cdots - C\cdot v_{0,n}\cdot A_n^m\cdot\Gamma(1+m/B_n)(t-T_{change(n-1)})\le 0 \tag{4.5}$$

where $T_{change(i)}$ is the time the vessel is moved from climate *i* to a different location.

The probability of failure of a component in fatigue for $t > T_{change(i)}$ is

$$P_f = P\left[M_{j\to k}(t)\le 0\right] \tag{4.6}$$

Figure 4.2 shows a comparison between the cumulative failure probability and annual hazard rate for both harsh-to-benign and benign-to-harsh cases. It might be observed that both cases converge to the same cumulative failure probability after 20 years of service. This coincidence is due to the cumulative nature of fatigue damage and to the fact that the vessel, for both cases, is subjected to the two different climates during the same period of time for, i.e. 10 years in harsh and 10 years in benign climate, and vice versa. This is also a proof of correctness of the formulation. On the other hand, the annual hazard rate behaves differently. After 20 years, the benign–harsh case shows larger annual failure probability than that of harsh–benign. It is also observed that the latter shows a remarkable drop in annual failure rate once the vessel is moved from harsh to benign conditions, whereas the benign-harsh curve does not present a sudden jump but a smooth change on annual failure rate. The curves of both cumulative and annual failure probabilities for the case the vessel operates 20 years under harsh conditions only (harsh–harsh) are also shown for reference.

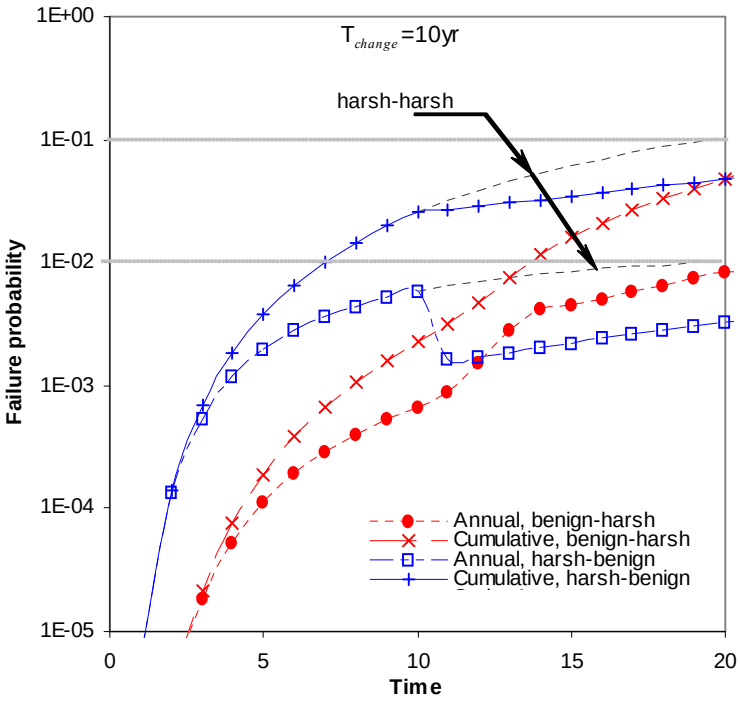

Figure 4.2. Cumulative failure probability vs. annual hazard rate

4.4. Reliability updating with inspection in sequentially different environments

Updating of reliability after inspections carried out in a production ship operating in sequentially different environments may be formulated as follows. Let the FPS be initially designed and installed in environment j, e.g. North Sea, and after some time being moved to climate k, e.g. Gulf of Mexico. Then, the inspection events with No detection, carried out at time t could be expressed as

$$I_{ND}(t): \quad a_D - a_j > 0 \qquad \text{for} \quad t < T_{change} \tag{4.7}$$

If an inspection is carried out with *No crack detection* after the vessel has been moved to a different location, i.e. time $t > T_{change}$, the inspection event is defined as

$$I_{ND}(t): \quad a_D - a_{j\to k} > 0 \tag{4.8}$$

where a_D is the minimum detectable crack size and it is regarded as a random variable whose distribution function is equal POD curve.

The inspection events performed at time t < T_{change} (climate *j*) have been discussed in Chapter 3. The inspection event with *no crack detection*, carried out at time t > T_{change}, (climate *k* conditions) i.e. after the vessel has been moved (*j*→*k*), may be expressed analogously to the safety margin given in Eq. (4.4), namely

$$I_{ND,j\to k}(t)=\int_{a_0}^{a_D}\frac{da}{Y(a)^m\left(\pi a\right)^{m/2}}-C\cdot v_{0_j}\,A_j^{\,m}\cdot\Gamma\left(1+\frac{m}{B_j}\right)T_{change} \\ -C\cdot v_{0_k}\,A_k^{\,m}\cdot\Gamma\left(1+\frac{m}{B_k}\right)\left(t-T_{change}\right)>0 \tag{4.9}$$

This event is positive since it implies that the crack size developed up to time T_{insp} is smaller than the detectable crack size a_D, which is a random variable, and $T_{insp}>T_{change}$. The inspection event of *crack detection* is negative, namely $I_{D,j\to k}(T_j)=a_D-a(T_j)<0$. The updated failure probability for a joint with inspections performed either before or after T_{change} is given by

$$P_{f,UPD}=\begin{cases}P\left[M_j(t)\le 0\middle|I_{ND}(t)>0\right]; & for \quad t<T_{change}\\ P\left[M_{j\to k}(t)\le 0\middle|I_{ND,j\to k}(t)>0\right]; & for \quad t>T_{change}\end{cases} \tag{4.10}$$

The safety margins in Eq. (4.10) are given by Eqs. (3.5) and (4.4), respectively.

4.4.1. Reliability updating with two inspection events

Article 2 describes a reliability updating formulation considering 2 inspections events performed simultaneously: inspection of crack and thickness measurement.

The failure probabilities of the formulation presented in *Article 2* are calculated by means of second-order reliability method, SORM, which showed to be more appropriate for the reliability model presented herein. The use of FORM may give non-conservative results for values of $t>T_{change}$. The calculations using SORM showed a better agreement with those obtained by means of axis orthogonal simulation. Details are given in *Article 2*.

4.4.2. Effect of inspection quality

In this section an NDT, such as magnetic particle inspection (MPI) or eddy current technique is compared to a close visual inspection (CVI) procedure. The POD curves for NDT and CVI are assumed to be exponential distributions with mean detectable crack size values of 2.0 and 16.6 mm, respectively. The sensitivity study showed that the updating effect is larger when the vessel has initially been exposed to harsh environment and then benign environment, with an inspection with no crack detected at T=15 years. This feature is illustrated in Figure 4.3.

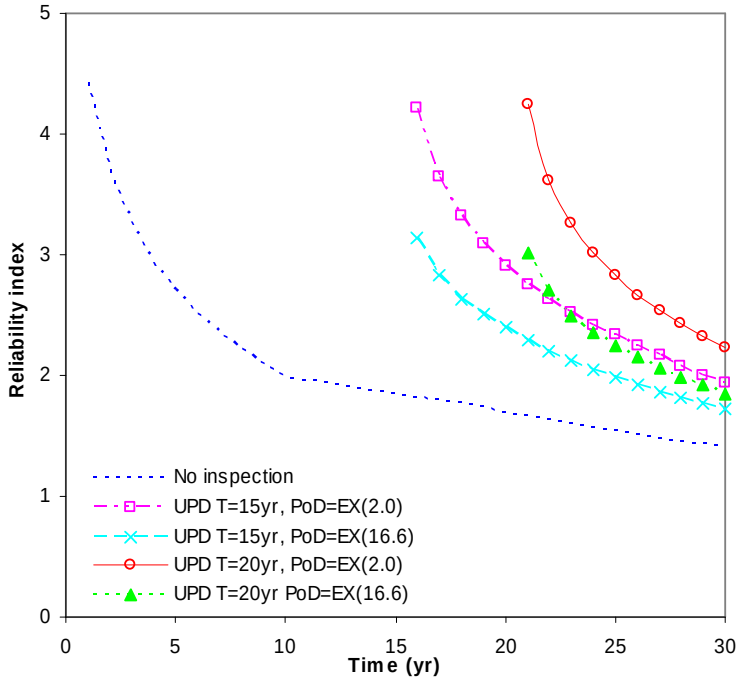

Figure 4.3. Sensitivity of updated reliability to the quality of inspection with no crack found, for a vessel operating 10 years in a harsh environment, then in benign conditions.

4.4.3. Effect of plate thickness reduction due to corrosion

The results shown in Figure 4.4, *harsh to benign*, show the effect of crack growth and corrosion-induced plate thinning on the fatigue reliability. It is assumed that the vessel operates in two different environment conditions: 10 years in a harsh environment and 10 years in benign climate. The reliability is updated by inspection after 20 years and it is assumed that no crack is detected. When the coating effect is considered, the time of coating failure T_0 is assumed as normally distributed with mean of 5 years and CoV=0.5. For the purpose of the sensitivity study, the corrosion fatigue effect is not accounted for, i.e. material parameters C and m are not modified after the coating system fails. The increasing effect on the stress range due to corrosion-induced thickness loss is accounted as formulated *Article 2*. From Figure 4.4 it may be observed that for the case of the structure under initially *harsh* conditions and then moved to more *benign* climate, there is a remarkable effect of updating. Figure 4.4 also shows the sensitivity of the corrosion rate R_{corr}.

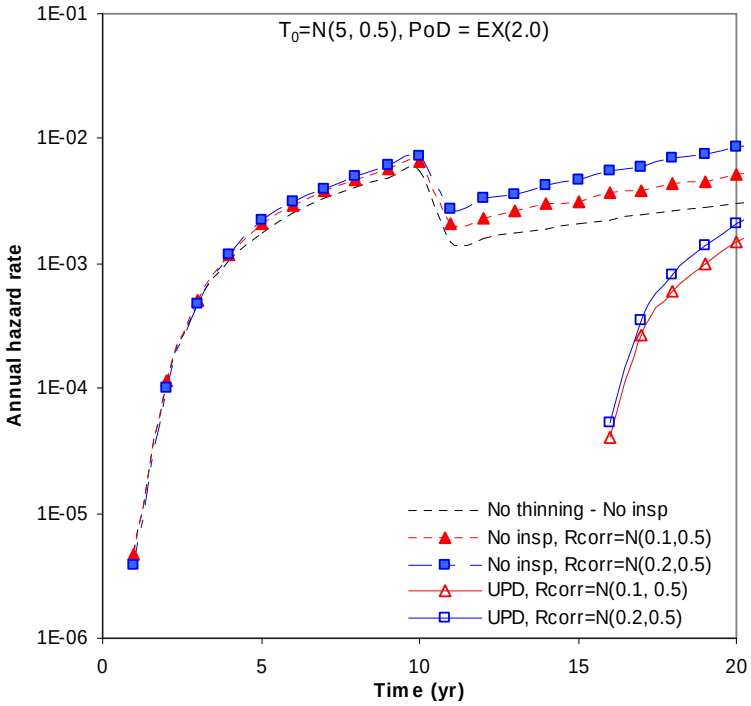

a) Annual hazard rate

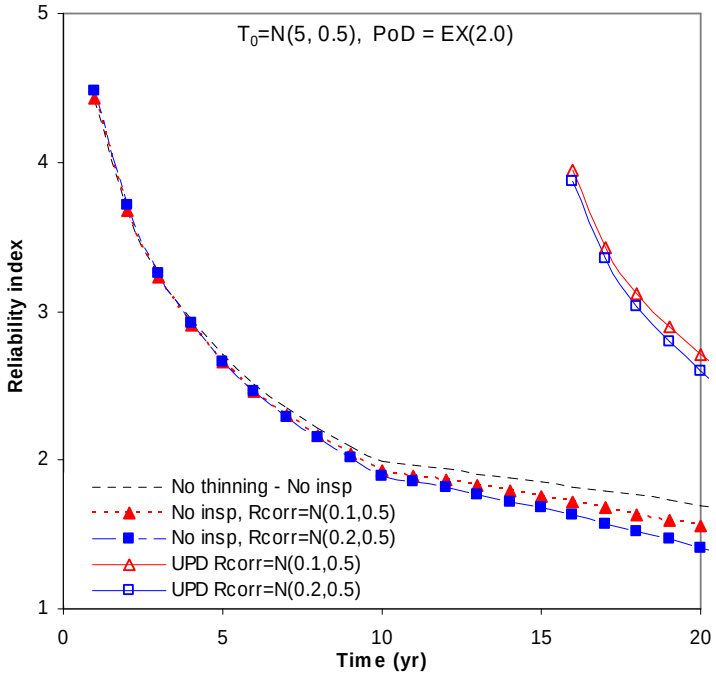

b) Reliability index

Figure 4.4. Sensitivity of updated fatigue reliability to the corrosion rate, 10 years in harsh environmental conditions, then benign. Updating after T=20yr, no crack found. The time of coating failure T0 is assumed as normally distributed with mean 5 years and COV=0.5.

CHAPTER 5

Reliability assessment of fatigue-induced fracture

5.1. General

First passage problems in structural reliability analysis are, in most of the cases, rather complex and computationally expensive. Nevertheless, the use of time-variant reliability methods to estimate the probability of overload failure of deteriorating structures is getting more commonly used. Application of such methods is especially relevant for structures that need to be used beyond their initially intended service life.

As shown in the previous chapters, fatigue reliability problems are successfully treated with time-invariant techniques, by randomizing the parameters involved in the model, which are based on linear elastic fracture mechanics principles. On the other hand, fracture of fatigue-cracked structural components may occur either as ductile, brittle or a combination of both failure modes. Assessment of flawed components in fracture failure mode is recommended by using elastic-plastic principles, e.g. BS7910 (1999). Failure probabilities for ductile/brittle fracture of structural components may also be obtained with time-invariant reliability methods. Fatigue-induced fracture in offshore structures and ships require the use of a coupled model to account for the interaction between fatigue crack growth random process and an eventual overload failure in fracture of the fatigue-cracked structural component. Furthermore, the accelerating effect of corrosion on fatigue may also be accounted for. In principle, time-variant approaches are needed to properly account for the time-dependent strength deterioration and its variability, which is also time dependent.

During the last decades, few researchers have studied the reliability of fracture-fatigue coupled phenomena. Karamchandani et al (1992) and Dalane (1993) proposed a time-

invariant reliability method to be applied to complex structural systems integrated by tubular components, where the effects of fatigue degradation are considered in determining the most probable failure mechanism or failure path. The failure criterion of a through-thickness cracked tubular joint is based on a ductile fracture criterion of the ligament. Marley (1991) and Marley and Moan (1992) proposed a time-invariant approach validated with a time-variant method using Monte Carlo simulation. Their methodology is intended for assessing the overload reliability of a fatigue-cracked tubular joint of an offshore structure subjected to extreme wave loading, based on a long-term approach. Beck and Melchers (2004a) utilize a random process approach to describe the crack growth deterioration to calculate time-variant failure probability of overload fracture of a centre-cracked stiffened panel.

5.2. Ultimate hull failure assessment

For FPSOs wave-induced load effects are site-specific and still-water load effects are given by the continuous loading-offloading of crude oil production. The stochastic combination of both (wave and still-water) global load effects on the hull girder has a direct implication in the fatigue and overload failure modes which are to be handled differently to that of on-going ships.

Overall system safety of the vessel during the service life, in terms of hull girder ultimate strength, is of main concern with respect to loss of lives, economical and environmental consequences. Different overall failure modes of the hull girder are identified, including fracture failure, which may occur as either "brittle" or ductile fracture or a combination of both. Ductile failure on hull structures has been accounted for by some researchers to evaluate safety levels of hull girder ultimate strength on merchant ships, e.g. Paik et al (2003b), Guedes and Garbatov (1999), Amlashi and Moan (2008), Mansour et al (1997). Such studies determine hull girder safety in terms of likelihood of buckling collapse or tensile rupture of the net cross section reduced by the presence of fatigue cracks, considering as well the material loss due to corrosion. No interaction effect between fatigue cracking and corrosion is considered in these references.

Very often in ships, cracks are detected with close visual inspection when they are already through-thickness cracks, usually with detectable crack size larger than 100mm in length, depending upon accessibility and location of the structural detail. In relevant areas through-thickness cracks may be detected by leak. Depending on the size and location/ease of repair, it takes some time before they are repaired. There is evidence of very long cracks found in trading tankers, e.g. over 1 m long as reported by Bjørheim et al (2004). On the other hand, some studies suggest that in general stiffened panels, and therefore hull girder structures, are fatigue tolerant to long cracks due to the presence of stiffeners, complex residual stress fields and structural redundancy, e.g. Nussbaumer et al (1999). However, as the size and number of cracks increase, the likelihood of ductile and brittle fracture of the hull section under overload conditions increases when subjected to extreme conditions, mainly due to the existing correlation in location and loading, among the different structural components (stiffened panels) of an amidships cross section.

Adequate safety of an FPSO is guaranteed throughout the service life by appropriate design and operational measures, including periodical in-service inspection, maintenance and repair (IMR) activities necessary in the different parts of the vessel. Safety management of an FPSO is a particularly challenging task considering the various implications on the operation of a ship as a production-storage offshore structure. IMR activities required to keep a certain safety level throughout the service life of the vessel have to be performed in-situ since it may

result impractical and costly to deploy a permanent production ship to a dry dock to periodically perform such tasks. This means that if, for instance, an abnormal through-thickness crack develops in the bottom plating (i.e. leakage) it will take some time until the repair takes place. Then, the safety of the vessel under such conditions needs to be assessed. In this context, reliability-based approaches are useful tools for the decision making process during the operation of a vessel that enables to optimize the balance between safety and cost.

The aim of this chapter is to highlight the main aspects related to the safety assessment of an aging FPSO hull girder with the presence of an abnormal long crack, by applying an efficient time-variant reliability formulation, which is presented in *Article 3* of this dissertation. The probability of brittle fracture of a stiffened panel on the hull girder with a randomly propagating through-thickness crack is evaluated by taking explicit account of both wave loading and mean stress level of still-water (SW) loading.

In order to evaluate the time-variant overload failure probability of a stiffened panel with the presence of long cracks, it is necessary to solve the first passage problem of a scalar stochastic process (loading process) through a time-variant resistance threshold. For simplicity it is often assumed that the resistance degradation as function of time is regarded as deterministic values on the parameters involved, but in reality resistance degradation is of random nature in time. Further simplification is to consider the different deteriorating phenomena, such as fatigue and corrosion, to develop independently from each other throughout the service life of the structure. This assumption is no longer valid for aging infrastructure as fatigue damage is enhanced by the presence of corrosion.

When the resistance of a structure is treated as a random phenomenon in time, which is the case on deteriorating infrastructure, the resistance degradation may be defined in time in two ways: 1) by means of a degradation function and a vector of random parameters (random variable approach), or 2) by means of transition probability density functions, i.e. changing with time, which is called random process approach. The implications of both cases are that the former is perfectly correlated in time, whereas for the latter the random variables are not perfectly correlated (Beck and Melchers, 2004a). In general, the two different approaches may be used for estimating time-variant reliability of a deteriorating structure. The former is used in the annexed *Article 3* (Ayala-Uraga and Moan, 2007b).

5.3. Fracture failure criterion

5.3.1. Methods to assess fracture

Fracture strength of ships is traditionally based on Charpy methodology. More sophisticated assessments can be performed by means of FAD, (fracture assessment diagram), or the JQM-approach (e.g. Andersen, 1991). The first method is established as an industrial standard through BS7910. Several other methods are available, but these methods are not widely applied, and they are more on a research level.

5.3.2. Charpy testing

The Charpy testing was introduced in the first part of the last century, but did not become industrial standard before after the Second World War. The adoption of the Charpy testing procedure, as industrial practice, significantly improved the statistics on lost ships.

The idea of the test is that the energy it takes to build a crack, tells something about the material's ductility and toughness towards fracture. A V-notched test specimen with a cross-

section of 10 by 10 mm is clamped in a Charpy impact test machine. A pendulum, with certain velocity energy, hits the specimen. The energy-loss due to the fracture of the specimen is registered and checked towards acceptance criteria. The method could be said to be qualitative rather than quantitative, in the way that test results can be applied for ranking purposes, and check towards artificial acceptance criteria. Results from Charpy testing can however not be directly applied for damage evaluation, to decide if a certain crack is stable or not.

The development of materials and weld materials has, however, proceeded since the Charpy method first was introduced. The materials that the method originally was developed for are not available any longer. Current materials are far tougher, much stronger and more ductile. In addition other material-toughness parameters, such as CTOD and the J integral, have been introduced.

5.3.3. Master curve approach

The master curve approach (BS 7910, 1999) is a methodology based on data of Charpy V-notch test specimens correlated fracture toughness data on ferritic materials. This correlation of fracture toughness data accounts for thickness effects as well as the scatter and probability level. This correlation is well validated between the 27J Charpy transition temperature and the 3160 N/mm$^{3/2}$ (100 MPa$\sqrt{m}$) fracture toughness transition temperature, namely:

$$T_{100\ MPa\sqrt{m}} = T_{27\ J} - 18^{o}C\ (\pm 21^{o}C) \tag{5.1}$$

According to the BS 7910 (1999) the fracture toughness transition curve for brittle fracture is approximates the master curve given by:

$$K_{mat} = 630+[350 + 2435\ \exp\{0.019(T - T_{27\ J} - 3)\}]\ (25/B)^{1/4}\ [\ln\{1/(1 - P_f)\}]^{1/4} \tag{5.2}$$

where the fracture toughness is given in N/mm$^{3/2}$; T is the temperature in ^{o}C at which K_{mat} is to be determined; $T_{27\ J}$ is the 27 J Charpy transition temperature (^{o}C); B is the thickness of the material in mm; P_f is the probability exceedance corresponding to the data.

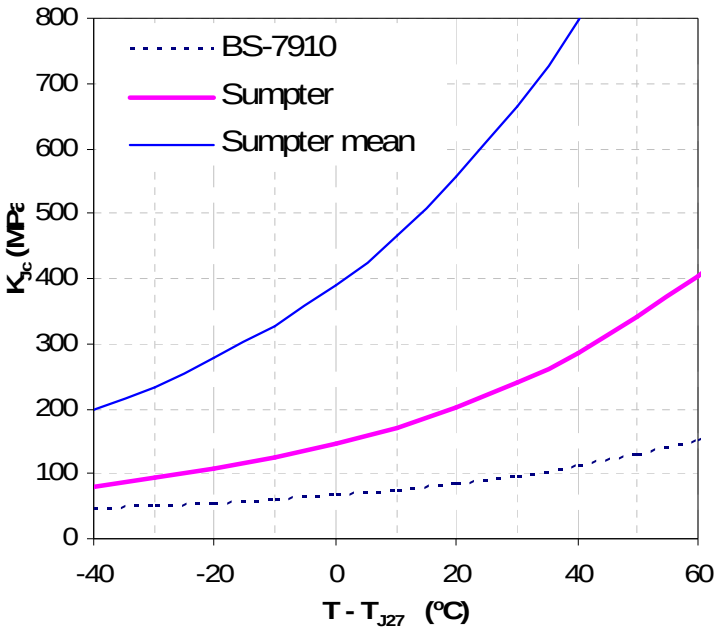

Figure 5.1. Comparison of master curves by BS 7910 and Sumpter's fitted model

Kent and Sumpter (2004), based on an extensive database, fitted a curve based on test carried out on mild steel that resulted in the following mean toughness line. A Weibull distribution is used to fit the variability in toughness with temperature and the 1% probability level is assumed to be adequate for plates up to 15 mm in thickness with through cracks, i.e. plane stress. This curve is utilized in *Article 3* for determining the threshold value in brittle fracture of a fatigue-cracked plate, instead of the curve recommended by the BS 7910, see Figure 5.1.

5.4. Time-variant reliability formulations of deteriorating structures

Time-dependent reliability is used to determine the likelihood in time of an excursion of the random vector X(t) out of a safe domain **D** defined by **G**(X)**>0**. The first-passage probability may be equivalent to the probability $P_f(t)$ of structural failure during a certain period [0,T], e.g. Melchers (1999).

$$P_f(t) = 1 - P\left[N(t) = 0 \mid X(0) \in D\right] P\left[X(0) \in D\right] \tag{5.3}$$

where $X(0) \in D$ signifies that the process $X(t)$ starts in the safe domain ***D*** at zero time and $N(t)$ is the number of outcrossings in the time interval [0,t].

The general solution of (5.3) is rather difficult to obtain owing to the need to account for the complete history of the process ***X***(t) in the interval [0,t]. Usually the solution will depend on the nature of the process **X(**t). For reliability problems, outcrossings usually occur so rarely that often it is satisfactory for the individual outcrossings to be assumed independent events, and therefore independent of the probability of any earlier outcrossings, including one at t=0. The probability of no outcrossings in [0,t] may then be approximated using the Poisson distribution. Then failure probability reads (e.g. Melchers, 1999):

$$P_f(t) \approx 1 - \exp\left(-\int_o^T \upsilon^+(r,t)\,dt\right) \tag{5.4}$$

This approximation is good for rare out-crossings, i.e. the out-crossings are independent events, but it is not a good choice for cases where the barrier is low or close to the origin, which implies that the assumption of independent crossings is not completely valid. Hence the first passage failure probability can approximately be calculated in cases of relatively high thresholds and not-too-narrow banded processes, i.e. the assumption of independent out-crossings is valid for rare process excursions, provided that the statistics of the out-crossing rate are known, (Melchers, 1999).

Reliability assessment of existing structures is already a common practice among engineering practitioners in different industries, like aerospace, offshore, and bridge engineering. The term “existing structure” implies that the structures have been operating for a certain period of time during which a certain degree of deterioration on the structural components has taken place, the strength reduction needs to be explicitly considered in the assessment.

In offshore structures, deteriorating agents such as fatigue and corrosion are of great concern, since their negative effects on the resistance of components, and hence structural systems, may lead to an increased likelihood of overload failure. One of the failure modes induced or increased by the combined effect of fatigue cracking and corrosion is the unstable

fracture. Floating offshore structures like production ships are integrated by stiffened panels supported by transverse frames.

The time-variant reliability problem of a deteriorating stiffened panel is to be dealt with as a first passage problem, with a decreasing threshold, i.e. deteriorating strength $\eta(t)$. The mean up-crossing rate $\upsilon^+(t)$ of the process X(t) out of the function $\eta(t)$ during a certain time interval, e.g. service life or one year, may be determined.

For the case of fracture failure probability of a cracked stiffened panel, this needs to be evaluated for every crack size step, i.e. a conditional failure probability is obtained for every outcome **r** of the resistance vector **R** as

$$P_f(T \mid \mathbf{r}) \le P_f(0 \mid \mathbf{r}) + \left[1 - \exp\left(-\int_0^T \upsilon^+\left(r(\mathbf{r},t)\right)\right)\right] \tag{5.5}$$

The first term in the right hand side is the initial Pf at T=0, **r** is the vector of random variables for every time step, $r(\mathbf{r}, t)$ is the resistance degradation scalar and $\upsilon^+\left(r(\mathbf{r},t)\right)$ is the up-crossing rate of the barrier $r(\mathbf{r}, t)$. The unconditional failure probability is obtained as

$$P_f(T) = \int_{\mathbf{R}} P_f(T \mid \mathbf{r}) f_{\mathbf{R}}(\mathbf{r}) d\mathbf{r} \tag{5.6}$$

To solve Eq. (5.6) Wen and Chen (1987) proposed the so-called *fast probability integration* (FPI) approach based on the first order approximation by solving the following limit state function

$$g(u_{n+1}, \mathbf{u}) = u_{n+1} - \Phi^{-1}\left[P_f\left(\mathbf{T}^{-1}(\mathbf{u})\right)\right] \tag{5.7}$$

where $\mathbf{u} = \mathbf{T}(\mathbf{r})$ is the transformation to the standard normal space and u_{n+1} is an auxiliary standard normal variate independent of **u** in the transformed space. This implies to calculate the time variant problem with a nested FORM.

Another simplified approach is the *time integrated* (TI) approach (Melchers, 1999) which consists of considering the whole life time of the structure as a unit so that the probability distribution of maximum load effects and minimum resistance are referred to such a period of time. Marley and Moan (1992), assuming that the maximum load in the life time occurs at the end of the term and coincides with the minimum realization of resistance. However, it is very unlikely that the lifetime maximum load effect occurs exactly at the end of the service life, see Figure 5.2.

Under this scheme the resistance is characterized with a horizontal line corresponding to the minimum resistance in the interval $[0,T]$ and an associated uncertainty at time T. The probability distribution of the maximum load effect $S_{max}(T)$ may be obtained, for a certain time interval, by means of asymptotic extreme value approaches, i.e. defining the expected largest maximum. The failure probability is simply

$$P_f(T) = P\left[R \le S_{\max}(T)\right] \tag{5.8}$$

The TI approach may therefore be applied for a certain time interval, e.g. one year, where the expected largest loading is determined for one year assuming independent years. The year-to-year variability needs therefore to be accounted for, as studied by Moan et al (2005), which may be very relevant for assessment of existing offshore structures and hence for the

inspection, maintenance and repair management. Eq. (5.8) may be solved by any time-invariant reliability method e.g. FORM/SORM.

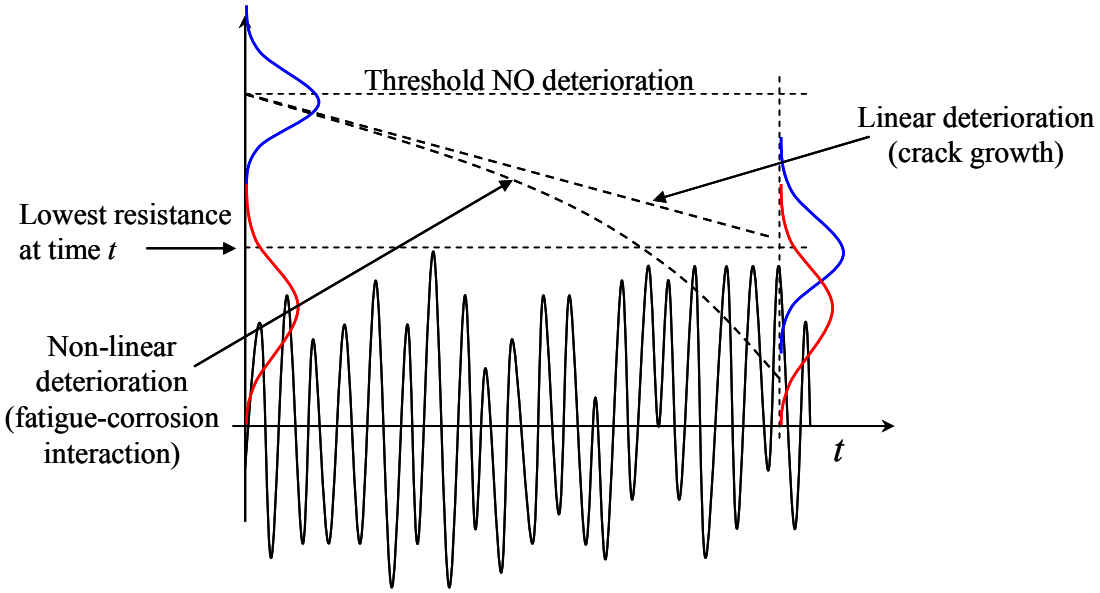

Figure 5.2. Time-reliability problem in deteriorating structures

5.5. Up-crossing rates

Calculation of up-crossing rates of a loading process over a resistance threshold or barrier depends upon the type of process under consideration. For scalar Gaussian processes there are solutions under the assumption of independence between the actual process and its time derivative. Solutions for up-crossing rates for high threshold levels, e.g. fracture failure, are based on the assumption of independent (rare) crossings, i.e. they follow a Poisson distribution. For problems where the resistance barrier decreases with time, e.g. due to deterioration, the assumption of independence between crossings may be not valid as there could be clustering of crossings, Beck and Melchers (2004b).

Recently, Beck and Melchers (2004b, 2005) studied the particular case when the outcrossing of a random process over a barrier is basically governed by a small realization of the latter, i.e. low resistant threshold induced by deterioration. This case in time-variant reliability theory is referred to as a barrier failure dominance problem.

The up-crossing rate obtained under the assumption of independent crossings over deterministic barriers is corrected, by interpolating rates obtained with both low and intermediate thresholds. Beck and Melchers (2004b) introduce a correction to the ensemble upcrossing rate and estimated the amount of error introduced in typical cases.

5.5.1. Parallel systems sensitivity measure

Based on unpublished work by H. O. Madsen, Hagen & Tvedt (1991) proposed a general procedure for estimating the mean up-crossing rate $\upsilon^{+}(t)$ of a scalar differentiable process $X(t)$, obtained as a parametric sensitivity measure of the probability of an associated parallel system. The method is applicable to Gaussian and non-Gaussian, stationary as well as non-

stationary random processes, and to time-dependent failure surfaces. It was originally derived for the case of a time-independent level η, the up-crossing rate of a scalar differentiable process $X(t)$, where the parallel system sensitivity measure reads:

$$\upsilon(\eta,t) = \lim_{\Delta t \to 0^+} P\left[X(t) < \eta \cap X(t+\Delta t) > \eta \right] \tag{5.9}$$

$$\begin{aligned} \upsilon(\eta,t) = \lim_{\Delta t \to 0^+} \Big\{ & P\left[\dot{X}(t) > 0 \cap X(t) + \dot{X}(t)\Delta t > \eta \right] \\ & - P\left[\dot{X}(t) > 0 \cap X(t) > \eta \right] \Big\} \end{aligned} \tag{5.10}$$

$$\begin{aligned} \upsilon(\eta,t) &= \frac{d}{d\theta} P\left[\dot{X}(t) > 0 \cap X(t) + \dot{X}(t)\theta > \eta \right]_{\theta=0} \\ &= \frac{d}{d\theta} P(t,\theta)_{\theta=0} \end{aligned} \tag{5.11}$$

where $P(t,\theta)$ is the probability of the associated parallel system domain. The approach requires that the joint distribution of $[\mathbf{Z}(t), \dot{\mathbf{Z}}(t)]$ is known and that a transformation of the jointly random variables $[\mathbf{Z}(t), \dot{\mathbf{Z}}(t)]$ into a set if independent standard normal random variables is also possible at each time $t \in (0,T)$. Thus, methods for calculating parametric sensitivity factors for time-independent parallel systems, solved by FORM/SORM, are then applicable to determine the mean up-crossing rate. The advantage of this approach is that it may be extended to the case of uncertain failure surfaces.

5.5.2. Ensemble up-crossing rate

The so called ensemble up-crossing rate (EUR), which is an averaged rate, is formally obtained by averaging over a deterministic resistance, but it may be obtained by introducing the variability of the resistance parameters in the parallel system sensitivity analysis, (e.g. Wen and Chen, 1989; Beck and Melchers, 2004b).

The averaged up-crossing rate of a random loading process through a deterministic barrier level is given by (e.g. Beck and Melchers, 2004b)

$$\upsilon_{ED}^{+}(t) = \int_R \upsilon^{+}(r,t) f_R(r,t)\, dr \tag{5.12}$$

where $f_R(r,t)$ is the resistance transition probability density at time t. Herein, the subscript ED is given to denote that the ensemble averaged rate implies certain level of dependency among the crossings, in contrast with the assumption of independent crossings implied by e.g. Eq. (5.12)

In order to correct the values obtained with the ensemble up-crossing rate approach over relatively low barriers, Beck and Melchers (2004b) estimated the error of EUR approximation with respect to a conditional (independent crossing) up-crossing rate described with an "exact" Poisson process.

The corrected upcrossing rate is given by (Beck and Melchers, 2005)

$$\upsilon^+(r,t) = \upsilon_S^+(r,t)\left[\frac{\upsilon_S^+(r,t)}{\upsilon_S^+(o,t)} + 1 - \exp\left(\frac{\upsilon_A^+(r,t)}{\upsilon_S^+(r,t)}\right)\right] \tag{5.13}$$

which is an interpolation between crossings by the load process $\upsilon_S^+(r,t)$ at very low barriers *r(t)*, crossings by the amplitude process $\upsilon_A^+(r,t)$, and crossings by the load process at high barrier levels, (Beck and Melchers, 2004b).

However, these authors argue that the EUR approximation may lead to large errors of failure probabilities if the variance of the resistance threshold is large in comparison to the variance of the load process. These kinds of problems are referred to as barrier failure dominance problems in time-variant reliability (Beck and Melchers, 2005).

For the particular case of a stiffened panel in a ship structure with a through-thickness crack under wave random loading, the overload failure probability, e.g. brittle fracture, may be dominated by the uncertainty of the degrading strength, induced by crack growth. Furthermore, as explained in previous chapters, the fatigue-corrosion interaction problem may introduce additional uncertainties, sometimes difficult to quantify. These factors make it even more challenging to use the EUR approach.

5.5.3. Long-term approximation of crossing rate

The loading quantities of relevance to the fatigue/fracture reliability problem are a) the "mean crack driving load" and b) the extreme load giving rise to final failure. Often the long term distributions of these quantities may be obtained or approximated. Then, the reliability problem may be posed in terms of time independent **Z** variables only and the methods presented in Chapters 3 and 4 applied directly. This means that the resistance deterioration, conditional on a vector of random variables, is controlled by the mean load effect. The out-crossing of this resistance is additionally dependent on the long term statistics of extreme loads.

For a non-Gaussian process, e.g. Weibull process describing the stress amplitude, the up-crossing rate may be approximated by (Marley and Moan, 1992):

$$\begin{aligned}\upsilon^+(\eta,t) &= \upsilon_0^+\left\{-\ln\left(1-\exp\left[-\left(\frac{\eta(t)}{A_\upsilon}\right)^B\right]\right)\right\} \\ &\approx \upsilon_0^+\exp\left[-\left(\frac{\eta(t)}{X_A\cdot A_\upsilon}\right)^B\right]\end{aligned} \tag{5.14}$$

where A_υ and B are the Weibull parameters of the process, υ_0^+ is the zero up-crossing rate, and X_A is the model uncertainty, i.e. variability of A_υ. This expression is used in *Article 3* to describe the long-term up-crossing rate.

5.6. Failure probability of fatigue-induce fracture

Cracks are commonly detected in ship structures by means of close visual inspection when they have already propagated through the thickness. Their presence may lead to eventual

occurrence of fracture when exposed to overloads, e.g. when a permanently moored FPSO is exposed to a storm. Such offshore vessels cannot periodically be dry-docked for inspection and repair and hence, it is not rare that non-accessible cracks are left unrepaired, e.g. Kent et al (2002). Although it has been found that stiffened panels, main longitudinal resistant components of hull girder structures, are tolerant to fatigue cracking, the safety of such structural components with the presence of long cracks may be threatened when exposed to overload extreme conditions.

Fatigue-induced fracture on aging hull structures is studied in the present research work. Failure probability of a stiffened panel at the bottom plating with the presence of long cracks is discussed in *Article 3*. The mean stress effects are explicitly accounted for in the crack growth calculation procedure, in order to include mean stress levels due to the continuously varying still-water loading as well as the residual stresses. As pointed out in *Article 3* of this dissertation, one of the main conclusions drawn is that the still-water mean stress has a significant effect on the failure probabilities of stiffened panels with long cracks under brittle fracture mode.

As discussed above, time-variant reliability problems are basically dealt with by solving the crossing rate of a scalar over a decreasing threshold. In *Article 3*, only brittle fracture mode is considered in the failure probability quantification, where the time-dependent threshold level depends upon the crack propagation estimated for the stiffened panel, based on integrated Paris' law. The resulting threshold model may be written as

$$R(t,\mathbf{z}) = \frac{K_{Jc}}{\gamma \cdot Y(a)\sqrt{\pi a}} = \frac{K_{Jc}}{\gamma\sqrt{\pi}}\left(c_0 - \sum_{i=1}^{n} c_i X_i \cdot t^i\right) \tag{5.15}$$

where γ is the model uncertainty, t is time and c_0 is a constant value. X_i are the time-invariant random variables that depend upon the crack propagation parameter C and the fatigue loading S_{eq}, i.e. equivalent stress range. For the special case that $Y(a)$=1.0, applicable for through thickness crack, Paris' law can be integrated analytically. The result is then:

$$R(t,\mathbf{z}) = \frac{K_{Jc}}{\gamma \cdot \sqrt{\pi}}\left(c_0 - \alpha X \cdot t\right) \tag{5.16}$$

where c_0 is equal to $1/\sqrt{a_0}$, with a_0 as the initial crack length. Here α represents the mean value resulting from the summation implied in Eq. (5.15) and X is a time invariant random variable describing the total crack growth randomness.

On the other hand, the fracture toughness K_{Jc} implied by Eq. (5.16) is assumed to be Weibull distributed as implied from the data fitted by Kent and Sumpter (2004), whose coefficient of variation is 0.44 and expected value is given by

$$E\left[K_{Jc}\right] = 20 + 0.93\left[11 + 77\exp\left\{0.019\left(T_{op} - T_{27J} + 78\right)\right\}\right]\left(\frac{25}{B}\right)^{1/4} \tag{5.17}$$

where B is the thickness of the plate, T_{op} is the operating temperature and T_{27J} is the transition temperature corresponding to the 27 Joule toughness of the material.

The brittle fracture limit state is therefore defined as

$$g(t) = R(t,\mathbf{z}) - Y(t) \tag{5.18}$$

where the load process $Y(t)$ is the combination of still-water and wave-induced stresses. Let process $X_w(t)$ be the wave-induced stresses and $X_{sw,i}$ the still-water stress in load condition i, assumed as time independent and described as implied by Figure 2 in *Article 3*. The load process $Y(t)_i$ then reads

$$Y(t)_i = X_w(t) + X_{sw,i} \tag{5.19}$$

In reality, a marine structure is subjected to a series of sea states in its service life. The procedures mentioned above may be utilized in principle to calculate the crossing rates and failure probabilities for a given sea state and still-water condition. Then, the long-term reliability problem is calculated by summing the weighed contributions to failure probability from each sea state. Since the number of sea states is large, a simplified approach is preferred. Marley (1991) carried out a full long-term simulation of fatigue-induced fracture of a marine structure, accounting for the crack growth contribution from each sea state. Based on long-term approximation of the load effects, both fatigue and extreme loading, Marley (1991) and Marley & Moan (1992, 1994) propose a simplified long term approach. The basis of this approach is then to determine the long term up-crossing frequency, as defined by Eq. (5.14).

The still water (SW) loading effects introduce mean stress levels that vary from laden to ballast conditions, which have an important implication in the fatigue calculations. In order to estimate the failure probability of fatigue-induced fracture on a stiffened panel with a randomly growing long crack, the SW loading effects are discretized into different stress levels. Hence, the failure probability corresponding to a *SW* stress level *i* (SW_i) is given by

$$P_f(T \mid \mathbf{z})_i = 1 - \exp\left(-\int_0^T \upsilon^+\left(R(\mathbf{z},t)\right) dt\right) \tag{5.20}$$

The unconditional failure probability implied in Eq. (5.20) is obtained as

$$P_f(T)_i = \int_{\mathbf{R}} P_f(T \mid \mathbf{z}) f_{\mathbf{R}}(\mathbf{z}) d\mathbf{z} \tag{5.21}$$

where $f_{\mathbf{R}}(\mathbf{z})$ is the joint density function of $\mathbf{Z}$. Eq. (5.21) is solved by using Monte Carlo simulation (MCS). The total failure probability for a given time is obtained as follows

$$P_f(T) = \sum_i P_{f|SW,i}(T) \cdot P_{SW,i} \tag{5.22}$$

where $P_{SW,i}$ is the probability of still water condition i.

The results are compared with a time invariant reliability approach which consists of calculating the failure probability by using a degrading threshold corresponding to the crack size at time T. The time-invariant failure probability is then evaluated by making the maximum load effect in the interval $[0, T]$ to occur at the time T of minimum resistance. The approach was validated by Marley and Moan (1992).

The procedure mentioned above is exemplified in *Article 3* with the calculation of failure probabilities on a stiffened panel located at the bottom plating of a hull structure, corresponding to every SW loading level, and the final failure probability is determined by a weighed sum of these probabilities. Moreover, the failure probabilities are obtained for two different operating temperatures, namely +10 and –10 ^{o}C.

Table 5.1 shows the failure probabilities corresponding to each of the SW stress levels, calculated at time T=1 and 2 years by means of the time-variant approach described above. The "weight" column defines the probability of each SW stress level to occur and weighs the corresponding failure probability, which is presented in the fourth and sixth columns. It is observed that the vessel under sagging condition at a still-water stress level of 85 MPa represents the larger individual failure probability, which is especially seen for T=2 years, however the final weighed P_f is largest for the stress level of 50 MPa. Hence a safety measure implied by these results is to avoid operating the vessel close to these stress level, i.e. to keep the time (weighing value) under such conditions as low as possible until repair is carried out.

Table 5.1. SWBM-induced mean stresses in an FPSO including the corresponding weights used to calculate an equivalent stress range. Operating temperature= +10 ^{o}C.

i-th SW stress level (MPa)	Weight	Time = 1 year		Time = 2 years	
		P_f for *i*-th stress level	Weighed Pf-*i*	P_f for *i*-th stress level	Weighed Pf-*i*
Hogging (30%)					
–30	0.1155	2.74E-02	3.16E-03	1.39E-01	1.61E-02
–10	0.1844	2.97E-02	5.48E-03	1.45E-01	2.67E-02
Sagging (70%)					
20	0.2854	3.43E-02	9.79E-03	1.56E-01	4.45E-02
50	0.3726	3.91E-02	1.46E-02	1.67E-01	6.22E-02
85	0.0421	4.59E-02	1.93E-03	1.82E-01	7.66E-03
		Total P_f	**3.49E-02**		**1.57E-01**

CHAPTER 6

Conclusions

Summary of accomplishments

This work deals with the application of reliability-based techniques to evaluate the effect of deteriorating phenomena on the structural safety of existing ship-shaped production vessels. The proposed methodologies and formulations reported herein are aimed at evaluating the effects on safety of structural components when exposed to fatigue cracking, corrosion-enhanced crack growth and the likelihood of fracture of a cracked joint or component.

The research work was intended to go a step forward in the assessment of structural reliability of fatigue prone components of ship-shaped existing production vessels. It has been discussed that as structural systems age, the interaction between the different deteriorating phenomena, namely fatigue, corrosion and fracture, increase in time, thus, it results indispensable to explicitly account for this interaction to achieve reliable results. Nevertheless, it is challenging to model the interacting effects between fatigue, corrosion and fracture, considering the individual random nature of each of these phenomena, but it even more demanding the difficulty to characterize their interaction.

In the sequel, the main contributions achieved on each of the three articles presented in this dissertation are discussed.

Article 1:

Fatigue reliability assessment of welded joints applying consistent fracture mechanics formulations

This article discusses a comprehensive study on the use of reliability-based models to characterize the safety of a welded joint with respect to surface fatigue cracks. Such models include SN-based models as well as formulations based on fracture mechanics (FM) of both linear and bi-linear crack growth laws.

The FM bi-linear model recommended by the BS7910 (1999) has also been validated, taking explicit account of the uncertainty level corresponding to each of the segments that describe the crack growth law. In order for the reliability calculations to be conservative when applying the bi-linear crack growth law, it is recommended to assume both segments to be highly correlated. Moreover, it has been shown that calibration of the bi-linear FM model to the SN model with respect to the reliability index is not as simple as for the linear FM case. For the bi-linear FM approach, a calibration strategy based upon 3 parameters may be necessary. It is observed that in order for the fatigue design curve corresponding to joint *C* (flush-welded joint, S-N curve C) an initiation time of 2 years was utilized compared to 1 year corresponding to joint F (T-butted joint), which agrees with the fact that for the latter the initiation time is shorter due to the stress rising effect of the weld.

Further, it has been demonstrated that the effect of inspection on reliability, i.e. reliability updating, for the bi-linear FM model needs to be carried out by means of Monte Carlo simulation, as the FORM/SORM approaches result to be non-conservative.

The main contributions of this article are:

- Derivation of a reliability-based formulation for the bi-linear fracture mechanics law recommended by the BS7910. It is demonstrated that linear crack growth laws result in too conservative reliability levels.
- Validation of the bi-linear crack growth formulation with respect to the existing correlation level between segments of the bi-linear model.
- Calibration of the bi-linear fracture mechanics model with SN curves considering three parameters related to the crack growth process, namely, initial crack size, aspect ratio development and initiation time. The latter has been found to be a determining parameter in the calibration.
- Definition of the inspection event required to determine updated reliabilities when applying the bi-linear crack growth formulation. Through sensitivity studies it was determined that accurate reliability updating calculations are to be performed by means of Monte Carlo simulation as FORM/SORM provide non-conservative results.

Article 2:

Reliability-based assessment of deteriorating ship structures operating in multiple sea loading climates

A robust fatigue reliability model based on an event formulation is proposed to efficiently assess, by means of a second order reliability method (SORM), the safety of welded joints of an existing ship subjected to two different consecutive climate conditions throughout the service life.

Fatigue and corrosion full interaction phenomena are accounted for in the formulation, considering the increased crack growth rate induced by the rise of stress range due to the corrosion wastage (plate thinning). The model also allows for the corrosion fatigue phenomenon.

The effect of inspection is considered to emphasize its effect after the vessel has been moved and hence exposed to different climate conditions. Both the cumulative failure probability throughout the service life, commonly used in evaluating fatigue failure, and the annual hazard rate are calculated. The latter approach is shown to be very valuable when considering an extension in the service life of the ship.

The case studies show that the results are non-conservative when the interaction between crack growth and corrosion thinning is ignored in the evaluation of the fatigue failure probability. However, it is a challenging task to evaluate corrosion rates, especially their dependence on local conditions. There is, as expected, a larger effect in the updating when the structure has spent 10 years under harsh conditions and conditions and moved to benign climates.

The main contributions of this article are:

- Derivation of a robust fatigue reliability formulation to assess the safety of ship structural details when exposed to two different consecutive climate conditions. This formulation can be extended to evaluate fatigue reliability in ships under multiple consecutive climate conditions. Explicit consideration of uncertainties corresponding to each climate condition is accounted for.
- The interaction between fatigue and corrosion is modeled in terms of increased crack growth rate. Such an interacting effect is introduced together with the model that accounts for the changing climate conditions, mentioned above, under a reliability framework. This formulation represents a useful reliability-based decision support tool applicable for, e.g. service life extension of existing FPSOs or ships, or condition assessment of ships before being converted to FPSOs.
- Appropriate inspection events are derived, considering fatigue and corrosion interaction, in order to update reliability levels on structural details of ships exposed to two different consecutive climate conditions.

Article 3:

Time-variant reliability assessment of FPSO hull girder with long cracks

An efficient time-variant reliability analysis formulation for a stiffened panel with long cracks has been proposed. Fracture failure probability of the panel induced by the random fatigue propagation of an existing long crack, is evaluated with a robust formulation based on the master curve approach.

The effect of mean stress on fatigue propagation due to the slowly varying still-water loading is presented, including in the formulation the residual stress effect. The results obtained with this formulation can serve as a basis for decisions in the safety management of FPSOs with respect to the still-water (SW) loading which is a man-dependent process.

For the present case it is found that the time-invariant approach is a good approximation when dealing with the time-variant reliability problem. In this manner, major repairs may be more efficiently applied and better planned. One of the main conclusions drawn from this study is that the effect of still-water mean stresses in the propagation of long cracks is the most significant one and it is conservative to disregard the residual stress field.

The main contributions of this article are:

- Fatigue-induced fracture formulation of randomly growing through-thickness crack in a stiffened panel
- Still-water load effect on the fatigue damage calculation for an FPSO is explicitly introduced in the methodology.
- A comprehensive yet efficient methodology to assess time-variant reliability of a stiffened panel with a long crack is established, which puts together different topics whose individual complexity is of consideration, namely: mean stress effects on fatigue damage (e.g. due to SW

loading and residual stresses), random crack propagation of a long crack in a stiffened plate, probabilistic description of fracture failure of a randomly growing flaw (long crack), and time-variant reliability analysis.

Recommended further research work

In the study reported herein the interacting effect of fatigue and corrosion is considered in assessing the failure probability of structural components. Such an interaction is given in terms of the increase of nominal stresses introduced by the material loss due to general corrosion. However, pits are formed at the plating that in many cases may also represent a stress riser, especially if they are located at e.g. weld toes. The way corrosion pits affect the crack initiation period and development needs to be studied to achieve a complete picture of the interacting effect between fatigue and corrosion on long welds.

A natural extension to the crack growth analysis on stiffened panels is to perform further research on the propagation and coalescence of multiple cracks initiated along welds of uniformly loaded details, as it is the case of long welds existing in ship structures, e.g. fillet welds at the connection of bulkheads or transverse frame web with the bottom/deck plating. Coalescence of multiple cracks may lead to very long cracks that grow more rapidly than a single semi-elliptical shaped crack does. The density and distribution of multiple cracks along the weld is of random nature, hence a probabilistic approach of coalescence is recommended to be investigated.

Mean stress effect on fatigue crack growth was dealt with to estimate crack propagation of a long crack on a stiffened panel subject to random variation of still-water loading of the vessel. A comprehensive study on variable amplitude loading fatigue of surface and through-thickness cracks under a probabilistic framework is recommended to be performed.

With respect to the fatigue-induced fracture likelihood in a long term approach, the calculation of up-crossing rates of the resistance barrier by the loading process is to be improved, especially for cases where the barrier or threshold is reduced, e.g. due to combined deteriorating effects of fatigue and corrosion. In such cases, the fact that wave-induced response, often described by means of a Gaussian process, may imply clustering effect crossings with low thresholds, i.e. the independence among crossings is no longer valid. Further research is necessary to deal with estimation of long-term crossing rates for the cases of barrier failure dominance.

References

ABS (2001). Understanding recent product tankers casualties. The American Bureau of Shipping. http://www.eagle.org/news/speeches/seatradefinal/sld001.htm

Akpan,U.O., Koko, T.S., Ayyub, B., and Dumbar, T.E. (2002), "Risk assessment of aging ship hull structures in the presence of corrosion and fatigue". Marine Structures **15**: 211-231.

Almar-Naess, A. (1985). "Fatigue Handbook – Offshore Steel Structures". Tapir Publishers, Trondheim, Norway

Amlashi, H.K.K. and Moan, T. (2008), "Ultimate strength analysis of a bulk carrier hull girder under alternate hold loading condition – A case study: Part 1: Nonlinear finite element modelling and ultimate hull girder capacity". Marine Structures **21**(4): 327-352

Andersen, T.L. (1991), "Fracture Mechanics – Fundamentals and Application", CRC Press.

Ang, A. H-S., and Tang, W.H. (1984). "Probability concepts in Engineering Planning and Desing. –Vol II – Decision, Risk, and Reliability". John Wiley & Sons, New York, USA.

Ayala-Uraga, E. and Moan, T. (2002), "System Reliability Issues of Offshore Structures Considering Fatigue Failure and Updating Based on Inspection", In: Proc. of 1st International ASRANet Colloquium, Glasgow, Scotland, UK.

Ayala-Uraga, E., and Moan, T. (2005a). "Reliability based assessment of welded joints using alternative fatigue failure functions". In: Augusti G., Schuëller GI & Ciampoli M, editors. Proc. of International Conference on Structural Safety and Reliability ICOSSAR 2005, Rome, Italy.

Ayala-Uraga, E., Moan, T., (2005b), "Time-variant reliability assessment of FPSO hull girder with long cracks". In: Proc. 24th Int. Conf. of Offshore Mech. and Arctic Eng., Halkidiki, Greece.

Ayala-Uraga, E. and Moan, T. (2007a), "Fatigue reliability-based assessment of welded joints applying consistent fracture mechanics formulations", International Journal of Fatigue **29** (3): 444-456.

Ayala-Uraga, E. and Moan, T. (2007b), "Time-variant reliability assessment of FPSO hull girder with long cracks", Journal of Offshore Mechanics and Arctic Engineering **129** (2): 81-89.

Beck, A.T., and Melchers, R.E, (2004a). "Overload failure of structural components under random crack propagation and loading – a random process approach". Structural Safety **26**:471-488.

Beck, A.T., and Melchers, R.E., (2004b). "On the ensemble crossing rate approach to time variant reliability analysis of uncertain structures". Probability Engineering Mechanics **19**:9-19.

Beck, A.T., and Melchers, R.E., (2005). "Barrier failure dominance in time variant reliability analysis". Probability Engineering Mechanics **20**:79-85.

Bjørheim, L.G. (2006). “Failure assessment of long through thickness fatigue cracks in ships hulls”, PhD Thesis, Dept. of Marine Technology, Norwegian University of Science and Technology, Trondheim, Norway

Bjørheim, L.G., Berge, S., and Skaret, H., (2004). “Damage tolerance of FPSOs with fatigue cracks”. In: Proceedings of 14th Intnal. Offshore and Polar Engineering Conference, Toulon, France, paper no. JSC-451.

Bokalrud, T., and Karlsen, A. (1981). ”Probabilistic Fracture Mechanics evaluation of fatigue failure from weld defects in butt weld joints”. In: Proceedings on Conf. on Fitness for Purpose Validation of Welded Constructions. London, UK, paper 28.

Bouchard, R., Vosikovsky, O., and Rivard, A. (1991). Fatigue life of welded plate T joints under variable-amplitude loading. Int J Fatigue 13 (1): 7-15.

Bowness, D., and Lee, M.M.K. (1999). Weld toe magnification factors for semi-elliptical cracks in T-butt joints. Offshore Technology Report – OTO 1999 014. Health Safety Executive.

BS 7608, (1993). “Code practice for Fatigue design and assessment of steel structures”, BS 7608. British Standard Institution, London, UK.

BS 7910 (1999). “Guide on methods for assessing the acceptability of flaws in fusion welded structures”, BS 7910:1999, British Standard Institution, London, UK

Burns, D.J., Lambert, S.B., and Mohaupt, U.H., (1987). “Crack growth behaviour and fracture mechanics approach”. In: Noordhoek and Back (eds) Steel in Marine Structures, Amsterdam: Elsevier Science Publishers.

Dalane, J. I., (1993). “System Reliability in Design and Maintenance of Fixed Offshore Structures”, Dr.ing. Thesis, Department of Marine Structures, The Norwegian Institute of Technology (NTH), The University of Trondheim, Norway.

Dexter, R.J., and Pilarski, P.J. (2000). “Effect of welded stiffeners on fatigue crack growth rate”. Report SSC-413, Ship Structure Committee, Washington, DC.

Dexter, R.J., Pilarski, P.J., and Mahmoud, H.N. (2003). “Analysis of crack propagation in welded stiffened panels”. International Journal of Fatigue **25**: 1169-1174.

Dexter, R.J., and Mahmoud, H.N., (2004). “Predicting stable fatigue crack propagation in stiffened panels”. Report SSC-435, Ship Structure Committee, Washington, DC.

DNV (1995). DnV Hull Structural Rules – Development, background, motives. Det Norske Veritas, Høvik

DNV (1996). “PROBAN – General purpose probabilistic analysis program, User’s manual, Rev. 1, Veritas Research DNV, Høvik, Norway.

DNV CN30.7 (2001), “Fatigue assessment of ships structures – Classification Notes 30.7”. Det Norske Veritas, Høvik, Norway.

Dover, W.D., Dharmavasan, S., Brennan, F.P. and Marsh, K.J., Eds., (1995). "Fatigue Crack Growth in Offshore Structures", Engineering Materials Advisory Services Ltd, London, UK.

Dover, W.D., Stacey, A., Tantbirojn, N. and Brennan, F.P. (2002). “Variable amplitude corrosion fatigue tests on high strength jack-up steel”. In: Proc. 21st Intnal. Conference on Offshore Mechanics and Arctic Engineering, Oslo, Norway.

Eide, O.I., and Berge, S., (1987). “Fracture Mechanics analysis of welded girders in fatigue”. In: Proc International Conf on Fatigue of Welded Constructions, Brighton, UK, 7-9 April.

Frise, P.R and Bell, R. (1992). “Modelling Fatigue Crack Growth and Coalescence in Notches”, Int. J. Pres. Ves. & Piping 51, pp. 107-126

Fujimoto, Y., et al, (1996). “Study on fatigue reliability and inspection of ship structures based on enquete information”. J. Soc. Naval Arch. of Japan, 180:601-609.

Fujimoto, Y., et al. (1997). “Inspection planning of fatigue deteriorating structures using genetic algorithm”. J. Soc. Naval Arch. of Japan 182.

Garbatov, Y., Guedes Soares, C., and Wang, G. (2007). "Nonlinear time dependent corrosion wastage of deck plates of ballast and cargo tanks of tankers". J Offshore Mech & Arctic Eng **129**: 48-55

Guedes Soares, C., and Garbatov, Y., (1998a). "Reliability of maintained ship hull girders subjected to corrosion and fatigue". Structural Safety **20**: 201-219.

Guedes Soares, C., and Garbatov, Y., (1998b). "Reliability of corrosion protected and maintained ship hulls subjected to corrosion and fatigue". Journal of Ship Research **43**(2): 65-78.

Guedes Soares, C., and Garbatov, Y., (1999). Reliability of maintained ship hulls subjected to corrosion and fatigue under combined loading. J. Constructional Steel Research; **52**: 93-115.

Guedes Soares C., and Moan, T., (1991). "Model uncertainty in the long-term distribution of wave-induced bending moments for fatigue design of ship structures". Marine Structures **4**(4): 295-315.

Gurney TR. (1976). "Cumulative damage calculations taking account of low stresses in the spectrum". Welding Research Inst 6(2):51-76

Hagen, Ø., and Tvedt, L., (1991). "Vector process out-crossings as parallel system sensitivity measure". J Eng Mech 117(10):2201-2220.

Haibach, E., (1970). "Contribution to discussion". The Welding Institute Conference on Fatigue of Welded Structures, Brighton, UK.

Isida, M., (1973). "Analysis of stress intensity factors for the tension of a centrally cracked strip with stiffened edges". Eng Fracture Mech **5**(3):647-665.

Jiao, G., (1992). Stochastic analysis of fracture under combination of gaussian response processes. Engineering Fracture Mechanics **43**: 321-329

Kam, J.C.P., and Dover, W,D., (1989). "Corrosion fatigue of welded tubular joints: Fracture Mechanics modeling and data interpretation". In: Proc International Conference on Offshore Mechanics and Arctic Engineering, The Hague, The Netherlands.

Kam, J.C.P. (1990). "Recent development in the fast corrosion fatigue analysis of offshore structures subject to random wave loading". International Journal of Fatigue **12**(6): 458-468

Karamchandani, A., Dalane, J.I., Bjerager, P. (1992). "Systems reliability approach to fatigue of structures". Journal of Structural Engineering, ASCE **118** (3): 684-700.

Kent, J.S., Das, P.K., Barltrop, N.D.P., and Sumpter, J.D.G., (2002). "Probabilistic study of the effects of leaving fatigue cracks unrepaired in a ship". In: Proc. 21st Conference on Offshore Mechanics and Arctic Engineering, Oslo, Norway

Kent, J.S., and Sumpter, J.D.G., (2004). "Probability of brittle fracture of a cracked ship". In: Proceedings of 2nd International ASRANet Colloquium, Barcelona, Spain.

King, R.N. (1998). "A review of fatigue crack growth rates in air and sea water". Offshore Technology Report OTH 511. London: Health Safety Executive, HSE Books.

Lindley, C. and Rudd, W.J. (2001). "Influence of the level of cathodic protection on the corrosion fatigue properties of high-strength welded joints", Marine Structures **14**(3):397-416.

Lotsberg, I., and Landet, E., (2004). "Fatigue capacity of side longitudinals in floating structures"; In: Proc. of OMAE Specialty Symposium on FPSO Integrity, paper OMAE-FPSO'04-0015, Houston.

Lotsberg, I., and Sigurdsson, G., (2005). Assessment of input parameters in probabilistic inspection planning for fatigue cracks in offshore structures. In: 9th International Conference on Structural Safety and Reliability, ICOSSAR'05, Rome, Italy.

Ma, K.T., Holzman, R.S., and Demsetz, L. (1995). Ship Maintenance Project – Volume 4 Durability considerations. Report SSC-386-IV. Ship Structure Committee, Washington DC, USA, 1992.

Madsen, H.O., Krenk, S., and Lind, N.C. (1986). "Methods of Structural Safety". New Jersey: Prentice-Hall Inc.

Mann, N.R., Schafer, R.E., and Singpurwalla, N.D. (1974). "Methods for statistical analysis of reliability and life data". New Jersey: John Wiley & Sons.

Mansour, A.E., Wirsching, P., Luckett, M., and Plumpton, A., et al (1997). Assessment of reliability of existing ship structures. Report SSC-398, Ship Structure Committee, Washington DC.

Marley, M.J., (1991). "Time variant reliability under fatigue degradation". PhD Thesis, Division of Marine Structures, The Norwegian Institute of Technology, Trondheim, Norway.

Marley, M.J. and Moan, T. (1992). "Time Variant Formulation for Fatigue Reliability", In: Proc. of Offshore Mechanics and Arctic Eng. Conference Paper No. 92-1203, Calgary, Ca.

Marley, M.J.,and Moan, T., (1994). "Approximate time variant analysis for fatigue, structural safety and reliability". In: Schueller, Shinozuka & Yao, editors.

Melchers, R.E., (1999). "Structural reliability analysis and prediction". 2nd ed. West Sussex, UK: John Wiley & Sons.

Melchers, R.E. (2001). "Probabilistic models of corrosion for reliability assessment and maintenance planning". In: Proc 20th Intnal Conf OMAE; Rio de Janeiro: ASME, paper S&R-2108.

Melchers, R.E. (2003a). "Probabilistic models for corrosion in structural reliability assessment – Part 1: Empirical models". Vol. **125**: 264-271.

Melchers, R.E. (2003b). "Probabilistic models for corrosion in structural reliability assessment – Part 2: Models based on mechanics". Vol. **125**: 272-280.

Moan, T., (2005). "Reliability-based management of inspection, maintenance and repair of offshore structures". J Structure and Infrastructure Engineering, **1**(1): 33-62.

Moan, T., Hovde, G.O., and Blanker, A.M., (1993). "Reliability-based fatigue design criteria for offshore structures considering the effect of inspection and repair". In: Proc of 25th Offshore Technology Conference. Houston. Vol II pp. 591-600.

Moan, T., Vårdal, O.T., Hellevig, N.C., and Skjoldli, K. (2000). "Initial crack depth and POD values inferred from in-service observations of cracks in North Sea jackets". J Offshore Mechanics and Arctic Eng 122:157-162.

Moan, T., Ayala-Uraga, E., Amlashi, H., and Dong, G. (2004). "Safety formats for ultimate strength and corresponding load effect models for FPSOs", Report MK R/153, Department of Marine Technology, Norwegian University of Science and Technology, Trondheim, Norway.

Moan, T. and Ayala-Uraga, E., Wang, X. (2004). "Reliability-based service life assessment of FPSO structures". Trans. of the Soc. of Naval Architects and Marine Eng., Vol. 112, pp. 314-342.

Moan, T., Gao, Z., and Ayala-Uraga, E., (2005). "Uncertainty of wave-induced response of marine structures due to long-term variation of extratropical wave conditions", Mar Str **18**(4): 359-382.

Moan, T. and Ayala-Uraga, E. (2008). "Reliability-based assessment of deteriorating ship structures operating in multiple sea loading climates, Reliability Eng. & System Safety **93** (3): 433-446.

Newman, J.C., and Raju, J.S. (1981). "An empirical stress-intensity factor equation for the surface crack". Eng. Fracture Mech **15**(1-2):185-192.

NORSOK (1998). "N-004 – Design of steel structures". Oslo: Norwegian Technology Standards Institution.

Nussbaumer, A., Fisher, J.W, and Dexter, R.J. (1999). "Behaviour of long fatigue cracks in cellular box beam", Journal of Structural Engineering **125**: 1232-1238.

Offshore Magazine, (2005). "Worldwide survey of floating production, storage and offloading (FPSO) units". Offshore Magazine, Houston. Poster 57.

OLF., (2002). A summary report on lessons learned, gathered from 4 Norwegian FPSOs. Norwegian Oil Industry Asociation, OLF (Oljeindustris Landsforening), Olso.

Otegui, J. L., Kerr, H. W., Burns, D. J. and Mohaupt, U. H. (1989). "Fatigue crack initiation from defects at weld toes in steel". Int. J. Pres. Ves. & Piping **39** (1989) 385-417.

Otegui, J.L., Burns, D.J., Kerr, H.W., and Mohaupt, U.H., (1991). "Growth and coalescence of fatigue cracks at weld toes in steel". Int J Pres Ves & Piping **48**:129-165.

Paik, J.K., Lee, J.M., Hwang, J.S., and Park, Y.I. (2003a). A time-dependent corrosion wastage model for the structures of single- and double-hull tankers, and FPSs and FPSOs. Marine Technology. Vol. **41**(3): 201-217.

Paik, J.K., Thayamballi, A.K., Lee, J.M., and Park, Y.I., (2003b), "Time-dependent risk assessment of aging ships accounting for general/pit corrosion, fatigue cracking and local denting damage". In: Proc of 2003 SNAME Annual Meeting, San Francisco, USA.

Rauta, D., Gunner, T., and Eliasson, J. (2004). Double hull tankers and corrosion protection. In: Proc of Annual SNAME Maritime Tech and Expo Conference, Washington, DC

Righiniotis, T.D., and Chryssanthopoulos, M.K, (2004). "Fatigue and fracture simulation of welded bridge details through a bi-linear crack growth law", Structural Safety **26**: 141-158.

Rodriguez-Sanchez, J. E., Brennan, F. P., and Dover, W. D. (1998). "Minimization of Stress Concentration Factors in Fatigue Crack Repairs," Int. J. Fatigue 20(10), pp. 719–725.

Schijve, J., (2002). "Fatigue of structures and materials". Kluwer Academic Press.

SSC-386, (1995a), "Ship Maintenance Project – Volume 1 Fatigue Damage Evaluation", Ship Structure Committee, Washington DC, USA

SSC-386, (1995b), "Ship Maintenance Project – Volume 2 Corrosion Damage Evaluation", Ship Structure Committee, Washington DC, USA

SSC-386, (1995c), "Ship Maintenance Project – Volume 3 Repair and Maintenance", Ship Structure Committee, Washington DC, USA

SSC-397, (1997), "Commercial Ship Design for Corrosion Control", Ship Structure Committee, Washington DC, USA

Sucharski, D. (1997). "Crude oil tanker hull structure fracturing: an operator's perspective". In: Ship Structure Committee. Proc. Symposium and workshop on the prevention of fracture in ship structure, Washington, D.C., pp. 87-124.

Sumpter, J.D.G., and Kent, J.S., (2004). "Prediction of ship brittle fracture casualty rates by a probabilistic method". Marine Structures **17** (8): 575-584.

TSCF. (1997). "Guidance Manual for Tankers Structures". Tanker Structure Co-operative Forum & IACS. Whitherby Publishers, London, UK

Visser, W., Dover, W.L., and Rudlin, J.R. (1996). "Review of UCL underwater inspection trails". Report OTN 96 179, Health & Safety Executive, UK.

Visser, W., (2000). POD/POS curves for non-destructive examination. Offshore Technology Report OTO 2000/018, Health & Safety Executive, UK.

Vosikovsky, O., Bell, R., Burns, D.J, and Mohaupt, U.H., (1985). "Fracture Mechanics assessment of fatigue life of welded T-joints including thickness effect". In: Proc 4th Int Conf Behavior of Offshore Structures, BOSS 85. Elsevier, Amsterdam, pp. 453-464.

Wang, G., Spencer, J., and Sun, H. (2003). "Assessment of corrosion risks to aging ships using an experience database". In: Proc of Offshore Mechanics and Arctic Eng; Cancun, Mex. OMAE, paper 37299.

Wen, Y.K., and Chen, H.C., (1987). "On fast integration for time variant structural reliability". Prob Eng Mech 2(3):156-162.

Wen, Y.K., and Chen, H.C., (1989). "System reliability under time varying loads: I". J Eng Mech 115(4):808-823.

Yamamoto, N., and Yao, T. (2001) "Hull girder strength of a tanker under longitudinal bending considering strength diminution due to corrosion". In: Corotis et al (eds); Structural Safety and Reliabilit: Swets & Zeitlinger.

Zhang, R. and Mahadevan, S., (2001). "Reliability-based reassessment of corrosion fatigue life", Structural Safety **23**: 77-91.

Zhang, B., and Moan, T., (2005). "Analysis of fatigue crack propagation in typical welded joints of FPSOs". In: Proc. Offshore Mech. Arctic Eng., paper OMAE2005-67058, Halkidiki, Greece .

APPENDIX A

Published Articles

The articles developed as product of the research work reported in this dissertation are listed below. In the sequel each of the three papers is briefly introduced before it is presented as published.

1. **Ayala-Uraga, E. and Moan, T.**, "Fatigue reliability-based assessment of welded joints applying consistent fracture mechanics formulations", *International Journal of Fatigue*, Vol. **29** No. 3, pages 444-456, 2007

2. **Moan, T. and Ayala-Uraga, E.**, Reliability-based assessment of deteriorating ship structures operating in multiple sea loading climates, *Reliability Engineering and System Safety*, Vol. **93** No. 3, pages 433-446, 2008.

3. **Ayala-Uraga, E. and Moan, T.**, "Time-variant reliability assessment of FPSO hull girder with long cracks", *Journal of Offshore Mechanics and Arctic Engineering*, Vol. **129** No. 2, pages 81-89, 2007

Article 1. Fatigue reliability assessment of welded joints applying consistent fracture mechanics formulations

Authors: **Ayala-Uraga, Efren** and **Moan, Torgeir**,

Published in: *International Journal of Fatigue*, Vol. **29** (2007), No. 3, pp. 444-456.

Refereed article

Preface

In this paper, alternative SN and fracture mechanics formulations of fatigue reliability analysis are proposed. They include a crack growth formulation based on bi-linear crack growth law as recommended by the BS7910 (1999). The effect of inspection in the updated reliabilities is illustrated using various methods including Monte Carlo simulation. The calibration of the FM method is performed with respect to SN design curves, based upon consideration of the crack initiation time, initial crack size and the crack aspect ratio.

Available online at www.sciencedirect.com
ScienceDirect
International Journal of Fatigue 29 (2007) 444–456
International Journal of Fatigue
www.elsevier.com/locate/ijfatigue

Fatigue reliability-based assessment of welded joints applying consistent fracture mechanics formulations

Efren Ayala-Uraga [a], Torgeir Moan [b,*]

[a] Department of Marine Technology, Norwegian University of Science and Technology, Otto Nielsens vei 10, N-7491 Trondheim, Norway
[b] Centre for Ships and Ocean Structures, Norwegian University of Science and Technology, Otto Nielsens vei 10, N-7491 Trondheim, Norway

Received 11 August 2005; received in revised form 15 May 2006; accepted 21 May 2006
Available online 1 August 2006

Abstract

Design of welded structures for fatigue limit state is normally carried out by means of either single- or two-sloped SN curves. To properly assess the effect of an inspection and repair strategy of structures degrading due to crack growth, fracture mechanics (FM) models need to be applied to describe crack propagation. To provide a proper tool for making decisions regarding the balance between design criteria and an optimal plan for inspection and repair in view of the inherent uncertainties, reliability methods should be applied. In this paper, alternative SN and FM formulations of fatigue are investigated. They include a crack growth formulation based on bi-linear crack growth law, considering both segments of the crack growth law as correlated and non-correlated in the failure probability calculation. The effect of inspection in the updated reliabilities is illustrated using first and second-order reliability methods as well as Monte Carlo simulation. It is argued that FM formulations need to be calibrated based upon SN-data. This is because the initiation of crack and its initial stages are subjected to uncertainties which are hard to quantify. The calibration of the FM method is specially based upon consideration of the crack initiation time, initial crack size and the crack aspect ratio.

Keywords: Fatigue; Welded joints; Crack growth; Reliability-based

1. Introduction

Fatigue damage becomes an important limit state for design of infrastructure because of the introduction of materials with higher static strength. Structures with significant dynamic loading are prone to develop fatigue damage during their service lives, especially those whose utilization is to be extended beyond the initial defined life time. The aircraft industry was the first to introduce fatigue as a criterion for design, and later other industries followed, such as the nuclear, steel bridge engineering, offshore, and later in the shipping industry as well. In the latter the use of high strength steels has led to the definition of an explicit fatigue limit state for design. Design criteria against fatigue failure are based upon SN data, obtained from tests on typical structural details. Good design practices also imply the use of in-service inspection, maintenance and repair (IMR), to keep adequate structural safety and system integrity during the service life. The introduction and development of fracture mechanics (FM) and reliability-based methods for crack growth assessment has signified substantial benefit and understanding of the different parameters and corresponding uncertainties involved in the fatigue damage process.

SN curves combined with the hypothesis of linear cumulative damage are applied to carry out the fatigue design check under variable amplitude loading, e.g. NORSOK [1]. Besides adequate design against fatigue failure, inspection and repair can be used to increase the reliability in view of crack growth. In order to guarantee the effect of inspection more details about the crack growth than provided by SN-data are required. Fracture mechanics then

* Corresponding author. Tel.: +47 73595541; fax: +47 73595528.
E-mail address: Torgeir.Moan@ntnu.no (T. Moan).

0142-1123/$ - see front matter © 2006 Elsevier Ltd. All rights reserved.
doi:10.1016/j.ijfatigue.2006.05.010

represents a potential tool to describe the gradual development of crack and hence account for the effect of inspection and possible repair at the different stages of crack growth. Due to the inherent uncertainties of the crack growth method and data, as well as those in the inspection procedure, reliability methods can be used to support the decisions regarding the balance between design, inspection and repair plan, e.g. Moan [2]. Recently, the use of an FM-based bi-linear crack growth law for fatigue analysis has been introduced (BS7910 [3]), which reduces the excessive conservatism believed to be implicit in the single slope Paris' law approach.

It is argued that FM formulations need to be calibrated based upon SN-data. Among the parameters involved in the FM models, the initiation time as well as the initial crack size and shape include uncertainties which are hard to quantify. Therefore, the calibration of the FM method is specially based upon consideration of the crack initiation time, initial crack size and the crack aspect ratio. The implications of using different methods to calculate the failure probability, namely first and second-order reliability methods and importance of sampling simulation, are also shown.

The purpose of this paper is to assess various fatigue reliability formulations based on either SN or FM approaches including an FM bi-linear crack growth law. In the latter formulation, it is considered that both segments of the crack growth law are either correlated or uncorrelated in the failure probability calculation. The corresponding inspection event margins are also defined for reliability updating and hence the effect of inspection is assessed and compared with the single slope law. The amount of conservatism of the single-sloped model with respect to the bi-linear one is illustrated.

2. Fatigue reliability

The basic failure probability may be defined by

$$P_{\mathrm{f}} = P[g(t) \leqslant 0] = \Phi(-\beta) \tag{1}$$

where $g(t)$ is the failure function and β is the reliability index. Most of the examples shown in the sections below are expressed in terms of the reliability index. $\Phi(\,)$ is the standard normal distribution function (see e.g. Melchers [4]).

The failure probability or the reliability index may also be updated with new information collected during the service life of the structure, e.g. with inspection results, based on the definition of conditional probability as

$$P_{\mathrm{f}_i,\mathrm{UP}} = P[g(t) \leqslant 0|\mathrm{IE}] = \frac{P[g(t) \leqslant 0 \cap \mathrm{IE}]}{P[\mathrm{IE}]} = \Phi(-\beta_{\mathrm{up}}) \tag{2}$$

where the inspection event IE may e.g. represent either "*no crack detection*" or "*crack detection*". The inspection events used herein are defined below.

Failure probabilities implied by Eqs. (1) and (2) may be calculated by means of well-established methods such as first-order reliability method (FORM), second-order reliability method (SORM) and Monte Carlo simulation (MCS) techniques, see e.g. Melchers [4], Madsen et al. [5]. The latter method is especially necessary to use when calculating reliability updating for the FM bi-linear model, as discussed in the sensitivity studies shown below. In the subsequent sections, SORM is applied to calculate the failure probability if not specified otherwise.

2.1. SN-based failure functions

New design approaches based on the SN curves, e.g. BS 7608 [6], NORSOK [1], include two-slope curves to account for the effect of variable amplitude loading. Gurney [7] first proposed using a detailed fracture mechanics model of fatigue crack initiation and growth in joints with fillet and butt welds. Haibach [8] proposed an integrated approach, also using fracture mechanics, and derived a two-slope SN curve. The first segment of the SN curve extends until a limit of constant-amplitude validity, whereas the second (lower) segment was found to have a slope equal to $2m_1 - 1$, with m_1 being the slope of the first (upper) segment. However, the criterion behind the definition of slope and position of the knuckle of both slopes seems to be not clear in design codes. For instance, the BS 7608 and NORSOK codes define the knuckle at 10^7 cycles in the SN curve, whereas the IIW [9] sets this value at 5×10^6 cycles. The BS 7608 assigns a slope of the lower segment equal to the slope of the upper segment plus 2; NORSOK recommends a fixed value of 5 and the IIW recommends using $2m_1 - 1$. This may be an indication that the lower segment implies uncertainties difficult to be quantified.

Recalling from Miner's rule the number of cycles contributing to fatigue damage N, i.e. $N = KS^{-m}$, where K is a constant defined under constant amplitude loading, S is the stress range and m is the slope of the curve. If the long-term stress range is assumed to be Weibull distributed with scale and shape parameters A and B, respectively,

$$F_{\mathrm{S}}(s) = 1 - \exp\left[-(s/A)^B\right] \quad \text{for } s > 0 \tag{3}$$

The fatigue damage may be expressed as (e.g. Nolte and Hansford [10])

$$D = \sum \frac{n_i}{N_i} = \frac{N}{K}\int_0^\infty s^m f_{\mathrm{S}}(s)\,\mathrm{d}s = \frac{N}{K}A^m\Gamma\left(1+\frac{m}{B}\right) \tag{4}$$

where $f_{\mathrm{S}}(s)$ is probability density of the long-term stress range s, assumed to be Weibull distributed as in Eq. (3).

In a two-sloped SN curve, the constant K_2 for the second slope is determined by

$$K_2 = K_1 S_0^{m_2 - m_1} \tag{5}$$

where m_1 and m_2 are the corresponding slopes and S_0 is the stress range at the knuckle of the slopes. This implies that the uncertainty corresponding to the first slope (i.e. CoV of K_1) is the same for the second slope. In principle, the uncertainty for the latter fatigue life is larger as this corresponds to long fatigue endurances, for which there are limited

data. This uncertainty is also reflected in the debate about which slope should be applied for the lower segment.

From the cumulative damage expression for a single slope SN curve model of Eq. (4), the damage in the 2-slope model is given by

$$D = N\left\{\frac{A^{m_1}}{K_1}\Gamma\left[1+\frac{m_1}{B};\left(\frac{S_0}{A}\right)^B\right]+\frac{A^{m_2}}{K_2}\gamma\left[1+\frac{m_2}{B};\left(\frac{S_0}{A}\right)^B\right]\right\} \tag{6}$$

From Eq. (5) it is readily seen that

$$D = \frac{N}{K_1}A^{m_1}\left\{\Gamma\left[1+\frac{m_1}{B};\left(\frac{S_0}{A}\right)^B\right]+\left(\frac{S_0}{A}\right)^{m_1-m_2}\gamma\left[1+\frac{m_2}{B};\left(\frac{S_0}{A}\right)^B\right]\right\} \tag{7}$$

The safety margin is expressed as $g(t) = \Delta - D \leqslant 0$, then for the 2-slope model it may be expressed as

$$g(t) = \Delta - \frac{N}{K}A^{m_1}\Gamma\left[1+\frac{m_1}{B};\left(\frac{S_0}{A}\right)^B\right] \times\left\{1+\left(\frac{S_0}{A}\right)^{m_1-m_2}\frac{\gamma[1+m_2/B;(S_0/A)^B]}{\Gamma[1+m_1/B;(S_0/A)^B]}\right\} \tag{8}$$

where Δ is the fatigue damage at failure, $\Gamma[;]$ and $\gamma[;]$ are the complimentary incomplete gamma and incomplete gamma functions, respectively.

The fatigue design criteria can be expressed by

$$D_c \leqslant \Delta_d \tag{9}$$

where D_c is the characteristic damage value determined by expected values of N, A in a long term period, and characteristic value (mean minus two standard deviations) for K.

A common design practice in the shipping industry is to consider a cumulative fatigue damage of $\Delta_d = 1$ in a 20-year service life. In the offshore industry, structures are designed against fatigue degradation considering fatigue damage ranging from Δ_d equal to 0.1 to 1.0, depending on the consequences of failure and accessibility of inspection (e.g. [1]). The equivalent stress range level corresponding to a certain damage D defined with a two-sloped SN curve (cf. Eq. (4)) is larger than that obtained by assuming single-sloped SN curve (Eq. (1)).

Fig. 1 shows the results of reliability calculations using safety margins corresponding to a single- (margin 1 slope) and two-slope (margin 2-slope) SN models for curve C according to BS 7608 [6]. See Table A1 for details about the input data. The design SN curve C corresponds to a flat plate or flushed welded joint. The stress levels are defined by using single slope curve (referred to in the figure as stress 1-slope) and two-slope (stress 2-slope). For the case of $\Delta_d = 1$, i.e. largest stress level, the reliability level for the case of "stress 2-slope, margin 2-slope" is virtually the same to the case "stress 1-slope, margin 1-slope" after 20 years. However, at a low stress level corresponding to $\Delta_d = 0.1$ the difference is large. This implies that at low stress levels the effect of the second slope has, as expected,

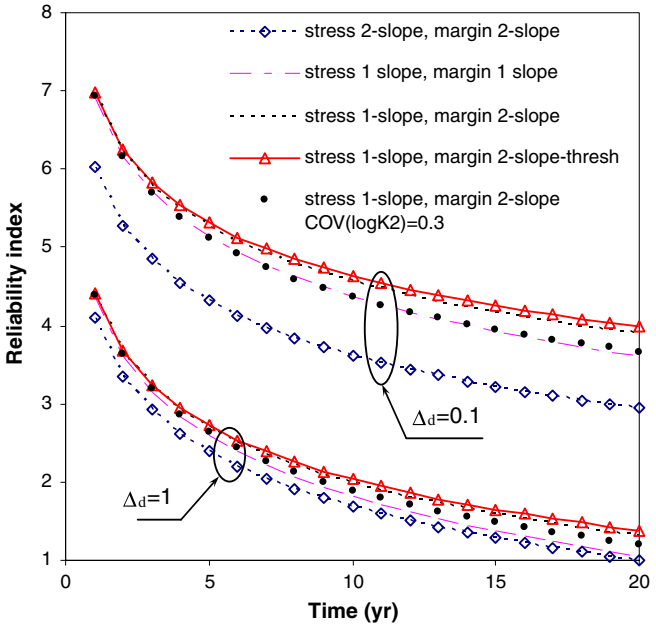

Fig. 1. Comparison of reliability levels obtained for $\Delta_d = 1$ and 0.1, using safety margins corresponding to one- and two-slope models for SN curve C, under different stress levels.

a significant effect. The case of "2-slope margin" under a stress level defined with 1-slope is also included. This figure also shows the case of a larger uncertainty for the second slope, in this case assumed to have a standard deviation of $\sigma_{\log K_2} = 0.3$, compared to the base case $\sigma_{\log K_1} = 0.204$ of the first slope included in the other reliability curves (see Table A2). As observed, the case of $\Delta_d = 0.1$ is more sensitive to the larger uncertainty in K_2, but the effect is relatively small.

Fig. 2 depicts the comparison of reliability calculations using different SN safety margins for a T-butt welded joint corresponding to an SN curve F. The stress level is defined with $\Delta_d = 1$ and $\Delta_d = 0.1$. This case is seen to be more sensitive to the model, as compared to the case with SN curve C.

2.2. Models based on fracture mechanics

The fatigue reliability and updating formulation often used is based on a fracture mechanics approach given by the Paris' crack propagation law (e.g. Madsen et al. [5]; Moan et al. [11]; Lotsberg and Sigurdsson [12]). In general, the Paris' law may be used in a multi-segmented one-dimensional crack growth as follows:

$$\frac{da}{dN} = \begin{cases} 0 & \text{for } \Delta K \leqslant \Delta K_{th} \\ C_1(\Delta K)^{m_1} & \text{for } \Delta K_{th} < \Delta K \leqslant \Delta K_1 \\ \vdots & \\ C_{n+1}(\Delta K)^{m_{n+1}} & \text{for } \Delta K > \Delta K_n \end{cases} \tag{10}$$

where a is crack depth, N is number of cycles, C_i is the crack growth rate parameter for segment i and m is its

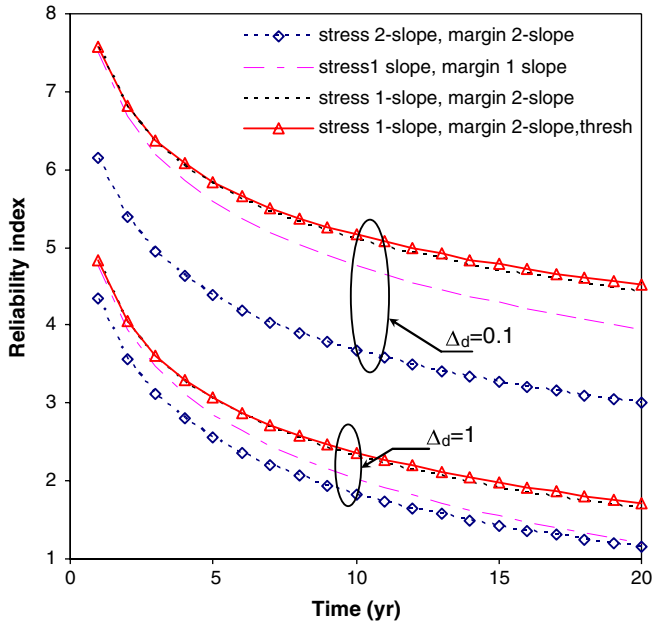

Fig. 2. Comparison of reliability levels obtained for $\Delta_d = 1$ and $\Delta_d = 0.1$, using safety margins corresponding to one- and two-slope models for SN curve F, under different stress levels.

corresponding slope, ΔK_{th} is a threshold of the stress intensity factor range and ΔK_i is the point of intersection of two consecutive segments. ΔK is given as a function of the crack depth a, as follows:

$$\Delta K = Y(a) \cdot S\sqrt{\pi a} = (Y_m S_m + Y_b S_b)\sqrt{\pi a} \tag{11}$$

where the one-dimensional compliance function $Y(a)$ is based on constant aspect ratio a/c; S is the stress range and the sub-indices m and b refer to the membrane and bending stress, respectively. This one-dimension model may be extended by generalizing Eq. (10) to cover crack growth in a (depth) as well as in c (length). The definition of the stress intensity factor range ΔK is a crucial aspect in evaluating the fatigue life of a welded joint.

For the particular case, where a constant geometry function Y is assumed and $\Delta K_{th} = 0$, the crack growth at time t may be easily integrated resulting in closed form expressions. This procedure is, however, non-conservative in welded joints, e.g. butt joints and fillet welded joints, where the weld toe magnifying effect has important implications. In general the geometry function, which is dependent upon the crack size and shape, may be defined as:

$$Y(a) = Y_{plate}(a) \cdot M_k(a) \tag{12}$$

where $Y_{plate}(a)$ is the geometry function corresponding to a semi-elliptical surface crack as proposed by Newman and Raju [13] from finite element analysis in flat plates subjected to axial and bending remote stresses. $M_k(a)$ is a magnification factor (or correction factor) which depends on the local weld geometry and accounts for the crack size and loading. The cases studied herein considering the $M_k(a)$ effect (joint F) is based on the formulation proposed by Bowness and Lee [14] and recommended in the BS 7910 [3]. Often, a model uncertainty γ_{geom} is introduced for the geometry function in the reliability analysis.

If the geometry function is to be considered as defined in Eq. (12), the failure function for fatigue as function of time can be written as $g(t) = a_f - a(t)$ (e.g. Madsen et al. [5]), or

$$g(t) = \int_{a_0}^{a_f} \frac{da}{G(a)[Y(a)\sqrt{\pi a}]^m} - C \cdot v_0 \cdot A^m \Gamma\left(1 + \frac{m}{B}\right) \cdot t \tag{13}$$

where a_0 and a_f are initial and final crack depths, respectively. This safety margin may be expressed in terms of the number of cycles N as the product of time t, and the average stress cycle frequency, v_0. In case of through thickness crack, a_f = plate thickness. Is it noted that all variables, except a_0 and a_f, in the fracture mechanics model are proportional to time, t, see Eq. (13). Hence, the relative magnitude of uncertainty varies with time. $G(a)$ is an auxiliary function that helps account for the threshold of stress intensity range ΔK_{th}, and it is defined by

$$G(a) = \frac{\Gamma\left(1 + \frac{m}{B}; \left(\frac{\Delta K_{th}}{A \cdot Y\sqrt{\pi a}}\right)^B\right)}{\Gamma\left(1 + \frac{m}{B}\right)} \tag{14}$$

$\Gamma(\cdot)$ and $\Gamma(\cdot;\cdot)$ are the Gamma and the complementary incomplete Gamma functions, respectively.

2.3. Bi-linear crack growth model

The British Standard BS7910 [3] recommends the use of a bi-linear crack growth law for fatigue assessment of welded structures, which is based on the study carried out by King [15]. King performed a comprehensive collection of data obtained from different sources and ended up recommending a two-segment crack growth law for steels. The uncertainties reported for both segments of the crack growth are different, with the largest variability in the (lower) near-threshold segment. The larger variability in the near-threshold segment may be explained by the inherent uncertainty of the ΔK threshold below of which no crack growth is experience, and due to the proximity to the small-crack regime. On the other hand, the lower uncertainty of the upper segment corresponds to the crack growth rates behavior well inside the stable region with high values of ΔK. However, there is no information provided on the correlation level between the two segments. Ayala-Uraga and Moan [16], Righiniotis and Chryssanthopoulos [17] assumed that the two segments of the crack growth law are uncorrelated. The effect of correlation in failure probability is investigated below.

Following Paris' law, a weighed (averaged) crack growth rate may be estimated based on the multi-segmented crack growth law implied by Eq. (10). Then, the crack growth rate for the bi-linear model may be expressed as (e.g. Kam and Dover [18])

$$\frac{da}{dN} = C_1(\Delta K)^{m_1} + C_2(\Delta K)^{m_2} \quad (15)$$

From Eq. (15) and with the assumption of Weibull distributed stress range as suggested in Eq. (3), this expression becomes

$$\frac{da}{dN} = C_1 A^{m_1}(Y(a)\sqrt{\pi a})^{m_1} \cdot G_1(a) + C_2 A^{m_2}(Y(a)\sqrt{\pi a})^{m_2} \cdot G_2(a) \quad (16)$$

The auxiliary (weighing) functions of Eqs. (15) and (16) $G_1(a)$ and $G_2(a)$ are, respectively, given by

$$G_1(a) = \Gamma\left[1 + m_1/B; \left(\frac{\Delta K_{th}}{A \cdot Y(a)\sqrt{\pi a}}\right)^B\right] - \Gamma\left[1 + m_1/B; \left(\frac{\Delta K_0}{A \cdot Y(a)\sqrt{\pi a}}\right)^B\right] \quad (17)$$

$$G_2(a) = \Gamma\left[1 + \frac{m_2}{B}; \left(\frac{\Delta K_0}{A \cdot Y(a)\sqrt{\pi a}}\right)^B\right] \quad (18)$$

Here, $\Gamma[;]$ is the complimentary incomplete gamma function. The value of the stress intensity factor range corresponding to the intersecting point of the two slopes, ΔK_0, is given by:

$$\Delta K_0 = \exp\left(\frac{\ln C_1 - \ln C_2}{m_2 - m_1}\right) \quad (19)$$

From the integration of Eq. (16) the failure function at time t may be given by

$$g(t) = \int_{a_0}^{a_f} \left(\frac{da}{dN}\right)^{-1} da - v_0(t - t_0) \quad (20)$$

where t_0 is the initiation time.

2.4. Validity of FM bi-linear models

In general, according to the data provided in the BS7910 [3] and King [15] the uncertainties of the material parameter C corresponding to the lower segment are larger than that of the upper segment. This also implies that the near-threshold crack growth rates have an influence, due to both the inherent uncertainty of very small crack growth behavior and due to the difficulty of measuring such rates in the tests. In addition, there is a lack of information regarding the degree of correlation existing between both segments. This has a direct implication in the reliability calculations as explained below. In order to verify the validity of the models four bi-linear cases are analyzed in the sequel, namely:

(1) *Random ΔK_0 – non-correlated*. The randomness of the SIF at the knuckle of both slopes, ΔK_0, is determined based on the variability of constants C_1 and C_2. The realizations of the knuckle imply a large range of ΔK_0 and corresponding crack growth rates. Since the uncertainty of the lower slope is generally much larger C_1 than C_2, it may be possible that some of the results are too conservative.

(2) *Random ΔK_0 – correlated ($\ln C_1$, $\ln C_2$)*. In this case, the pattern of realizations of ΔK_0 corresponds to a more or less fixed crack growth rate, Fig. 3b.

(3) *Fixed ΔK_0 – non-correlated*. From Fig. 3c, it is observed that in some realizations there could be discontinuities in the crack growth rate that makes it a bit unrealistic.

(4) *Fixed ΔK_0 – correlated ($\ln C_1$, $\ln C_2$)*. If correlation is introduced to the item 3 above, the model looks like that in Fig. 3d.

In all these cases, no threshold of ΔK correlated is considered.

Fig. 5 shows reliability results of a weld-flushed joint (C joint) using the four bi-linear models mentioned above. The bi-linear crack growth data of the BS7910 for $R > 0.5$ is used in the calculations. The stress level assumed in the example is based on a cumulative fatigue damage of $\Delta_d = 1$ in a design life of 20 years using SN curve C. The corresponding equivalent stress range implies stress intensity factor range ΔK in the range of 18–245 N/mm$^{3/2}$, whereas ΔK_0 at the intersection of both slopes is at 195.6. This indicates that the crack growth is mostly governed by the lower segment if the segments were described by deterministic C parameters. However, the effect is different if the uncertainty in C and correlation between segments is considered.

Model (1) provides higher reliabilities compared to model (2) with correlated slopes. This is due to the fact that the larger uncertainty of C_1 makes the slope of the upper segment to give more contribution as the realizations of ΔK_0 may occur at lower values, i.e. the realizations of the knee (intersection) may occur along the shadowed area in Fig. 4 for model (1), whereas for model (2) the possible intersections of the slopes are only possible along the red dots. The curve for model (2) approaches to the linear model at the initial stages of crack propagation. Even though models (3) and (4) imply introducing unrealistic discontinuities in the crack growth rate as observed in Fig. 3c–d, the effect seems to be well compensated among the various possible realizations of pairs of slopes.

It is important to emphasize that in the context of a bi-linear FM law in in-air conditions, most part of the propagation of surface cracks is very much influenced by the uncertainties related to the near threshold crack growth rates, whereas for through-thickness cracks, the propagation is driven by larger crack growth rates far away from the influence of the uncertainties inherent to the knuckle of both slopes. The cases illustrated in this paper deal with surface cracks only.

In the sensitivity studies presented in the following sections, the correlated-random ΔK_0 model is used, which is believed to represent most appropriately the bi-linear FM probabilistic formulation.

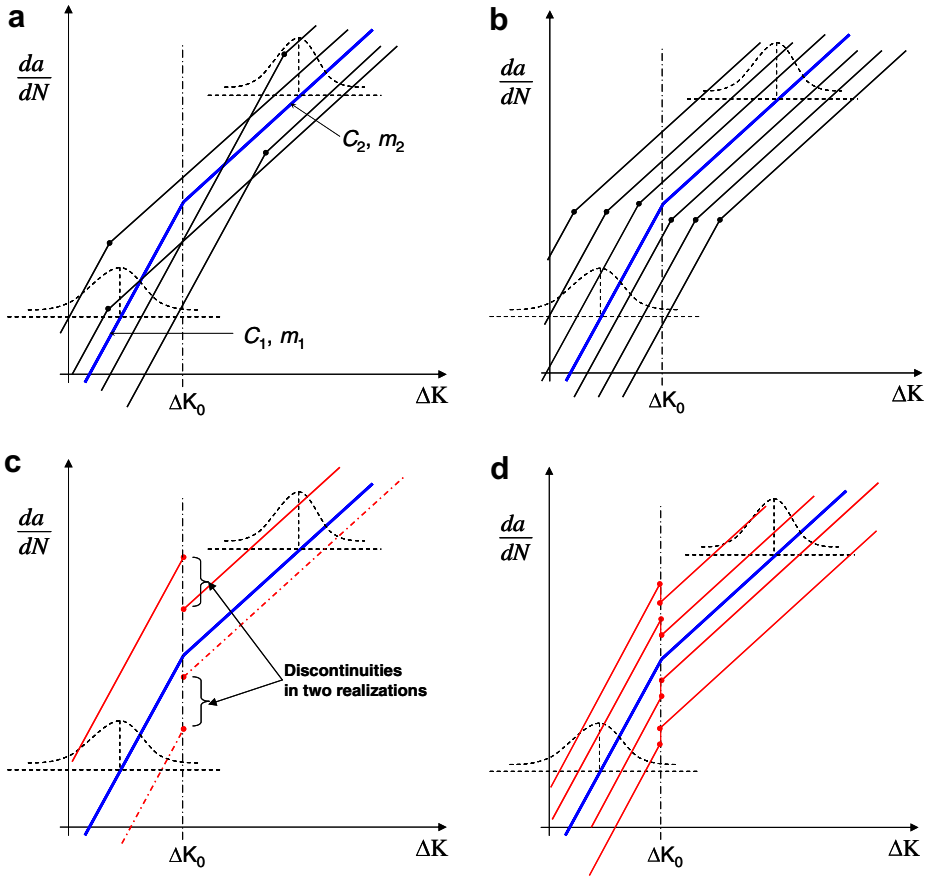

Fig. 3. Different bi-linear FM models: (a) random ΔK_0 – non-correlated; (b) random ΔK_0 – correlated ($\ln C_1$, $\ln C_2$); (c) fixed ΔK_0 – non-correlated and (d) fixed ΔK_0 – correlated ($\ln C_1$, $\ln C_2$).

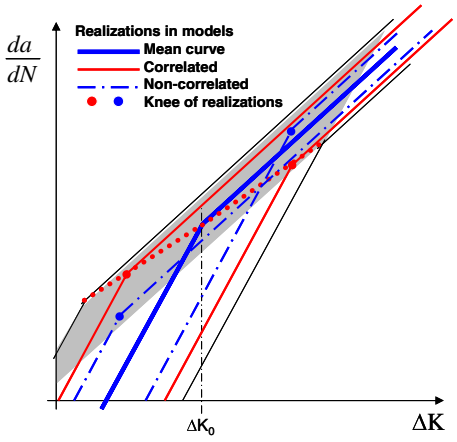

Fig. 4. Schematic representation of correlation effect in realizations of ΔK_0 in bi-linear crack growth model. Larger uncertainty in lower segment assumed.

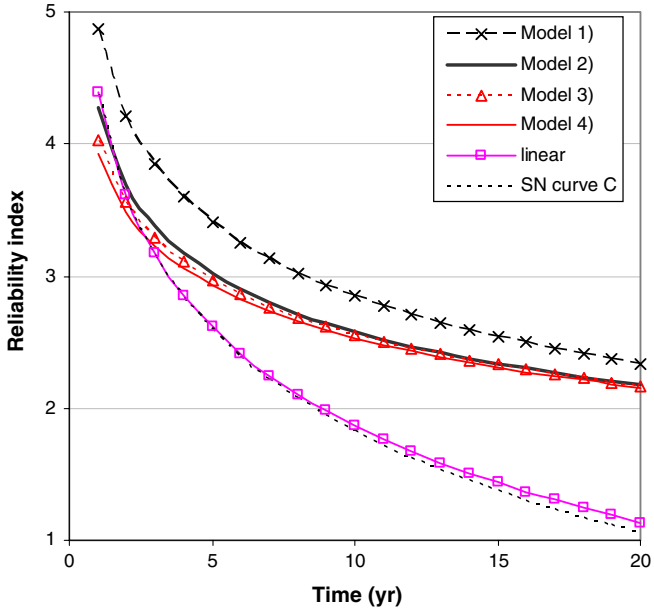

Fig. 5. Comparison of the different models in a flush-welded joint (joint C) using crack growth data from BS7910 for $R > 0.5$. Assumed: $a_0 = \mathrm{EX}(0.11)$, $\Delta_d = 1$, $a/c = 0.83$ and $\Delta K_{th} = 0$.

3. Sensitivity studies

As discussed in Ayala-Uraga and Moan [16], besides the uncertainty on the crack growth law parameter C, the uncertainties in the crack initiation period, the initial crack size as well as in the crack aspect ratio development, are those parameters that mostly influence the fatigue life and reliability of a welded component. It is argued, however, that the initiation time in welded structures is relatively small (10–15% of the total fatigue life) due to the

large number of microscopical defects introduced during the welding procedure as well as due to the stress raising effect of the weld geometry itself, e.g. Bouchard et al. [19], Otegui et al. [20]. Hence, the initiation time is neglected herein which is also a conservative assumption. In addition, the use of design curves obtained with constant amplitude loading.

Distribution of initial crack size should be defined with due account of the frequency of crack occurrence, e.g. per meter of weld (Moan et al., [21]). Bokalrud and Karlsen [22] found a_0 to be exponentially distributed with mean crack size of 0.11 mm, and 16 cracks per m. SN curves for weld specimens are usually obtained by test on narrow specimens, implying, maybe, 2 or more crack sites over the width. The expected value of the largest size of two independent cracks of the above type is for instance 0.17 mm.

The aspect ratio development of surface cracks depends on the applied stress profile throughout the thickness, as well as the density of initial defects along the weld toe, among other factors. The local weld geometry increases the likelihood of coalescence of the multiple surface cracks to form longer cracks at the toe, in e.g. fillet welds, which leads to shorter fatigue lives. Depending on the density of initial cracks per unit of length, the defects may coalesce to form longer cracks, i.e. smaller aspect ratio a/c. Some studies have dealt with the coalescence problem of multiple surface cracks and its effect in fatigue life estimation, e.g. Otegui et al. [20], Vosikovsky et al. [23], Eide and Berge [24], Burns et al. [25].

In the following sections, sensitivity studies are shown on the initial crack size a_0 and the crack aspect ratio a/c for a flush-welded joint (joint C) and a fillet-welded joint (joint F).

Fig. 6 shows a comparison of the fully correlated FM bi-linear model with the FM linear and SN-based (C curve) approaches corresponding to a flush-welded joint. Curves of two stress levels are included corresponding to $\Delta_d = 1$ and $\Delta_d = 0.1$. The curves related to the SN model are calculated using "stress 1-slope, margin 1-slope" as explained above. The FM calculations include linear models using data from BS7910 and DNV [26], cf. Table A4, as well as the bi-linear correlated model with BS data from [3], see Table A5. In all the cases, the material parameters used correspond to a stress ratio $R \geqslant 0.5$. It is observed that the reliability index curves corresponding to the bi-linear model drop at the beginning and rise and the end of the service life with respect to those of the FM linear and SN models. This effect is more pronounced for the case of lowest applied stresses, i.e. $\Delta_d = 0.1$, due to the fact that a larger amount of the crack growth is governed by the lower segment as compared to the case of $\Delta_d = 1$. Before 8 years, the reliability level is lower for the bi-linear compared to the SN model for $\Delta_d = 0.1$. It is also observed that the linear FM models may be fitted to the SN models, whereas the bi-linear ones seem to have a very different slope. No threshold has been included in neither FM nor SN curves.

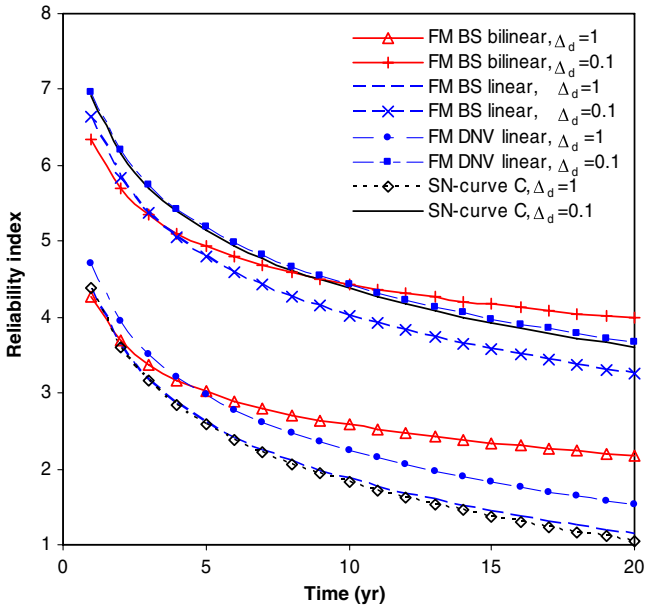

Fig. 6. Comparison of FM bi-linear and SN models for joint C. Assumed: $a_0 = \mathrm{EX}(0.11)$, $a/c = 0.83$; No threshold of ΔK.

3.1. Initial crack size

The initial crack size of a surface crack in welded joints induced by the welding process itself is of interest herein. In principle, the initial crack size may be defined as the depth (or length) from which a flaw has nucleated from surface defects and will grow under the stable crack propagation regime until a final crack size or fracture. Reliability-based crack growth analysis is very sensitive to the mean value of initial crack size (e.g. Moan [2]) and it is therefore an important parameter to be considered in the calibration procedure.

According to Bokalrud and Karlsen [22], the initial crack size obtained from actual welded details in ship hull structures was found to follow an exponential distribution with a mean value of 0.11 mm, and a rate of 16 cracks per m. In SN tests, however, small specimens are normally used. Then, assuming two independent initial cracks in a specimen as the type described above, the expected largest value would be of 0.17 mm, characterized by a Gamma distribution with standard deviation equal to 0.12 mm. Another study of initial crack sizes on real structures was reported in Moan et al. [21], where an extensive database of cracks detected in tubular joints of jacket located in the North Sea has been analyzed. The initial crack size derived was estimated to have a mean value of 0.19 mm exponentially distributed for an individual crack, whereas a mean value of 0.38 mm per hot spot was found. Carrying out fatigue tests on small specimens, Otegui et al. [20] reported an average of 8.8 initiation sites per 25 mm of weld toe. Their findings also indicate that for specimens under relatively high stress ranges up to 13 initiation sites were reported from undercut defects, whereas only 1 site

was found in a specimen subjected to 2.5 times lower stress range.

From Figs. 7 and 8, it may be observed that the flush-welded joint is more sensitive to the initial crack size than the fillet-welded joint, for both linear and bi-linear models. Both figures also include a case with initial crack size gamma distributed with mean of 0.17 mm and standard deviation of 0.12 mm.

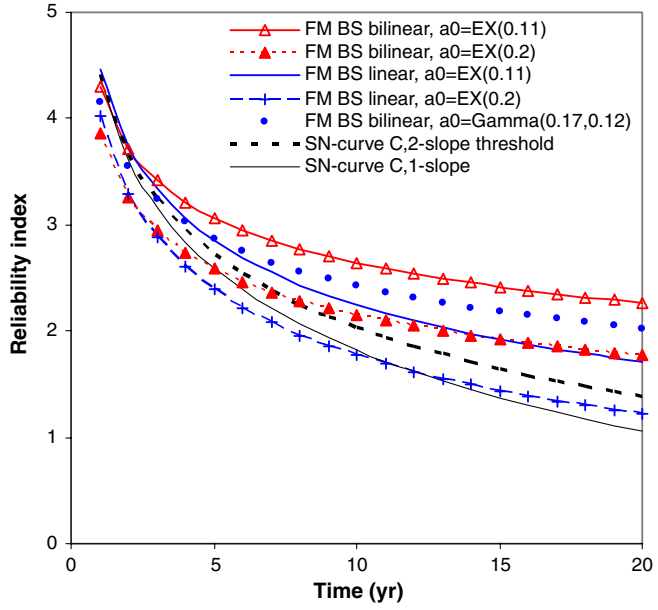

Fig. 7. Sensitivity of initial crack size a0 for joint C, $\Delta K_{th} = 63$, stress level for $\Delta_d = 1$.

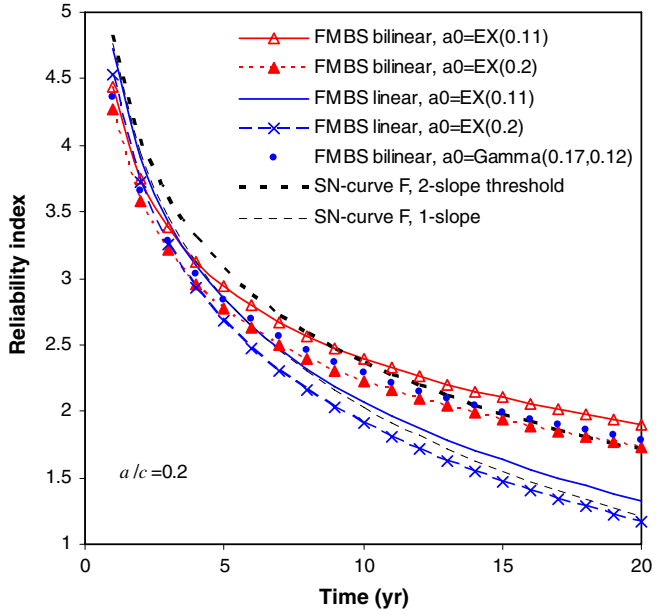

Fig. 8. Sensitivity of initial crack size a_0 for joint F (fillet-welded), $\Delta K_{th} = 63$, stress level for $\Delta_d = 1$, $a/c = 0.2$.

3.2. Crack aspect ratio development

In long fillet welds subjected to uniform stresses, as those in ship structures, the local weld geometry increases the likelihood of coalescence of single surface cracks, which leads to longer cracks (i.e. low aspect ratio), and hence shorter fatigue lives. In principle, the aspect ratio should be calculated by a two-dimensional crack growth model. If a constant aspect ratio is applied it ought to be weighted according to the time spent at various stages. The weight should be placed on the crack growth in the initial few mm.

The crack aspect ratio a/c varies as the crack propagates through the thickness, depending on the stress pattern and the effect of the local weld geometry, e.g. Burns et al. [25]. The use of forcing functions to describe the aspect ratio development is attractive for being used in a reliability framework, though their results are based on finite width specimens under specific loading conditions, which are sometimes difficult to generalize.

Multiple initial crack and coalescence models have been suggested. Vosikovsky et al. [23] fitted a model, where multiple initial defects have a semi-circular shape ($a/c \sim 1$). As the multiple micro cracks grow and coalescence takes place, the aspect ratio of the new coalesced crack decreases exponentially up to $a/c = 0.2$, which the value from which single crack growth was observed. The tests were performed under pure bending loading on fillet weld T-joints. Eide and Berge [24] carried out large scale fatigue tests of welded girders. The crack growth was focused on the weld of transverse stiffeners subjected to tensile stresses. They found that the aspect ratio at the very beginning shows a low value of ~0.2, which increases up to 0.6 before coalescence occurs, to then increase again to converge to a value of around 0.8. Otegui et al. [20] performed test in small T-butt specimens under bending loading. The aspect ratio shows a similar shape as reported by Eide and Berge at the first stage of the crack growth before the discontinuity of the curve due to coalescence. The single crack behavior was found to remain nearly constant at a value close to 0.2. They also found that the larger the stress level being applied the larger the frequency of crack initiation sites, which leads to earlier crack coalescence (i.e. low aspect ratio) and hence faster crack growth.

The use of forcing functions to describe the aspect ratio development as that recommended by Vosikovsky et al. [23] is attractive for being used in a reliability framework, though their results are based on finite width specimens under bending loading.

In general, the reliability analyses results showed that only the aspect ratio development taking place in the very few millimeters (e.g. less than 5 mm) are the most influential in the results, meaning that the single crack shape, after coalescence takes place, may be assigned a fixed value. Fig. 10 shows a comparison of reliability index calculations by using the forcing functions of Vosikovsky et al. [23] and

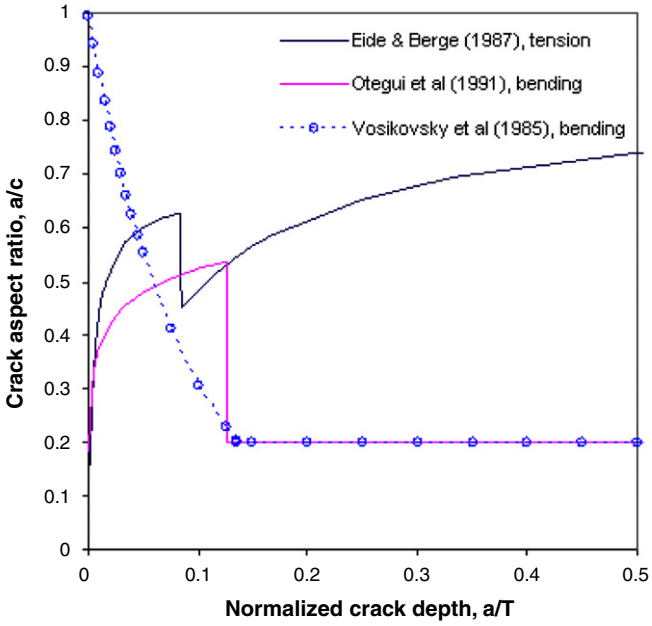

Fig. 9. Aspect ratio development according to different studies and loading modes.

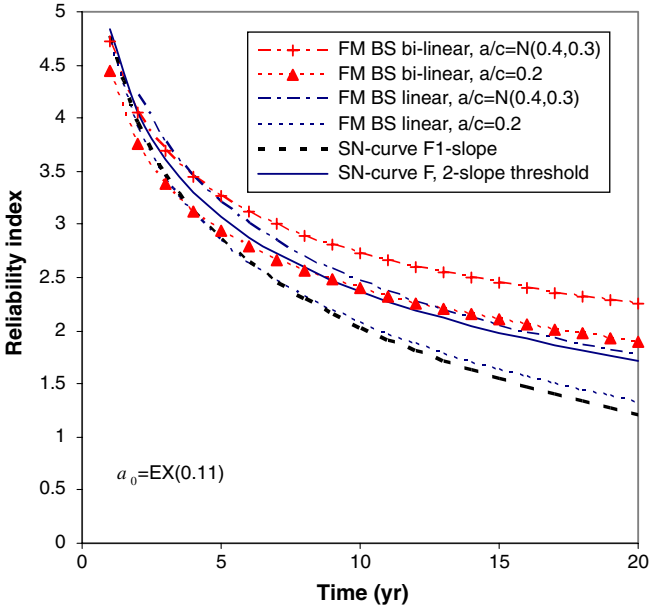

Fig. 11. Sensitivity of crack aspect ratio a/c for F joint, linear and bi-linear FM models. $a_0 = \mathrm{EX}(0.11)$; stress level according to $\Delta_d = 1.0$.

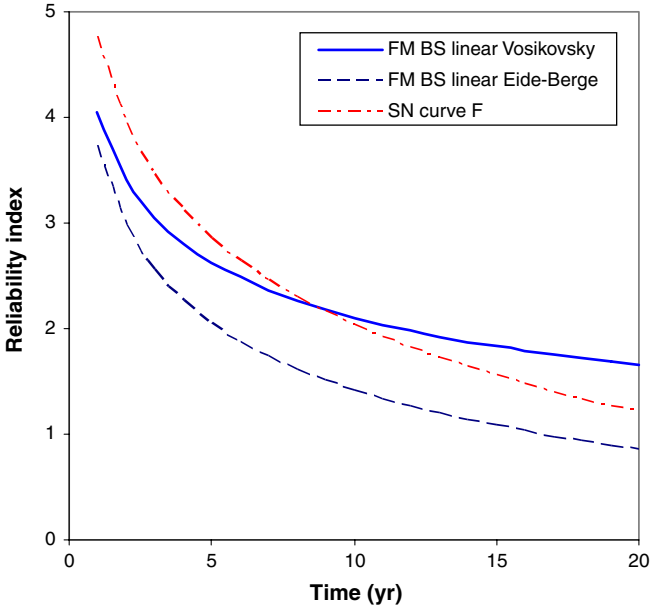

Fig. 10. Sensitivity of the aspect ratio development according to the models by Vosikovsky et al. [23] and Eide and Berge [24]. Linear FM model.

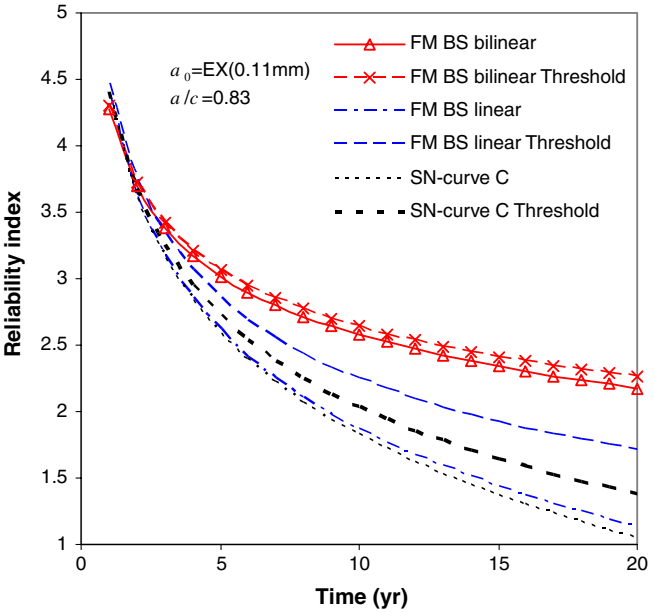

Fig. 12. Effect of threshold of ΔK in bi-linear and linear FM models.

Eide and Berge [24] shown in Fig. 9, to model the aspect ratio development. This figure also shows results obtained by Otegui et al. [20]. Fig. 10 shows that Vosikovsky's model is more conservative than Eide and Berge's, indicating that as most of the fatigue life is spent in the initial stages the larger aspect ratio of the former model results in larger reliability levels. However, neither of the curves seems to fit the reliability index curve obtained with SN curve F (see Figs. 11 and 12).

3.3. Threshold of ΔK

According to the data review by King [15] the threshold of the stress intensity factor range depends on the stress ratio R. For ferritic steels with yield stress less than 60 MPa the threshold increases as R reduces. However, the recommendation of BS7910 for welded joints is to assume a ΔK threshold value of 63 N mm$^{-3/2}$, which is adopted herein for both linear and bi-linear models, if not otherwise indicated.

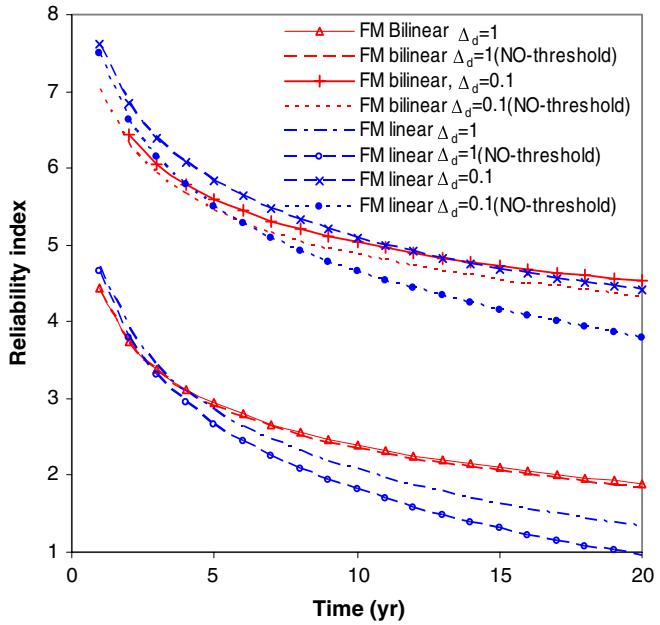

Fig. 13. Sensitivity of the threshold of ΔK in FM linear and bi-linear models for joint F. Assumed: $a_0 = \mathrm{EX}(0.11)$, $a/c = 0.2$; $\Delta K_{th} = 63$ N/mm$^{3/2}$.

As observed from Fig. 13 the safety of the joint, in terms of reliability index, is more sensitive for the linear FM model to the effect of SIF threshold than for the bi-linear FM model. For the latter the effect is negligible and it is therefore recommended to disregard the SIF threshold for the calculations, which is also reflected in reduced computational effort, especially for the case of low stress level, i.e. $\Delta_d = 0.1$, where convergence difficulties for the FORM/SORM may be found. It is also noticeable that the threshold effect has more relevance for joints under low stress level.

As is has been shown so far, the reliability index curves corresponding to the bi-linear FM model is difficult to be calibrated (fitted) to an SN-based reliability curve by utilizing a single parameter in the fitting procedure, as it is possible for the linear FM model. This means that a different strategy needs to be applied. Fig. 14 shows reliability index curves obtained with the linear FM model for both C- and F-joint, calibrated with respect to their corresponding 2-slope SN curve. The calibration procedure is achieved disregarding the initiation time, e.g. $T_0 = 0$ years. The mean value of the initial crack size results to be larger for the F joint ($\mu(a_0) = 0.2$ mm), than that for C joint ($\mu(a_0) = 0.15$ mm). Additionally, the crack aspect ratio is larger for the F joint, as it has been discussed before.

Fig. 15 shows calibrated bi-linear curves with respect to the corresponding 2-slope SN-curve for C- and F-joints. For both cases three parameters were used in the calibration procedure, namely initial crack size, aspect ratio and initiation time. It is observed that for the curve corresponding to joint-C an initiation time of $T_0 = 2$ years was utilized, as compared to $T_0 = 1$ year for joint-F, which agrees with the fact that for the latter the initiation time is shorter due to the stress amplification induced by the weld geometry effect. The other parameters used in the calibration for C- and F-joints are, correspondingly, the initial crack size $a_0 = \mathrm{EX}(0.11)$ and $\mathrm{EX}(0.2)$, as well as the aspect ratio which is Normally distributed with mean value of 0.7 and CoV of 0.3 for the former, and a fixed value of 0.2 for the latter.

3.4. Reliability updating with inspection

The advantage of using an FM formulation is that inspection results may be accounted for to update the estimated failure probabilities. The reliability updating

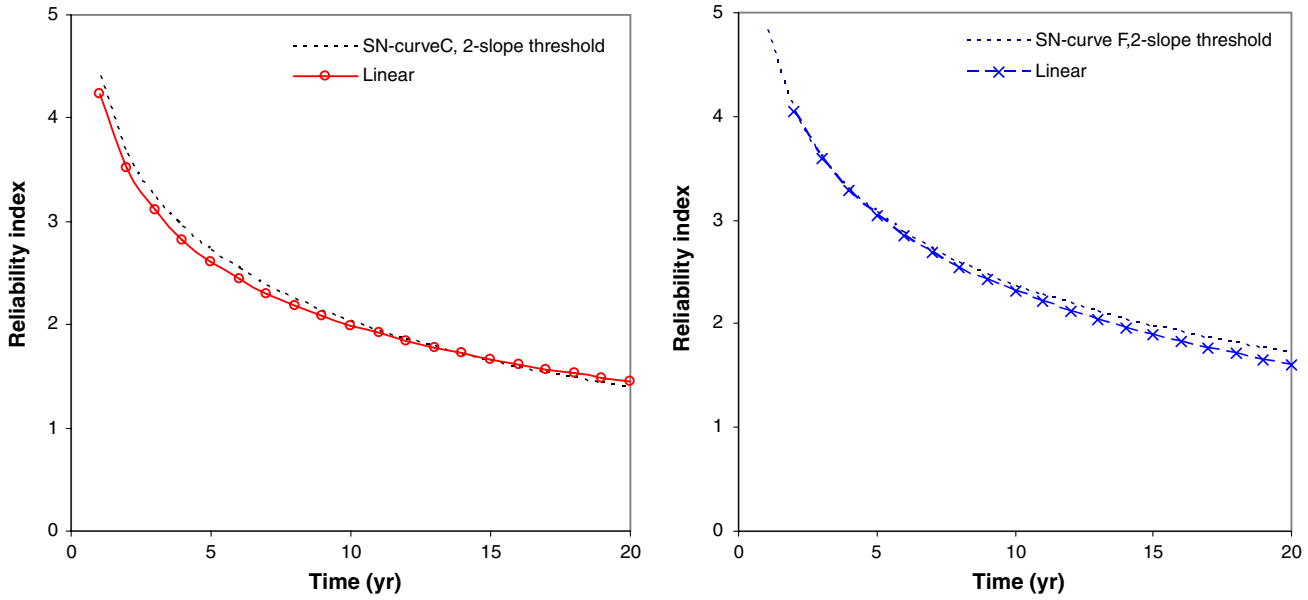

Fig. 14. Calibration of the linear FM model for C joint (left) and F joint (right).

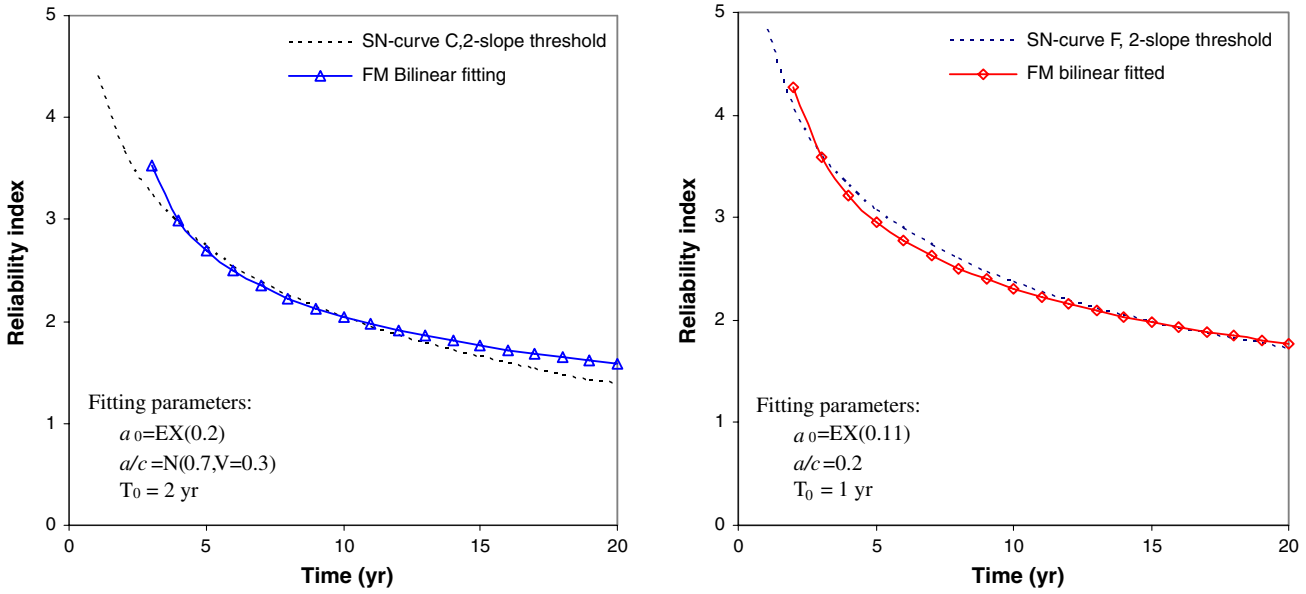

Fig. 15. Calibration of bi-linear FM model for C-joint (left) and F-joint (right).

approach used herein is based on definition of inspection events IE as implied in Eq. (2). The inspection event IE corresponding to the case of *no crack detection* at time t is given by:

$$I_{\mathrm{ND}}(t) = a_{\mathrm{D}} - a(t) > 0 \tag{21}$$

where the distribution function of the detectable crack size a_{D} is equal to the *probability of detection* (POD) curve. See e.g. Visser et al. [27] for typical values of POD curves. The inequality expressed by the inspection event of Eq. (21) implies that *no crack detection* is obtained when the detectable crack size is larger than the actual crack size at inspection time t. For the linear FM model, the inspection event $I_{\mathrm{ND}}(t)$ is equivalent to the failure function defined in Eq. (13), where the upper limit of the integral is substituted by a_{D}, i.e.

$$I_{\mathrm{ND}}(t) = \int_{a_0}^{a_{\mathrm{D}}} \frac{\mathrm{d}a}{G(a)[Y(a)\sqrt{\pi a}]^m} - C \cdot v_0 \cdot A^m \Gamma\left(1 + \frac{m}{B}\right) \cdot t > 0 \tag{22}$$

Similarly, for the bi-linear FM model, the event $I_{\mathrm{ND}}(t)$ is equivalent to Eq. (20) substituting the upper limit of the integral by a_{D} as well.

Fig. 16 shows the accuracy obtained by different reliability analysis methods in solving the failure probability problem with the bi-linear FM safety margin. In this case, an inspection is carried out at time $t = 10$ years with no crack found. It is observed the very good agreement between first-order (FORM) and second-order (SORM) methods with the results using Monte Carlo simulations for the fully correlated FM bi-linear model. However, the reliability updating curves (indicated as UPD in Figs. 16–18), i.e. considering inspection, obtained with FORM/SORM are below the results of MCS, implying that the non-linearity of the safety function introduces inaccuracies when the intersection of events suggested by Eq. (2) is calculated.

Figs. 17 and 18 show the updated reliability index curves resulting after an inspection at $t = 10$ years with no crack found, in both joints C and F, respectively. Both figures include reliability curves corresponding to linear and bi-linear FM models, as well as those obtained with SN curves (with threshold at 10^8 cycles). The basic curves without inspection are prolonged up to 20 years, for reference. It is observed that the updated curves corresponding to both linear and bi-linear FM models are very close to each other, even though the calibrated parameters used in both cases are different. The effect of updating, e.g. reliability curve at $t = 20$ years, is slightly larger for the F-joint than that obtained for joint C, with respect to the corresponding

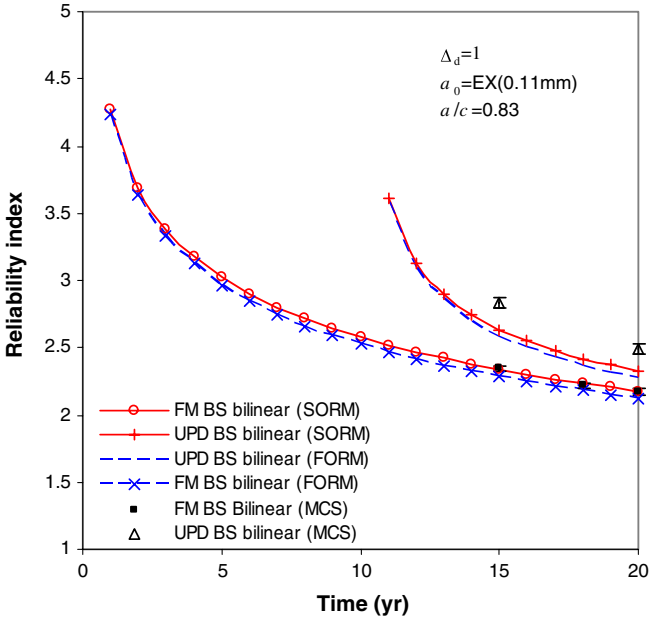

Fig. 16. Comparison among different reliability methods for the FM bi-linear model in a joint C case.

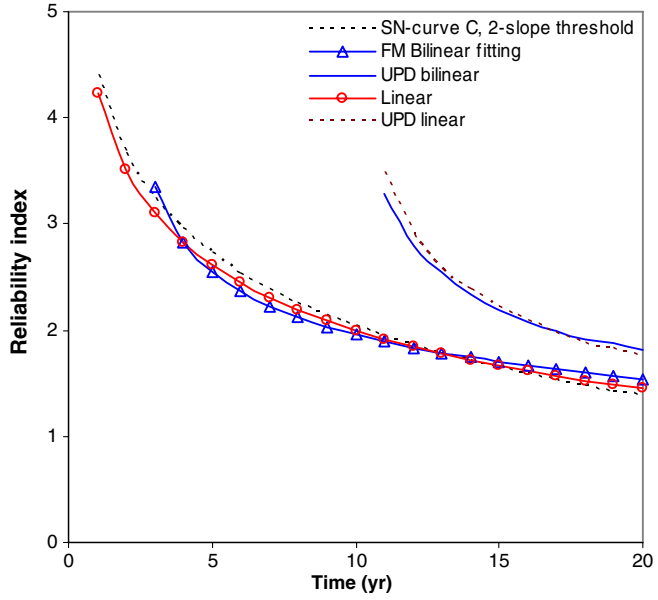

Fig. 17. Reliability updating using linear and bi-linear FM models in C joint. Assumed: $\Delta_d = 1.0$, $a_0 = \text{EX}(0.11)$, $a/c = 0.85$; $\Delta K_{th} = 63$ N/mm$^{3/2}$; SN-curve threshold at $N = 10^8$ cycles.

linear and bi-linear models. This is due to the fact that the crack growth rate is larger for joint F due to the raising effect of the weld geometry and hence, a larger crack size would be expected at time t. After the indication of no crack found at $t = 10$ years in the fillet-welded joint, with larger expected crack growth rate, shows slower decrease of the reliability level than that of the flushed joint.

The updated reliability index curves presented in both figures corresponding to linear and bi-linear FM models seem to be close to each other for these examples.

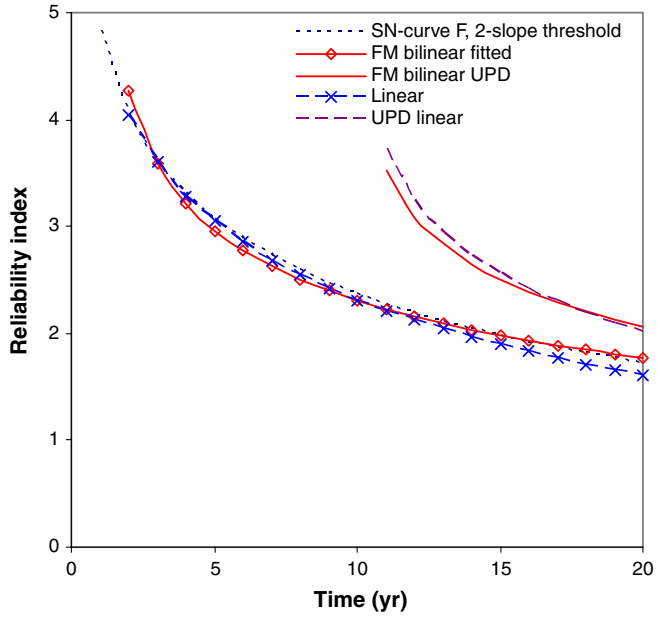

Fig. 18. Reliability updating using linear and bi-linear FM models in F joint. Assumed: $\Delta_d = 1.0$, $a_0 = \text{EX}(0.2)$, $a/c = 0.2$; $\Delta K_{th} = 63$ N/mm$^{3/2}$.

4. Conclusions

The use of reliability-based models to characterize the safety of a welded joint, including SN-, FM linear- and FM bi-linear models, has been presented. The FM bi-linear model validity has also been discussed.

It has been shown that calibration of the bi-linear FM model to the SN model with respect to the reliability index is not as simple as for the linear FM case. For the bi-linear FM approach, a calibration strategy based upon 2 or 3 parameters may be necessary.

The effect of inspection on reliability, i.e. reliability updating, for the bi-linear FM model needs to be carried out by means of Monte Carlo simulation, as the FORM/SORM approaches result to be non-conservative.

In order for the reliability calculations to be conservative when applying the bi-linear crack growth law, it is recommended to assume both segments to be highly correlated.

Acknowledgements

The first author acknowledges the financial support from the Department of Marine Technology, NTNU, and thanks Instituto Mexicano del Petróleo for providing the opportunity to pursue PhD studies at NTNU. The second author acknowledges the support from the Research Council of Norway to the Centre of Ships and Ocean Structures, NTNU.

Appendix. Input data

Table A1
Input for SN data (BS 7608 [6])

SN curve (joint type)	$N \leqslant 10^7$			$N > 10^7$	
	$\log K$	Std($\log K$)	m	$\log K$	m
C (flushed)	14.0342	0.2041	3.5	17.049	5
F (T-butt)	12.237	0.2183	3	15.728	5

Table A2
Basic data for FM models

Parameter	Distribution	Mean	Standard deviation
Initial crack size, a_0	Exponential	0.11	0.11
Scale parameter, $\ln A$	Normal	See Table A3	0.198
Shape parameter B	Fixed	1.14	
Average stress cycle, υ_0	Normal	0.158	0.07
Model uncertainty in geometry function, γ_{geom}	Normal	1.0	0.05
Stress ratio, $S_m/(S_m + S_b)$	Fixed	1.0	
Detectable crack size, a_d	Exponential	2.0	2.0
Wall thickness, critical crack size	Fixed	20	
Attachment length for M_k (only for joint F)	Fixed	25	
Threshold of SIF range, ΔK_{th}	Fixed	63	

Table A3
Weibull scale parameter A corresponding to stress levels for the different failure functions in SN and FM models used in the examples

SN curve	Δ_d	A (N/mm^2) (Mean ln A)	m
Single slope SN, no threshold			
C	1.0	23.72 (3.147)	3.5
	0.1	12.29 (2.489)	3.5
F	1.0	11.79 (2.448)	3
	0.1	5.472 (1.680)	3
Two-slope SN (limit of constant amplitude at N = 1E7)			
C	1.0	25.66 (3.225)	3.5; 5
	0.1	15.66 (2.731)	3.5; 5
F	1.0	13.484 (2.582)	3; 5
	0.1	8.117 (2.074)	3; 5

Table A4
Material parameters for linear crack growth laws

R	Mean (mean ln C)	Standard deviation (Std(ln C))	m
DNV [26] linear model			
	1.10E−13 (−29.97)	6.05E−14 (0.514)	3.1
BS 7910 [3] linear model			
In Air			
$R \geqslant 0.5$	2.5E−13 (−29.146)	1.355E−13 (0.508)	3.0

Table A5
Material parameters for bi-linear crack growth law in air corresponding to $R \geqslant 0.5$, according to the BS 7910 [3]

BS 7910 Bi-linear model						
Segment 1 (lower)			Segment 2 (upper)			ΔK_0[a]
Mean(C) ($\mu_{\ln C}$)	Stdv(C) ($\sigma_{\ln C}$)	m	Mean(C) ($\mu_{\ln C}$)	Stdv(C) ($\sigma_{\ln C}$)	m	
4.8E − 18 (−40.55)	8.10E − 18 (1.161)	5.1	5.86E − 13 (−28.32)	3.52E − 13 (0.555)	2.88	195.6

[a] Intersecting point ΔK_0 between segments 1 and 2. Units: N/mm$^{3/2}$.

References

[1] NORSOK Standard N-004. Design of steel structures. Oslo: Norwegian Technology Standards Institution; 1998.

[2] Moan T. Reliability-based management of inspection, maintenance and repair of offshore structures. J Struct Infrastruct Eng 2005;1(1):33–62.

[3] BS 7910. Guidance on methods for assessing the acceptability of flaws in fusion welded structures, BS 7910. London (UK): British Standards; 1999.

[4] Melchers RE. Structural reliability analysis and prediction. 2nd ed. West Sussex (UK): John Wiley & Sons; 1999.

[5] Madsen HO, Krenk S, Lind NC. Methods of structural safety. New Jersey: Prentice-Hall Inc.; 1986.

[6] BS 7608. Code practice for Fatigue design and assessment of steel structures, BS 7608. London (UK): British Standards; 1993.

[7] Gurney TR. Cumulative damage calculations taking account of low stresses in the spectrum. Weld Res Int 1976;6(2):51–76.

[8] Haibach E. Contribution to discussion. The welding institute conference on fatigue of welded structures. Brighton, UK; 1970.

[9] IIW. Recommendations for fatigue design of welded joints and components. International Institute of Welding, IIW document XIII-1539-96/XV-845-96. Paris, France; 2002.

[10] Nolte and Hansford. Closed-form expressions for determining the fatigue damage of structures due to ocean waves. In: Proceedings of the offshore technology conference, Dallas, TX, Paper 2606, 1976.

[11] Moan T, Hovde GO, Blanker AM. Reliability-based fatigue design criteria for offshore structures considering the effect of inspection and repair. In: Proceedings of 25th Offshore Technology Conference, Vol. II. Houston; 1993. p. 591–600.

[12] Lotsberg I, Sigurdsson G. Assessment of input parameters in probabilistic inspection planning for fatigue cracks in offshore structures. In: Proceedings of the ninth international conference on structural safety and reliability, ICOSSAR'05. Rome, Italy; 2005.

[13] Newman JC, Raju JS. An empirical stress-intensity factor equation for the surface crack. Eng. Fract Mech 1981;15(1–2):185–92.

[14] Bowness D, Lee MMK. Weld toe magnification factors for semi-elliptical cracks in T-butt joints. Offshore Technology Report – OTO 1999 014. Health Safety Executive; 1999.

[15] King RN. A review of fatigue crack growth rates in air and sea water. Offshore Technology Report OTH 511. London: Health Safety Executive, HSE Books; 1998.

[16] Ayala-Uraga E, Moan T. Reliability based assessment of welded joints using alternative fatigue failure functions. In: Augusti G, Schüeller GI, Ciampoli M, editors. Proceedings of the international conference on structural safety and reliability ICOSSAR 2005. Rome, Italy; 2005.

[17] Righiniotis TD, Chryssanthopoulos MK. Fatigue and fracture simulation of welded bridge details through a bi-linear crack growth law. Struct Saf 2004;26:141–58.

[18] Kam JCP, Dover WD. Corrosion fatigue of welded tubular joints: fracture mechanics modeling and data interpretation. In: Proceedings of the eighth international conference on offshore mechanics and arctic engineering. The Hague, The Nederlands; 1989.

[19] Bouchard R, Vosikovsky O, Rivard A. Fatigue life of welded plate T joints under variable-amplitude loading. Int J Fatigue 1991;13(1):7–15.

[20] Otegui JL, Burns DJ, Kerr HW, Mohaupt UH. Growth and coalescence of fatigue cracks at weld toes in steel. Int J Pres Ves Piping 1991;48:129–65.

[21] Moan T, Vårdal OT, Hellevig NC, Skjoldli K. Initial crack depth and POD values inferred from in-service observations of cracks in North Sea jackets. J Offshore Mech Arctic Eng 2000;122:157–62.

[22] Bokalrud T, Karlsen A. Probabilistic fracture mechanics evaluation of fatigue failure from weld defects in butt weld joints. In: Proceeding on conference on fitness for purpose validation of welded constructions. London, UK, Paper 28; 1981.

[23] Vosikovsky O, Bell R, Burns DJ, Mohaupt UH. Fracture mechanics assessment of fatigue life of welded T-joints including thickness effect. In: Proceedings of the fourth international conference on behavior of offshore structures, BOSS 85. Amsterdam: Elsevier; 1985. p. 453–64.

[24] Eide OI, Berge S. Fracture Mechanics analysis of welded girders in fatigue. In: Proceedings of the international conference on fatigue of welded constructions. Brighton, UK; 7–9 April, 1987.

[25] Burns DJ, Lambert SB, Mohaupt UH. Crack growth behaviour and fracture mechanics approach. In: Noordhoek C, Back L, editors. Steel in marine structures. Amsterdam: Elsevier Science Publishers; 1987.

[26] DNV. Classification Note No. 30.2 fatigue strength analysis for mobile offshore units. Det Norske Veritas, Høvik, Norway; 1984.

[27] Visser W. POD/POS curves for non-destructive examination. Offshore Technology Report OTO 2000/018. Health & Safety Executive, UK; 2000.

Article 2. Reliability-based assessment of deteriorating ship structures operating in multiple sea loading climates

Authors: **Moan, Torgeir** and **Ayala-Uraga, Efren**.

Published in: *Reliability Engineering and System Safety*, Vol. **93** (2008), No. 3, pp. 433-446.

Refereed article

Preface

A reliability-based model for assessment of deteriorating ships subjected to multiple environmental conditions is established in this article. Deterioration due to combined crack growth and corrosion in structural components of a ship hull is accounted for based on a fracture mechanics formulation. The model takes into account the corrosion-induced increased crack growth rate due to the increased stress range produced by the plate thinning (wastage) effect. Sensitivity studies are carried out to evaluate the effect of inspection updating on a production ship subjected to two different climate conditions.

Available online at www.sciencedirect.com
ScienceDirect
Reliability Engineering and System Safety 93 (2008) 433–446
RELIABILITY ENGINEERING & SYSTEM SAFETY
www.elsevier.com/locate/ress

Reliability-based assessment of deteriorating ship structures operating in multiple sea loading climates

Torgeir Moan[a,*], Efren Ayala-Uraga[b]

[a]Centre for Ships and Ocean Structures, Norwegian University of Science and Technology, Marine Technology Centre, Tyholt, N 7491 Trondheim, Norway
[b]Department of Marine Technology, Norwegian University of Science and Technology, Marine Technology Centre, Tyholt, N 7491 Trondheim, Norway

Accepted 11 December 2006
Available online 12 January 2007

Abstract

A reliability-based model for assessment of deteriorating ships subjected to multiple environmental conditions is established. Deterioration due to combined crack growth and corrosion in structural components of a ship hull is accounted for based on a fracture mechanics formulation. The model enables to take into account the corrosion-induced increased crack growth rate in two ways: (1) the increased stress range produced by the plate thinning (wastage) effect and (2) corrosion fatigue itself. Sensitivity studies are carried out to evaluate the effect of inspection updating on a production ship subjected to two different climate conditions. The hazard rate concept is adopted as a measure of reliability and emphasized throughout the different case studies.

Keywords: Reliability based; Fatigue; Corrosion; Deteriorating ships; Life extension

1. Introduction

A common practice nowadays in the offshore industry is to operate floating production ships (FPS) during a certain time in a given location and later deploy them to a different location, most likely in different climate conditions. Most of the applications are conversions of ocean-going oil tankers to relatively benign environmental areas such as Southeast Asia, West Africa and Offshore Brazil near the Equator. Conversion of tankers to FPSs may be carried out with ships of different age. Fatigue damage is very dependent on local wave conditions, and on the other hand, corrosion rates may also change from site to site.

Cracks in ship hull structures have always been an important concern for regulators and operators, as shown by the service experiences reported by Sucharski [1]. Until recently fatigue of trading vessels was implicitly covered by allowable stress (section modulus) requirements to wave loading. Use of high tensile steels, and particular local dynamic loads imply that fatigue might be a crucial design criterion.

Different measures are adopted during the design, fabrication and operation stages of ships in order to control fatigue cracking throughout the service life. This includes design, inspection and repair. Acquiring information of the integrity of a hull structure is a crucial task to be carried out during the operation of the vessel. Planning of inspection tasks is important in order to achieve economic and reliable results. Frequency, location and level of inspection are of course of concern during the planning process. An updated record of the inspection results, as well as the maintenance and repair task carried out to the structure during the service life is indispensable.

Another strength degradation phenomenon is corrosion, generally accounted for as uniform corrosion wastage. Studies, e.g. [2–4] show corrosion rates ranging from 0.01 to 0.3 mm/yr for general corrosion. Corrosion wastage increases nominal stresses and hence, induces earlier fatigue failure, as well as reduces ultimate strength capacity. Corrosion damage is not commonly treated as a failure criterion in itself, but if corrosion allowance is exceeded, the component is to be replaced. In this paper, the effect of plate thinning on fatigue is considered.

*Corresponding author. Tel.: +47 7359 5541; fax: +47 7359 5528.
E-mail address: tormo@marin.ntnu.no (T. Moan).

0951-8320/$ - see front matter © 2007 Elsevier Ltd. All rights reserved.
doi:10.1016/j.ress.2006.12.008

During the design stage, the effect of corrosion is dealt with by specifying a coating, cathodic protection and/or a corrosion allowance on the plate thickness. However, during the service life of ships the corrosion protection system is prone to fail after some time in operation, so its negative effects on the ship hull's strength are to be explicitly considered especially if its service life is extended. Moreover, the fatigue strength will be affected by possible increased crack growth rate, i.e. corrosion fatigue, once the corrosion protection system has failed.

Fatigue and corrosion effects on the strength are dealt with by design, as well as inspection and repair during operation. Such degradation becomes particularly important in connection with service life extension. Due to the significant uncertainties inherent in the degradation process and the uncertainties in the inspection and repair reliability model is preferable to obtain a measure of safety. Updating of the reliability can be made using Bayesian methods based on additional information by either updating variables, as made by Shinozuka, Yang, Itagaki and reviewed by Yang [5], or event updating, see e.g. Madsen et al. [6].

The aim of this paper is to establish a reliability-based procedure for assessment of deteriorating ship structures which are operated under multiple climate conditions, by accounting for the interaction between fatigue and corrosion wastage in terms of an accelerated crack growth rate due to plate thinning. A component-based model for fatigue reliability is proposed through a fracture mechanics crack growth formulation, which considers the uncertainties related to the stress intensity factors and weld toe effects.

Additionally, a robust fatigue reliability formulation is proposed to efficiently assess, by means of SORM, the safety of welded joints of a ship subjected to two different (or multiple) climate conditions throughout the service life. This formulation is also compared with a simplified fracture mechanics approach, i.e. geometry function Y constant, in order to highlight the efficiency and robustness of the proposed model. Accordingly, a series of inspection events are also defined for reliability updating in view of fatigue cracks and thickness measurement, both before and after the vessel has changed its location and, thereby, climate conditions. The formulation is demonstrated by a case study.

2. Reliability model considering fatigue failure and corrosion

2.1. Stress ranges in different sea climates

The long-term stress range distribution is calculated as a weighed average of the short-term distributions, with the weights proportional to the number of stress cycles in every sea state, described by the significant wave height, zero-crossing period and mean wave direction, e.g. a wave scatter diagram. The wave scatter diagram is a joint probability table of significant wave heights and wave periods defined from data collected over a long period of time. The largest uncertainties are expected from the inherent variability of the waves as well as from those related to the environmental description through the scatter diagram, including directionality and wave energy spreading.

Fatigue load effects are described by the long-term distribution of stress ranges, S. In general, the following two-parameter Weibull distribution is applied, which has been found to properly describe the long-term distribution for fatigue analysis in marine structures, see e.g. Nordenström [7]. This distribution has the form

$$F_S(s) = 1 - \exp\left[-\left(\frac{s}{A}\right)^B\right] \tag{1}$$

for $s>0$, where A and B are the scale and shape parameters of the distribution, respectively. The corresponding uncertainty is modeled by the parameters A and B, which then depend upon uncertainties associated with environmental conditions, wave load model and structural modeling. Guedes Soares and Moan [8] have studied the uncertainties involved in fitting the long-term load effects in ships for fatigue design. In this reference the shape parameter B has been reported to be typically around 1.0 for FPS and tankers operating in the northern North Sea. However, this value may be much lower for locations with tropical climate and sheltered waters, e.g. Gulf of Mexico (GoM), or Campos Basin in Brazil.

By assuming S_0 to be the maximum wave-induced stress response out of N_0 wave cycles, i.e. with probability of exceedance of $1/N_0$, the Weibull scale parameter may be determined as follows:

$$P(S \leqslant S_0) = 1 - \exp(-(S_0/A)^B) = 1 - 1/N_0, \tag{2}$$

then

$$A = S_0(\ln N_0)^{-1/B}. \tag{3}$$

The number of wave cycles may be different from site to site around the globe. In the Northern North Sea (NNS), for instance, the average long-term zero upcrossing frequency is typically 0.13–0.16 cycles per second ($4.1–5\times10^6$ cycles/year), whereas for a site in the GoM is around 0.2 cycles/s (6.4×10^6 cycles/year). Based on the assumptions of fatigue loading given by the Weibull distribution and resistance given by the S–N curve $N = KS^{-m}$, where K and m are constants which depend on the welded geometry, Guedes Soares and Moan [8] have shown that the major contribution for fatigue occurs around the stress range given by

$$S = S_0\left(\frac{m+B-1}{B\ln N_0}\right)^{1/B}. \tag{4}$$

A very useful definition in simplified fatigue analysis is the definition of the mth statistical moment of the expected long-term stress range. Hence, if the stress range is assumed Weibull distributed, it may be expressed in terms of the scale and shape parameters of the distribution,

as follows:

$$E[S^m] = \int_0^\infty s^m f_S(s)\,\mathrm{d}s = A^m \Gamma\left(1+\frac{m}{B}\right). \tag{5}$$

2.2. Fatigue failure

The fatigue reliability and updating formulation defined in this paper is based on a fracture mechanics approach given by the Paris' crack propagation law, namely

$$\frac{\mathrm{d}a}{\mathrm{d}N} = \begin{cases} C(\Delta K)^m, & \text{for } \Delta K > \Delta K_{\mathrm{th}}, \\ 0, & \text{for } \Delta K \leqslant \Delta K_{\mathrm{th}}, \end{cases} \tag{6}$$

where a is crack depth, N is number of cycles, C is crack growth parameter, m is the inverse slope of the SN curve, and ΔK_{th} is a threshold of the stress intensity factor range ΔK given as a function of a as

$$\Delta K = Y(a) S \sqrt{\pi a} = (Y_{\mathrm{m}} S_{\mathrm{m}} + Y_{\mathrm{b}} S_{\mathrm{b}}) \sqrt{\pi a}, \tag{7}$$

with a one-dimensional compliance function $Y(a)$ based on constant aspect ratio a/c. S is the stress range and the sub-indices m and b refer to membrane and bending stress, respectively. In general, the geometry function, which is dependent upon the crack size, may be defined as

$$Y(a) = Y_{\mathrm{plate}}(a) M_k(a), \tag{8}$$

where $Y_{\mathrm{plate}}(a)$ is the geometry function corresponding to a semi-elliptical surface crack as proposed by Newman and Raju [9], which is dependent upon crack size and shape and determined by fitting results from finite element analysis in flat plates subjected to axial and bending remote stresses. The crack aspect ratio, a/c, varies throughout the crack growth, and it is an important parameter to be accounted for, see e.g. Burns et al. [10]. $M_k(a)$ is a magnification factor (or correction factor) which depends on the local weld geometry and accounts for the crack size and loading, as proposed by Bowness and Lee [11] and adopted in the BS 7910 [12].

By integrating Eq. (6) the failure function for fatigue of the form $M(t) = a_f - a(t) \leqslant 0$ may be formulated, e.g. as shown by Madsen et al. [6], as

$$M(t) = \int_{a_0}^{a_{\mathrm{f}}} \frac{\mathrm{d}a}{G(a)\left[Y(a)\sqrt{\pi a}\right]^m} - C v_0 A^m \Gamma\left(1+\frac{m}{B}\right) t \leqslant 0, \tag{9}$$

where a_0 and a_{f} are initial and final crack depths, respectively. Here, the number of cycles N is the product of time t, and the average stress cycle frequency, v_0. The long-term stress range is assumed Weibull distributed, in which A and B are the scale and shape parameters of the distribution. In case of through thickness crack, a_{f} = plate thickness. $G(a)$ is defined by

$$G(a) = \frac{\Gamma\left(1+(m/B);\ \left(\Delta K_{\mathrm{th}}/\left(A Y \sqrt{\pi a}\right)\right)^B\right)}{\Gamma\left(1+(m/B)\right)}, \tag{10}$$

where $\Gamma(\cdot)$ and $\Gamma(\cdot;\cdot)$ are the gamma and the complementary incomplete gamma functions, respectively.

The failure probability is calculated as $P_{\mathrm{f}} = P[M(t) \leqslant 0]$.

2.3. Effect of corrosion on fatigue damage

Some researchers, e.g. [13–15], have studied the effect of corrosion and fatigue in assessing the safety of aging ship structures. However, the interaction between these two deteriorating agents has not been treated in such studies.

In this study, the fatigue–corrosion interaction is accounted for by

- introducing a correction factor to the material parameter C, e.g. C_{corr}. This correction factor is equal to 1 before failure of the coating, and greater than 1 after no corrosion protection exists. The crack growth rate under free corrosion conditions may correspond to a factor C_{corr} of 3 [16,17].
- modifying the long-term stress ranges in the corroded plate to account for the corrosion wastage (plate thinning). A probabilistic model to account for this effect is described in the following.

The corrosion process is assumed to start when the corrosion protection system, e.g. coating, fails. The coating protection time, t_0, is the average time the coating system is effectively working in the structure. The time it takes for the coating protection to fail has a large scatter, as it may fluctuate between 5 and 15 years, e.g. [16]. This parameter has to be treated as a random variable. Once the corrosion protection fails the metal starts to corrode with a certain corrosion wastage rate, which is dependent upon the location within the ship structure and geometry of the component. The effect of pitting/grooving corrosion may be relevant in certain particular cases, not treated herein.

Assuming a fixed annual thickness reduction rate due to corrosion throughout the service life of a certain component, the long-term stress range may be defined as function of the corrosion rate R_{corr}. Considering that the long-term stress range is Weibull distributed, hence a time-varying scale parameter A may be derived as shown in the following. Let the wall thickness h at time t be given by

$$h(t) = h_0 - W(t), \tag{11}$$

where h_0 is the initial value of the wall thickness and $W(t)$ is the thickness wastage due to corrosion. The time-dependent corrosion wastage may be defined as

$$W(t) = R_{\mathrm{corr}} \alpha (t - t_0), \tag{12}$$

for $t \geqslant 0$, where R_{corr} is the annual wastage rate or corrosion rate, whose mean values are exemplified in [3,4] for different structural components; α is a factor equal to 1 if the corrosion rate is one-sided or 2 if it is two-sided.

By using Eqs. (11) and (12), the time dependent wall thickness reads

$$h(t) = h_0 - R_{\text{corr}}\alpha(t - t_0). \tag{13}$$

Assuming that membrane stresses in a certain structural component are induced by global wave load effects, the equivalent stress range in intact (initial) conditions S_0 is as shown in Fig. 1. After the coating fails at time t_0 corrosion starts to induce a thickness loss with a fixed annual rate, i.e. the stress level is increased due to the plate thickness reduction. At any time t after coating failure the relationship $S_0h_0 = S(t)h(t)$ holds true. From this relationship and by using the definition of Eq. (13) it is readily seen that the increment in the equivalent stress range during the time interval Δt is given by

$$S(\Delta t) = \frac{S_0}{1 - \alpha R_{\text{corr}}(\Delta t)/h_0}. \tag{14}$$

According to the definition of the mth moment of the expected long-term stress range given by Eq. (5), from Fig. 1 it may be observed that an equivalent stress which accounts for the thinning effect of corrosion may be expressed as follows:

$$S(t)^m = \frac{1}{t}\left[t_0 S_0^m + S_0^m \sum_{i=1}^{n} \Delta t \left(\frac{1}{1 - \alpha R_{\text{corr}}(\Delta t)\text{i}/h_0}\right)^m\right]. \tag{15}$$

If the time interval $\Delta t \to 0$, then

$$S(t)^m = \frac{1}{t}\left[t_0 S_0^m + S_0^m \int_{t_0}^{t} \left(\frac{1}{1 - \alpha R_{\text{corr}}(t - t_0)/h_0}\right)^m \mathrm{d}t\right]. \tag{16}$$

Finally, the equivalent long-term stress range yields

$$S(t)^m = S_0^m\left[\frac{t_0}{t} + \frac{(kt_0 - kt + 1)^{1-m} - 1}{kt(m-1)t}\right] \tag{17}$$

for $t > t_0$, where $k = \alpha R_{\text{corr}}/h_0$. Then, by substituting $S^m = A^m\Gamma(m/B + 1)$ in both sides of Eq. (17) and after rearranging, a time-dependent scale parameter is obtained, as follows:

$$A(t) = \begin{cases} A_0, & \text{for } t \leqslant t_0, \\ \gamma A_0\left[\frac{t_0}{t} + \frac{(kt_0 - kt + 1)^{1-m} - 1}{k(m-1)t}\right]^{1/m}, & \text{for } t > t_0, \end{cases} \tag{18}$$

where A_0 is the initial scale parameter, i.e. in intact conditions; α is a factor equal to 1 or 2 depending whether the corrosion is one-sided or two-sided, respectively; t_0 is the coating protection time, which is a random variable; γ is a model uncertainty introduced to account for the uncertainty in the global redistribution of stresses due to spatial variation of the corrosion rates throughout the hull structure. This means that the neutral axis of the hull cross-section remains insensitive to the spatial variability of the corrosion rates, i.e. the stress level of interest would depend upon an average thickness reduction. This model uncertainty is assumed to be lognormally distributed, with a mean value of 1.0, standard deviation of 0.1 and a lower limit of 0.

Interaction between fatigue and corrosion is therefore, obtained by applying the time-varying scale parameter $A(t)$ from Eq. (18) into the safety function defined in either Eq. (9) or safety margins and inspection events to be defined in sections below.

2.4. Fatigue reliability in different environments

Miner-Palmgren formulation: The total cumulative fatigue damage for a joint subjected to a combination of environments j during the service life may be expressed as $D_{\text{total}} = \sum_j D_j$, where D_j is the cumulative damage during the service time, T_{sj} the structure is exposed to environment j, which involves operation in harsh or benign climates, laid up periods and conversion periods. The fatigue life under environment j is then $T_{f,j} = T_{sj}/D_j$. Then

$$D_{\text{total}} = \sum_j D_j = \sum_j \frac{T_{sj}}{T_{f,j}} \leqslant \Delta_{\text{allowable}}. \tag{19}$$

The allowable fatigue damage, $\Delta_{\text{allowable}}$ should in general depend upon the uncertainties inherent in long-term distribution of stress cycles, SN-data and Miner-Palmgren's hypothesis as well as access for inspection/repair and consequences of fatigue failure.

Reliability formulation: Let a production ship be initially designed and installed in a harsh environment, e.g. the North Sea, and after some time be moved to a less severe climate (moderate or benign), e.g. the Gulf of Mexico. The fatigue crack growth in a plated joint being initially subjected to environmental conditions j, and then moved to a different location with climate conditions k, i.e. $a_{j\to k}$, may be expressed by the following safety margin:

$$M_{j\to k} = a_{\text{f}} - a_{j\to k} \leqslant 0. \tag{20}$$

Now, recalling the safety function as that defined in Eq. (9) and assuming $\Delta K_{\text{th}} = 0$ and the crack growth from the initial crack size a_0 to $a(t)$, then the first term of the right-hand side may be defined as a monotonously

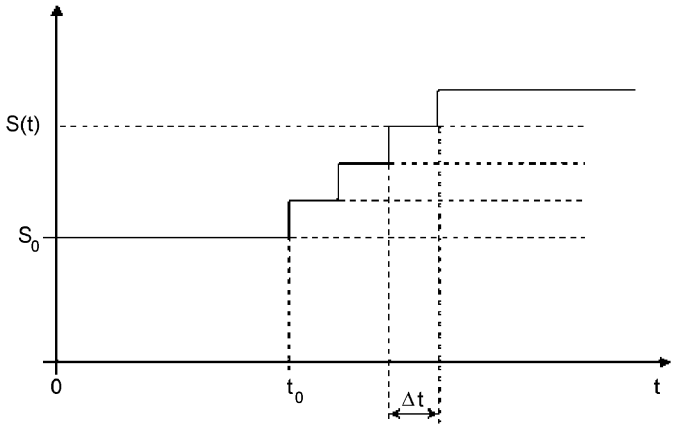

Fig. 1. Effect of corrosion on the equivalent long-term stress range.

increasing damage function $\Psi(a(t), a_0)$, namely

$$\Psi(a(t), a_0) = \int_{a_0}^{a(t)} \frac{\mathrm{d}a}{\left[Y(a)\sqrt{a\pi}\right]^m} = \phi(a(t)) - \phi(a_0). \quad (21)$$

Then, from the complete safety function of Eq. (9) and using the definition of damage function given by Eq. (21) the crack size at time t reads

$$a(t) = \phi^{-1}\left[\phi(a_0) + CA^m\Gamma(1 + m/B)tv_0\right]. \quad (22)$$

The crack size at the time T_{change}, i.e. from the time the vessel is installed under initial climate conditions j until it is moved to different climate conditions k, is given by

$$a_j(T_{\text{change}}) = \phi^{-1}\left[\phi(a_0) + CA_j^m\Gamma\left(1 + m/B_j\right)T_{\text{change}}v_{0,j}\right] = a_{k,0}, \quad (23)$$

where A_j and B_j represent the Weibull parameters corresponding to the climate conditions j and $v_{0,j}$ is the average frequency corresponding to the sea climate j. Notice that the fatigue damage a_j developed up to T_{change} becomes the initial crack size $a_{k,0}$ for crack growth under the new climate k. The crack growth as function of time t under the new climate conditions k, i.e. after T_{change}, is similarly to Eq. (23) given by

$$a_{j\to k}(t) = \phi^{-1}\left[\phi(a_{k,0}) + CA_k^m\Gamma\left(1 + m/B_k\right)\left(t - T_{\text{change}}\right)v_{0,k}\right]. \quad (24)$$

Substituting Eq. (23) into Eq. (24) the crack growth under two different climates, $a_{j\to k}(t)$ is obtained. Then the safety margin of Eq. (20) becomes

$$M_{j\to k}(t) = a_{\text{f}} - \phi^{-1}[\phi(a_0) + CA_j^m\Gamma(1 + m/B_j)T_{\text{change}}v_{0,j} + CA_k^m\Gamma(1 + m/B_k)(t - T_{\text{change}})v_{0,k}] \leqslant 0. \quad (25)$$

An equivalent safety function is given by

$$M'_{j\to k}(t) = \phi(a_{\text{f}}) - \phi(a_0) - CA_j^m\Gamma\left(1 + m/B_j\right)T_{\text{change}}v_{0,j} - CA_k^m\Gamma\left(1 + m/B_k\right)\left(t - T_{\text{change}}\right)v_{0,k} \leqslant 0. \quad (26)$$

After Eq. (21), the safety margin for fatigue life under multiple climate conditions is obtained as follows:

$$M_{j\to k}(t) = \int_{a_0}^{a_{\text{f}}} \frac{\mathrm{d}a}{\left[Y(a)\sqrt{a\pi}\right]^m} - Cv_{0,j}A_j^m\Gamma\left(1 + m/B_j\right)T_{\text{change}} - Cv_{0,k}A_k^m\Gamma\left(1 + m/B_k\right)\left(t - T_{\text{change}}\right) \leqslant 0. \quad (27)$$

Eq. (27) is valid for $t > T_{\text{change}}$.

Considering the special case for a constant value in the geometry function Y, a safety margin similar to that of Eq. (25) is derived

$$M_{j\to k}^{(Y)}(t) = a_{\text{f}} - [a_0^{1-m/2} + (1 - m/2)CY^m\pi^{m/2} \times (A_j^m\Gamma(1 + m/B_j)T_{\text{change}}v_{0,j} + A_k^m\Gamma(1 + m/B_k) \times v_{0,k}(t - T_{\text{change}}))]^{1/(1-m/2)} \leqslant 0. \quad (28)$$

Since the safety margin defined in Eq. (28) cannot be solved through FORM/SORM for $m > 2$, a transformed safety function needs to be used, namely

$$M_{j\to k}^{(Y)}(t) = a_{\text{f}}^{1-m/2} - a_0^{1-m/2} - (1 - m/2)CY^m\pi^{m/2} \times \left(A_j^m\Gamma(1 + m/B_j)T_{\text{change}}v_{0,j} + A_k^m \times\Gamma(1 + m/B_k)v_{0,k}\left(t - T_{\text{change}}\right)\right) \geqslant 0. \quad (29)$$

Observe that the inequality changes during the transformation of the safety margin, for values of m greater than 2.

In general, Eq. (27) may be expressed for a welded joint subjected to n different climate conditions as

$$M_{j\to k}(t) = \int_{a_0}^{a_{\text{f}}} \frac{\mathrm{d}a}{\left[Y(a)\sqrt{a\pi}\right]^m} - Cv_{0,j}A_j^m\Gamma(1 + m/B_j)T_{\text{change}(j)} - Cv_{0,k}A_k^m\Gamma\left(1 + m/B_k\right)\left(t - T_{\text{change}(j)}\right) - \cdots - Cv_{0,n}A_n^m\Gamma\left(1 + m/B_n\right)\left(t - T_{\text{change}(n-1)}\right) \leqslant 0, \quad (30)$$

where $T_{\text{change}(i)}$ is the time the vessel is moved from climate i to a different location.

The probability of failure of a component in fatigue for $t > T_{\text{change}(i)}$ is

$$P_{\text{f}} = P\left[M_{j\to k}(t) \leqslant 0\right]. \quad (31)$$

2.5. Reliability updating through inspection of cracks

The updating methodology is useful in connection with extension of service life for structures with joints governed by the fatigue criterion. In such cases, the design fatigue life is in principle exhausted at the end of the planned service life. However, if no cracks have been detected during inspections, a remaining fatigue life can be demonstrated.

The margin event $M(t)$ as defined in Eq. (9) for evaluating failure probability in fatigue of joint i is updated based on the definition of conditional probability as

$$P_{\text{f}_i,\text{UP}} = P\left[(M(t) \leqslant 0)|\text{IE}_j\right] = \frac{P\left[(M(t) \leqslant 0) \cap \text{IE}_j\right]}{P\left[\text{IE}_j\right]}, \quad (32)$$

where the inspection event IE may represent either "*no crack detection*" or "*crack detection*". The inspection event for *no crack detection* at time T_j, is in general defined as (e.g. [6])

$$I_{\text{ND}}(T_j) = a_{\text{D}} - a(T_j) > 0$$

or

$$I_{\text{ND}}\left(T_j\right) = \int_{a_0}^{a_{\text{D}}} \frac{\mathrm{d}a}{\left[Y(a)\sqrt{\pi a}\right]^m G(a)} - CA^m\Gamma\left(\frac{1}{B} + 1\right)v_0T_j > 0. \quad (33)$$

The distribution function of the detectable crack size a_{D} is equal to the *probability of detection* (POD) curve. If several inspections are carried out, the random variables a_{D} are mutually independent. The inspection event of *crack detection* is complementary to that expressed in Eq. (33). If the detected crack is measured at inspection T_j the inspection event margin reads as an equality of Eq. (33)

where a_D is substituted by a random variable a_m representing uncertainties inherent to the crack measurement, e.g. [6].

The safety margin of a joint may be updated when n inspection events are considered, e.g. *no detection* I_{ND}, *detection*, I_D and crack *measured* I_{MS} event margins, as follows:

$$P_{f,UP} = P\big(M(t)\leqslant 0 | I_{ND,1}>0 \cap I_{ND,2}>0 \cap \cdots \cap I_{D,j}\leqslant 0 \cap I_{MS,k}=0\big). \quad (34)$$

As the number of inspection outcomes increases, the calculation of Eq. (34) becomes more difficult to be performed. However, conservatively only the last inspection result may be considered if the previous inspection outcome history is *no detection*, see [18].

2.6. Updating with inspection in different environments

Updating after inspection carried out in a production ship operating in different environments is to be described as follows. Let the FPS be initially designed and installed in environment j and after some time be moved to climate k. Then, the inspection events carried out at time T_{insp} could be

$$\mathrm{IE}\big(T_{insp}\big) = \begin{cases} a_D - a_j > 0, & \text{for } T_{insp} < T_{change}, \\ a_D - a_{j\to k} > 0, & \text{for } T_{insp} > T_{change}. \end{cases} \quad (35)$$

If an inspection is carried out with *No crack detection* after the ship has been moved to a different location, the inspection event is defined as

$$I_{ND} = a_{j\to k} < a_D, \quad (36)$$

where a_D is the minimum detectable crack size and it is regarded as a random variable whose distribution function is equal POD curve.

The inspection events performed at time $t<T_{change}$ (climate j) have been discussed in Section 2.5. The inspection event with *no crack detection*, carried out at time $t>T_{change}$ (climate k conditions) i.e. after the vessel has been moved ($j\to k$), may be expressed analogously to the safety margin given in Eq. (27), namely

$$\mathrm{IE}_{j\to k}\big(T_{insp}\big) = \int_{a_0}^{a_D} \frac{da}{Y(a)^m(\pi a)^{m/2}} - Cv_{0_j}A_j^m\Gamma\left(1+\frac{m}{B_j}\right)T_{change} - Cv_{0_k}A_k^m\Gamma\left(1+\frac{m}{B_k}\right)\big(T_{insp}-T_{change}\big) > 0. \quad (37)$$

This event is positive since it implies that the crack size developed up to time T_{insp} is smaller than the detectable crack size a_D, which is a random variable. If several inspections are carried out, the random variables a_D are mutually independent. The inspection event of *crack detection* is negative, namely $\mathrm{IE}_{j\to k}(T_{insp})\leqslant 0$. The updated failure probability for a joint with inspections performed either before or after T_{change} is given by

$$P_{f,UPD} = \begin{cases} P\big[M_j(t)\leqslant 0 | \mathrm{IE}(T_{insp})\big], & \text{for } t<T_{change}, \\ P\big[M_{j\to k}(t)\leqslant 0 | \mathrm{IE}_{j\to k}(T_{insp})\big], & \text{for } t>T_{change}. \end{cases} \quad (38)$$

The safety margins in Eqs. (38) above, $M_j(t)\leqslant 0$ and $M_{j\to k}(t)\leqslant 0$ are given by Eqs. (9) and (27), respectively.

2.7. Updating with 2 inspection events: no crack found and thickness measurement

The inspection event corresponding to thickness measurement is given by

$$I_{ThM}(T_{insp}) = W(T_{insp}) - \Delta h_m = 0; \quad \text{for } T_{insp} > \text{mean value of } t_0, \quad (39)$$

where Δh_m is the measured thickness reduction, $W(T_{insp}) = R_{corr}\alpha(T_{insp}-t_0)$ is the estimated thickness reduction at time T_{insp}, i.e. the thickness wastage as defined in Eq. (12), and t_0 is a random variable corresponding to the time for the coating protection to fail. α is 1 if corrosion is one-sided or 2 if it is two-sided, and R_{corr} is the corrosion rate (thickness reduction). The updated fatigue failure probability for both climates j and k is given by

$$P_{f,UPD} = \begin{cases} P\big[M_j(t)\leqslant 0 | I_{ThM}(T_{insp})\big]; & \text{for } t<T_{change}, \\ P\big[M_{j\to k}(t)\leqslant 0 | I_{ThM}(T_{insp})\big]; & \text{for } t>T_{change}. \end{cases} \quad (40)$$

The updated failure probability of a joint under combined climate conditions j and k, considering inspection with no crack detection and thickness measurement performed at time T_{insp}, reads

$$P_{f,UPD} = \begin{cases} P\big[M_j(t)\leqslant 0 | I_{ND-j}(T_{insp}) \cap I_{ThM}(T_{insp})\big], \\ \quad \text{for} \quad t<T_{change}, \\ P\big[M_{j\to k}(t)\leqslant 0 | I_{ND-k}(T_{insp}) \cap I_{ThM}(T_{insp})\big], \\ \quad \text{for} \quad t>T_{change}. \end{cases} \quad (41)$$

The inspection events $I_{ND}(t)$ and $I_{ThM}(t)$ have been defined by Eqs. (33) or (37) and (39), respectively.

Two possible scenarios are envisaged when updating due to repair of corroded plate, namely: (a) plate replacement including both corroded and cracked areas, or (b) the corroded item only. In the former case, updating is carried out accounting for the repaired conditions, e.g. initial crack size as new structure, stress range level according to repaired conditions, new corrosion conditions. In the latter case, the stress level is to be updated according to the *new* repaired conditions. This model makes it possible to consider various conditions regarding the uncertainties involved, especially if the original ones differ with respect to the new ones.

2.8. Reliability formulation in terms of hazard function

So far the failure probability has been referred to a time period t. The hazard rate $h(t)$ is defined as, $h(t) = f(t)/(1 - F(t))$ where $F(t)$ is the distribution function of the time-to-failure of a random variable T, and let $f(t)$ be its probability density function (see e.g. [19, 20]). This expression represents the probability that the structure of age t will fail in the interval $t+\Delta t$, given that it has survived up to time t, namely

$$h(t) = P[T \leqslant (t + \Delta t) | T > t] = \frac{P[t \leqslant T \leqslant t + \Delta t]}{\Delta t(1 - P[T \leqslant t])} = \frac{\mathrm{d}P_{\mathrm{F}}(t)/\mathrm{d}t}{1 - P_{\mathrm{F}}(t)}. \quad (42)$$

To illustrate the concept of hazard rate for fatigue damage, let us consider a case where the implicit 20-year service life failure probability for an allowable cumulative damage of $\Delta = 1$, is of the order of 10^{-1}. While the average hazard rate is 5×10^{-3} for this case, the annual failure probability or hazard rate is 10^{-2} in the last year of service, as shown by the curves marked with harsh–harsh in Fig. 5 of Section 3.

2.9. Quality of inspection of cracks (POD)

Periodic updating of the fatigue reliability level of a welded connection in a vessel depends upon how likely it is that a crack is detected during an inspection. Much effort has been devoted in different industries to evaluate the quality of non-destructive techniques (NDT) for inspection of cracks in metals. The likelihood that a crack is detected is expressed by the POD curve corresponding to every NDT used.

POD curves for various applications of NDT obtained from different industrial projects have been compiled by Visser [21]. The Nordtest project [22] reports POD curves for different NDT for detecting surface cracks such as magnetic particle inspection (MPI) and dye penetrant, among other NDT for buried defects, obtained from a large database. UCL underwater inspection program (see e.g. [23]), and its extension projects ICON [24] and TIP [25] have been developed for the offshore industry. Besides MPI, Eddy current, alternate current methods (ACFM and ACPD) and ultrasonic inspection are also considered.

Typically, these projects indicate that surface cracks of 2–3 mm deep could be detected by a probability of 80%, i.e. a mean value around 1.4–1.8 mm if exponential distribution is assumed. Defects with depths less than 1 mm have introduced uncertainties in the results reported in [24], which may be dealt with by introducing a threshold for the initial crack size as suggested by Moan et al. [26]. Additionally, Moan et al. [27] inferred a POD curve with exponential distribution with mean value of 1.95 mm in depth, based on data from underwater inspection of cracks in tubular joints. Data from 4000 NDT inspections in jackets of the North Sea were applied. It is reasonable that the data from the latter reference represent an "upper bound" of the mean defect crack size, considering the difficult environment condition under which inspections are made. Fujimoto et al. [28,29] show POD curves for Close Visual Inspection (CVI) of ships (Fig. 2 and Table 1). This procedure is commonly used as initial inspection procedure, followed by an NDT inspection in areas more prone to cracking.

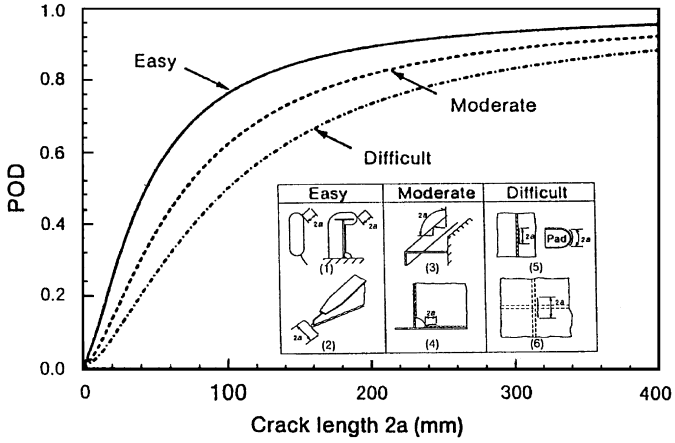

Fig. 2. POD curves for visual inspection depending upon access to crack site, [28].

Table 1
Mean detectable crack size through visual inspection (within 0.5 m distance) on trading vessels, depending upon access to crack site [28,29]

Access	Length (mm)
Easy	40
Moderate	70
Difficult	100

2.10. Target safety levels

Failure probabilities may be expressed as annual or service life values. The choice between the reference time period and the corresponding target value will have implications on the conclusions reached by the probabilistic safety analysis. The target level depends upon various factors such as the failure mode, the method to evaluate reliability, and the possible consequences in terms if risk to life, environment or economic loss. Commonly, when setting target levels for fatigue a comparison with the target level for ultimate strength might be useful, but difficult. Fatigue damage accumulates over fabrication, transport, installation and operation. However, for ships the operational phase would be dominant.

In general it is recommended to calibrate the target level to that implicit in structures, which are considered to have an acceptable safety, or modify it if this is not the case [30].

A starting point for setting the target level for fatigue is to estimate the implicit failure probability acceptable for welded joints, for which no account is made of inspection on reliability and for which fatigue failure implies "total

loss." Obviously, the relevant uncertainty measures for the structures needs to be assessed in this connection. Also, it is crucial to use the same reliability methodology as later will be used to demonstrate compliance with the target safety level. Target levels for other conditions can then be calibrated. This approach was applied in [31] to calibrate fatigue design criteria as a function of inspection, and is especially relevant in connection with assessment of service life extension [32,33].

The target level may be expressed by the annual or service life value. The annual value may conveniently be expressed by the (annual) hazard rate. However, since most fatigue requirements have not been consistently calibrated, the implied failure probability in relevant codes may vary and the target level would have to be based on a weighed mean of implied safety levels.

The cumulative nature of fatigue suggests using the cumulative probability as acceptance criterion. On the other hand, ultimate limit state criteria are either referred to annual or service life probability levels. It is commonly accepted that annual failure probability is relevant as a measure with respect to fatalities while failure probability in service life appears to be the most relevant when target values are determined by cost-benefit analyses. Fig. 3 shows the implied failure probability and hazard rate (target levels) as function of the fatigue design factor (see e.g. [16] for definition). Upper and lower bounds are defined assuming different uncertainty levels for the Weibull scale parameter of the long-term stress range distribution. This kind of analysis is proposed as basis for establishing target levels.

2.11. Calculation of failure probability

The failure probabilities of the case studies presented in Section 3 are calculated by means of second-order reliability method, SORM. Since the safety function of Eq. (27) and the updated probability with the use of the inspection event given by Eq. (37) are non-linear expressions, the use of FORM may give non-conservative results for $t > T_{\text{change}}$. This tendency may be observed when obtaining updated failure probabilities as shown in the annual hazard rate plot of Fig. 4. It is seen that just after T_{change}, the curves calculated with FORM show a decrease in the hazard rate, which is not correct. The calculations using SORM showed a better agreement with those obtained by means of axis orthogonal simulation, which is an improved importance sampling technique, see e.g. Hohenbichler and Rackwitz [34]. In order to achieve a coefficient of variation of the failure probability less than 0.02 using this simulation technique for the results shown in this figure, between 2000 and 5000 simulations were necessary. The calculation of probabilities was carried out by using the computer program Proban [35]. Detailed data are given in the case study in Section 3.

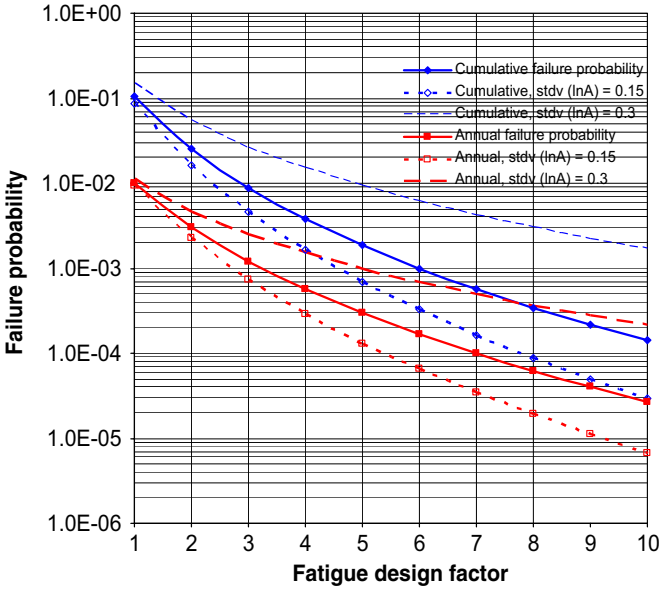

Fig. 3. Target levels as function of fatigue design factor.

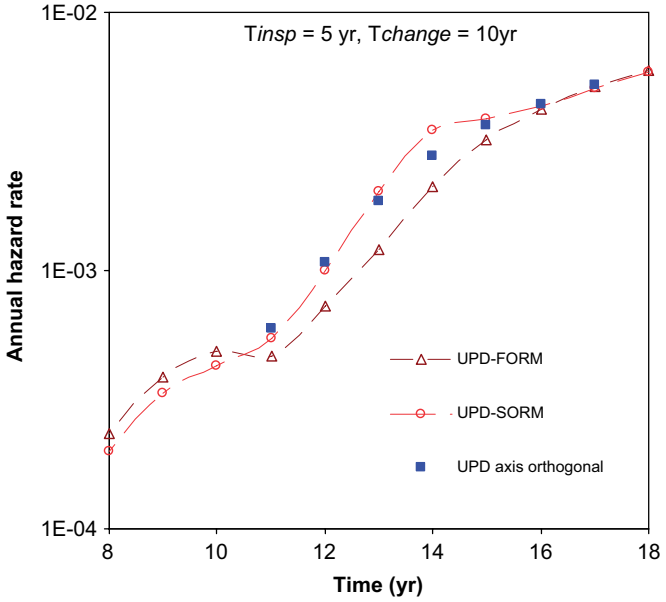

Fig. 4. Failure hazard rates calculated with FORM, SORM and axis orthogonal simulation.

3. Case study

The aim of the case study is to demonstrate the approach described above using the fatigue and corrosion reliability model under changing climate conditions. Sensitivity analyses with respect to climate conditions, corrosion rates and quality of inspections are studied. The results are presented in terms of annual (hazard rate) and service-life failure probabilities. Updating with inspection results is performed assuming that no crack is found and corrosion-induced thinning is measured.

The case study consists of a plated joint from a hull structure subjected to two different environmental conditions throughout the service life of the vessel. The stress

intensity factors are calculated assuming a semielliptical surface crack solution, considering a model uncertainty for the geometry function Y, namely γ_{geom}. The climate conditions are regarded herein as *harsh*, e.g. North Sea condition, and *benign* conditions, e.g. tropical climate. However, for the sensitivity studies the stress parameters are idealized as described in Table 2. The long-term stress range is assumed to be Weibull distributed. The scale parameter A corresponding to *harsh* conditions is defined so that the cumulative damage after 20 years of service is $D = 1.0$ with a shape parameter $B = 1.14$. Accordingly, for *benign* conditions the shape parameter is assumed to be $B = 0.66$ and the scale parameter is calibrated so that the damage after 20 years corresponds to $D = 0.33$. The same uncertainty is assumed for the scale parameter A, however this may not be true as explained in Section 2.1. The structure is assumed to be installed to initially operate under certain climate conditions (e.g. harsh) and moved at time $T_{change} = 10$ years to different climate conditions (e.g. benign), so that the case is named *harsh–benign*, whereas the opposite case is referred to as *benign–harsh*.

In Fig. 5, a comparison between cumulative failure probability and annual hazard rate is shown for both harsh-to-benign and benign-to-harsh cases. It might be observed that both cases converge to the same cumulative failure probability after 20 years of service. This coincidence is due to the cumulative nature of fatigue damage and to the fact that the vessel, for both cases, is subjected to the two different climates during the same period of time for, i.e. 10 years in harsh and 10 years in benign climate, and vise versa. This is also proof of correctness of the formulation. On the other hand, the annual hazard rate behaves differently. After 20 years, the benign–harsh case shows larger annual failure probability than that of harsh–benign. It is also observed that the latter shows a remarkable drop in annual failure rate once the vessel is moved from harsh to benign conditions, whereas the benign-harsh curve does not present a sudden jump but a smooth change on annual failure rate. The curves of both cumulative and annual failure probabilities for the case the vessel operates 20 years under harsh conditions only (harsh–harsh) are also shown for reference.

3.1. Sensitivity studies

3.1.1. Environment

Benign to harsh environment: Fatigue deterioration of joints subjected to different environments has been discussed in Section 2.4 and reliability updating has been introduced in Section 2.6. Let the vessel be subjected to *benign to harsh* conditions. The updated failure probability

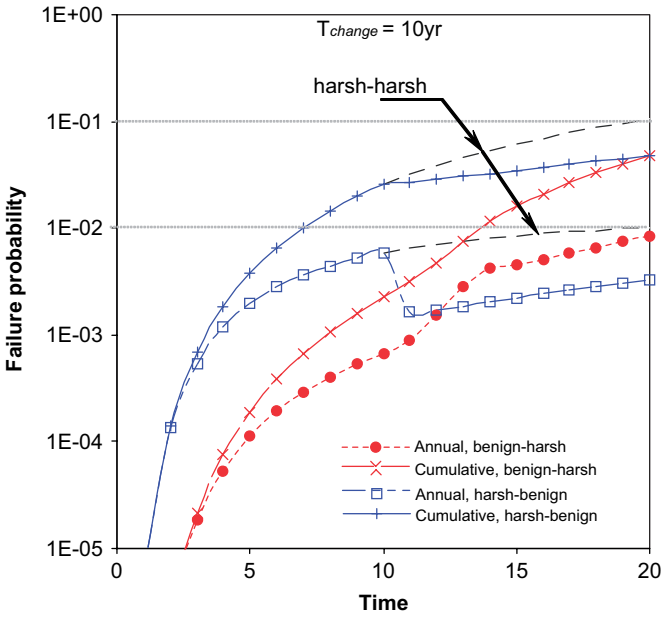

Fig. 5. Cumulative failure probability and annual hazard rate as function of time. Harsh-to-benign and benign-to-harsh conditions. The loading climate is changed from either harsh or benign conditions after $T_{change} = 10$ years.

Table 2
Typical input parameters for plated joint with shifting of environmental conditions (benign to harsh or vice-versa), assumed in the case study

Parameter	Distribution	Mean	Std. dev. (CoV)
Stress-scale param. ln A (benign conditions)	Normal	2.0288	0.198
Stress-shape param. B (benign conditions)	Normal	0.66	0.044
Stress-scale param. ln A (harsh conditions)	Normal	3.2288	0.198
Stress-shape param. B (harsh conditions)	Normal	1.14	0.044
Average stress cycle, υ_0 (harsh & benign)	Fixed	0.158	
Material parameter, ln C	Normal	−29.97	0.514
Material parameter, m	Fixed	3.1	
Geometry function, G_{Factor}	Normal	1.0	0.05
Aspect ratio, a/c	Fixed	0.83	
Membrane stress ratio, $S_m/(S_m+S_b)$	Fixed	1.0	
Initial crack size, a_0	Exponential	0.11	0.11
Detectable crack size, a_d	Exponential	2.0	2.0
Wall thickness, critical crack size	Fixed	20	
Corrosion wastage rate, R_{corr} (mm/yr)	Normal	0.1–0.2	(0.5)
Thickness measurement, Th-med	Normal	1.0–5.0	(0.1–0.3)
Time of coating, T_{coat}	Normal	5.0	(0.5)

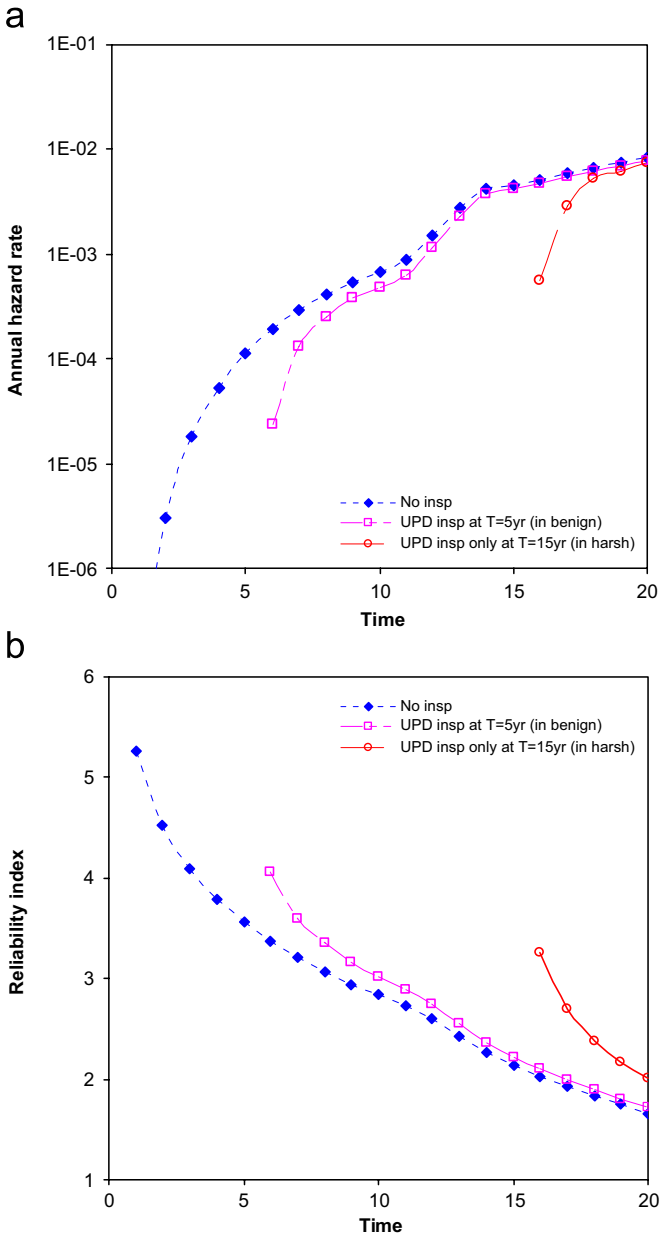

Fig. 6. Effect of inspection updating in different loading climates, assuming ten years in *benign*, then *harsh* climate conditions. Inspection with *no crack detection* at either $T = 5$ years (*benign*) or $T = 15$ years (*harsh*) (a) Annual hazard rate; (b) reliability index.

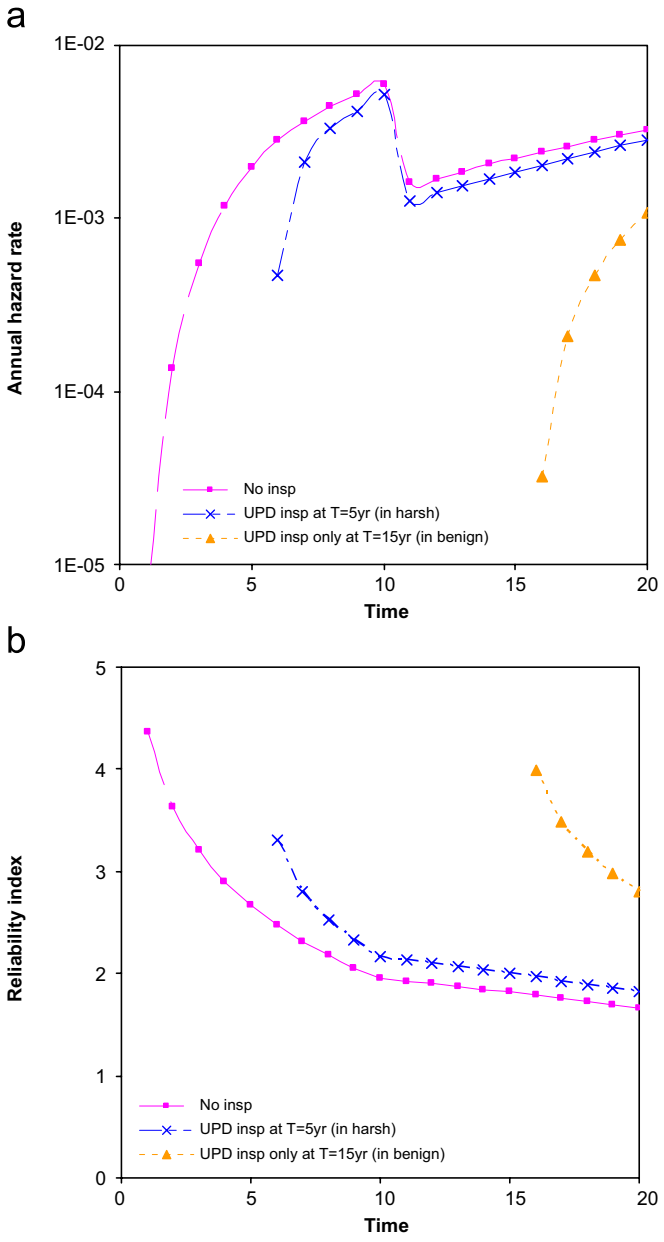

Fig. 7. Effect of inspection updating in different loading climates, assuming ten years in *harsh*, then *benign* climate conditions. Inspection with *no crack detection* at either $T = 5$ years (*harsh*) or $T = 15$ years (*benign*) (a) Annual hazard rate; (b) reliability index.

after inspection for benign to harsh sea loading is given by Eq. (38). Fig. 6a shows the hazard rate for the benign-to-harsh case, changing conditions at 10 years. Updating is done with inspection at $T_{\text{insp}} = 5$ years (in benign conditions) and $T_{\text{insp}} = 15$ years (in harsh conditions). It is observed that at $T = 20$ years, the rate is similar for both updated cases, approaching to the case of no inspection, although there is an important gain in reliability after the inspection at $T = 15$ year, as shown in Fig. 6b. No crack found is assumed during the inspection.

Harsh to benign conditions: Fig. 7a shows the hazard rate for the harsh-to-benign case, changing conditions at 10 years. Updating is done with inspection at $T_{\text{insp}} = 5$ years (in harsh conditions) and $T_{\text{insp}} = 15$ years (in benign conditions). It is observed that at $T = 20$ years, the rate is 3 times smaller when updating after 15 years, as also observed in the reliability plot shown in Fig. 7b.

3.1.2. *Plate thinning effect due to corrosion*

The results shown in Figs. 8 and 9 correspond to the interactive effect in fatigue reliability between the crack growth and corrosion-induced thinning in a hull structure subjected to two different environment conditions. For the purpose of the sensitivity study, the corrosion fatigue effect

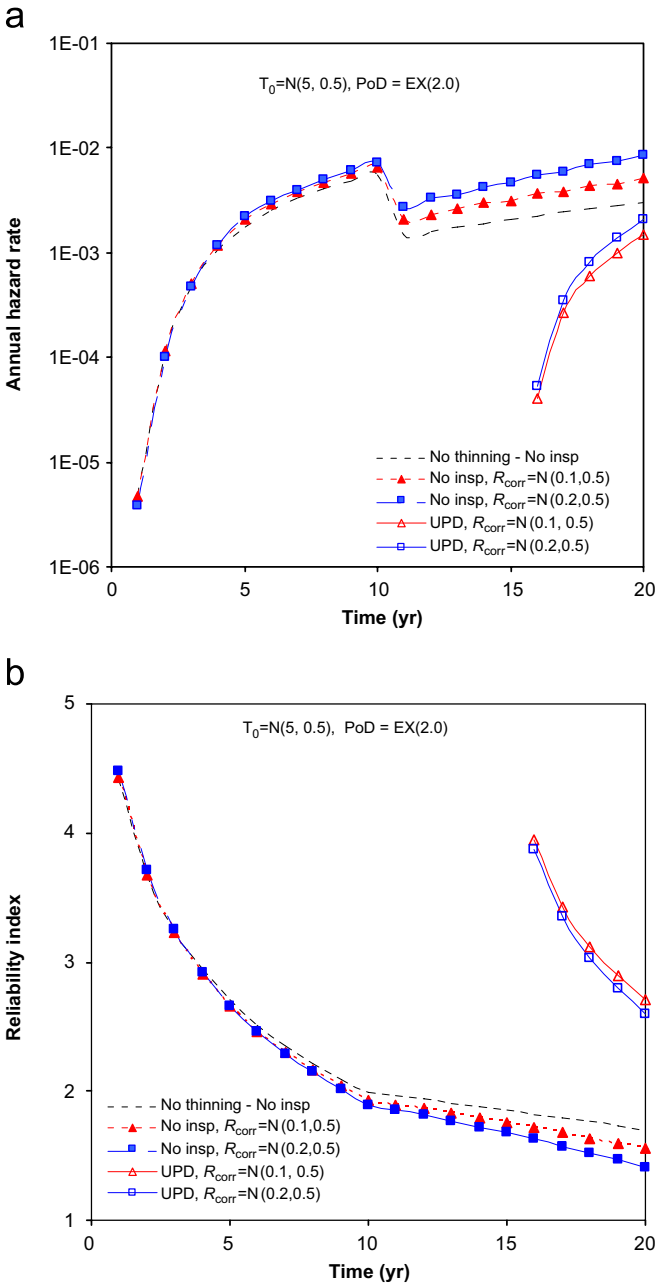

Fig. 8. Sensitivity of corrosion rates on fatigue reliability and updating. Ten years in *harsh*, then *benign* conditions. Updating after $T = 15$ years, no crack detection. The time of coating failure T_{coat} is assumed as normally disturbed with mean of 5 years and CoV = 0.5. $\alpha = \gamma = 1$. (a) Annual hazard rate; (b) reliability index.

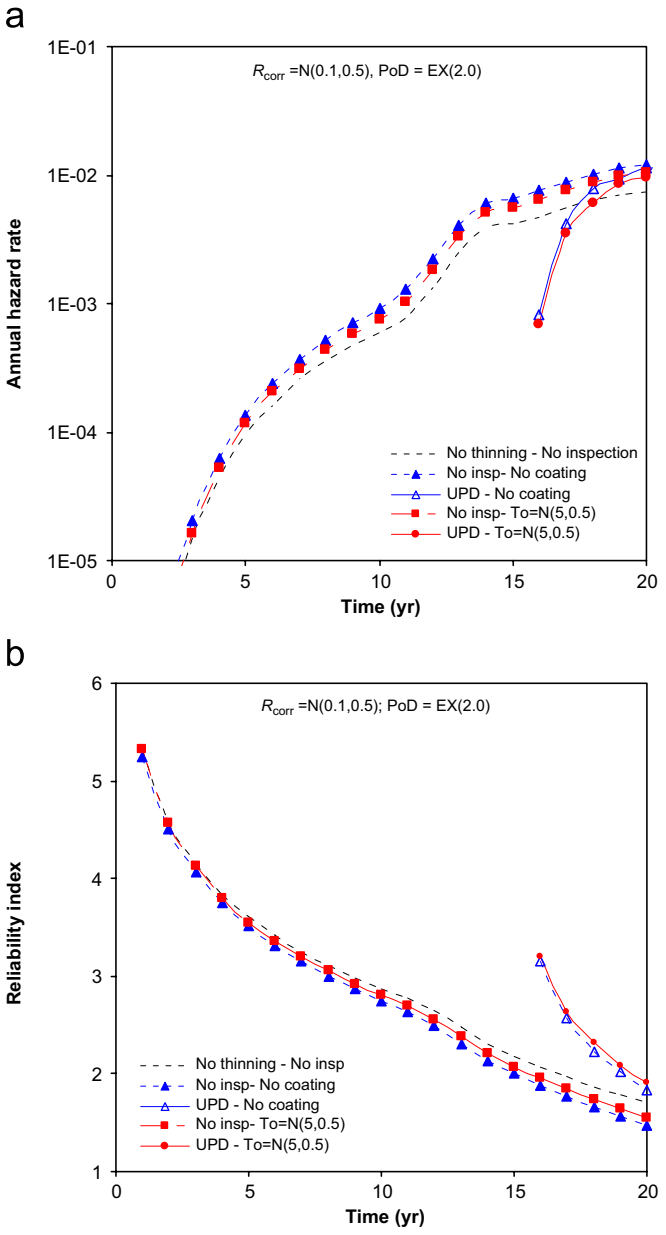

Fig. 9. Fatigue reliability and updating considering plate-thinning effect. Ten years in *benign*, then *harsh* conditions. Updating after $T = 15$ years, no crack detection. When coating effect is considered the time of coating failure T_{coat} is assumed as normally disturbed with mean of 5 years and CoV = 0.5. $\alpha = \gamma = 1$. (a) Annual hazard rate; (b) reliability index.

is not accounted for, i.e. material parameters C and m are not modified after the coating system fails. A considerable reduction in the reliability is observed when accounting for the corrosion wastage effect, even for reasonably small values of corrosion rate. From Fig. 8 it may be observed that for the case of the structure under initially harsh conditions and then moved to more benign climate, there is a larger effect after updating than for the opposite case shown in Fig. 9, i.e. in benign to harsh conditions. The former figure shows the sensitivity of the corrosion rate R_{corr}. The effect of failure time of the coating (T_{insp}) may be observed from the latter. The mean value considered of 5 year for the time to failure of the coating in this example has a little effect in the reliability index.

Fig. 10a and 10b exemplify, respectively, updated annual failure rates and updated reliability index, based on results of two inspection events, namely: no crack found and thickness loss measurement, performed at time $T = 15$ year. The POD is crack detection is exponentially distributed with mean of 2.0 mm. In this particular case, the measurement of thickness reduction is assumed as normally distributed with mean equal to 5 mm (with

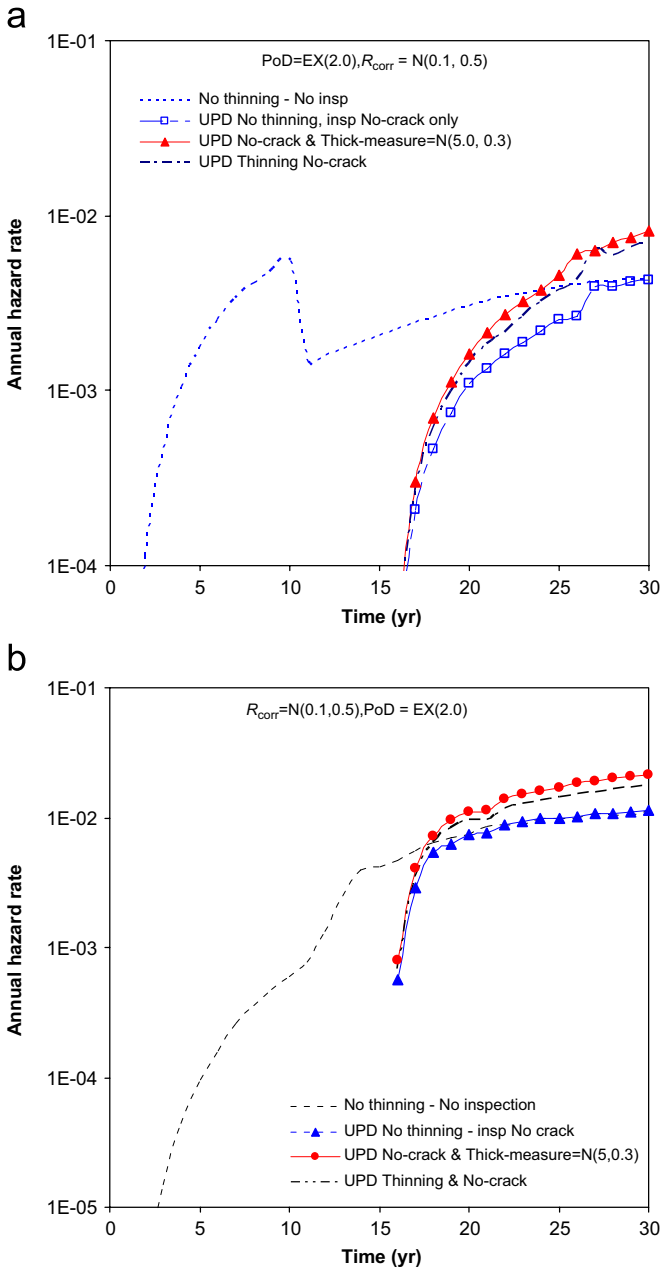

Fig. 10. Fatigue reliability updating at time $T = 15$ years, considering two inspection events: no crack detection and thickness measurement. (a) *harsh-benign*; (b) *benign-harsh* conditions. Corrosion wastage measured is normally distributed $\mu = 5$ mm, CoV = 0.3. T time of coating failure T_{coat} is assumed as $N(\mu = 5$ years, CoV = 0.5). $\alpha = \gamma = 1$. (a) annual hazard rate. Ten years in *harsh* climate, then *benign*; (b) annual hazard rate. Ten years in *benign* climate, then *harsh*.

CoV = 0.3). Such a thickness loss implies that no plate replacement would be necessary due to corrosion allowance in ships, since this reduction represents about 20% of the original plate thickness. Observe that the annual failure probability updated after inspection at 15 years with no crack detection and thickness reduction of 5 mm is larger than the updated annual rate when considering one inspection event (UPD thinning no-crack). This may be explained because the actual thickness loss (measured) is larger than that implied by the corrosion rate of 1.5 mm after 15 years. Hence, disregarding the effect of corrosion on fatigue damage on existing ships may lead to non-conservative decisions, e.g. for service life extension. Therefore, the measurement of material loss due to corrosion may provide further information that should be accounted for in assessing fatigue failure probability.

3.1.3. *Sensitivity of inspection quality*

Two POD curves are compared corresponding to an NDT such as magnetic particles inspection (MPI) technique, and compared to a visual inspection (CVI) procedure. The POD curves for MPI and CVI are assumed as exponential distributed with mean detectable crack size value of 2.0 and 16.6 mm, respectively. The latter corresponds to mean detectable depth size using the best quality of CVI specified in Table 1 as "easy access" (aspect ratio of 0.83 assumed), whose detectable mean value is 40 mm in length. It has to be pointed out that the actual depth may be affected by the thickness effect. No crack detection is the assumed outcome from inspections carried out at 15 and 20 years of service. From Fig. 11a it may be observed the effect of the POD curve selection in updating of a joint under multiple climate conditions, namely 10 years in benign then harsh conditions. It is readily observed the larger effect on updating for the case of the vessel being under harsh 10 years and then moved to benign conditions, see Fig. 11b.

4. Conclusions

A fatigue reliability-based formulation for assessment of existing ship hull structures subjected to multiple climate conditions throughout their service life has been established. Fatigue and corrosion phenomena are accounted for the formulation, considering the increased crack growth rate induced by the rise of stress range due to the corrosion wastage (plate thinning). The model also allows for the corrosion fatigue phenomenon. The effect of inspection is accounted for emphasizing its effect after the vessel has been moved and hence exposed to different climate conditions.

Both the cumulative failure probability, commonly used in evaluating fatigue failure, and the annual hazard rate are calculated. It is argued that annual failure probabilities are a better measure for the reliability than the cumulative probability with respect to consequences such as fatalities. This is very important issue when considering an extension in the service life of the ship.

The case studies show that the results are non-conservative when the interaction between crack growth and corrosion thinning is ignored in the evaluation of the fatigue failure probability. However, it is a challenging task to evaluate corrosion rates, especially their dependence on local conditions.

There is, as expected, a larger effect in the updating when the structure has spent 10 years under harsh conditions and

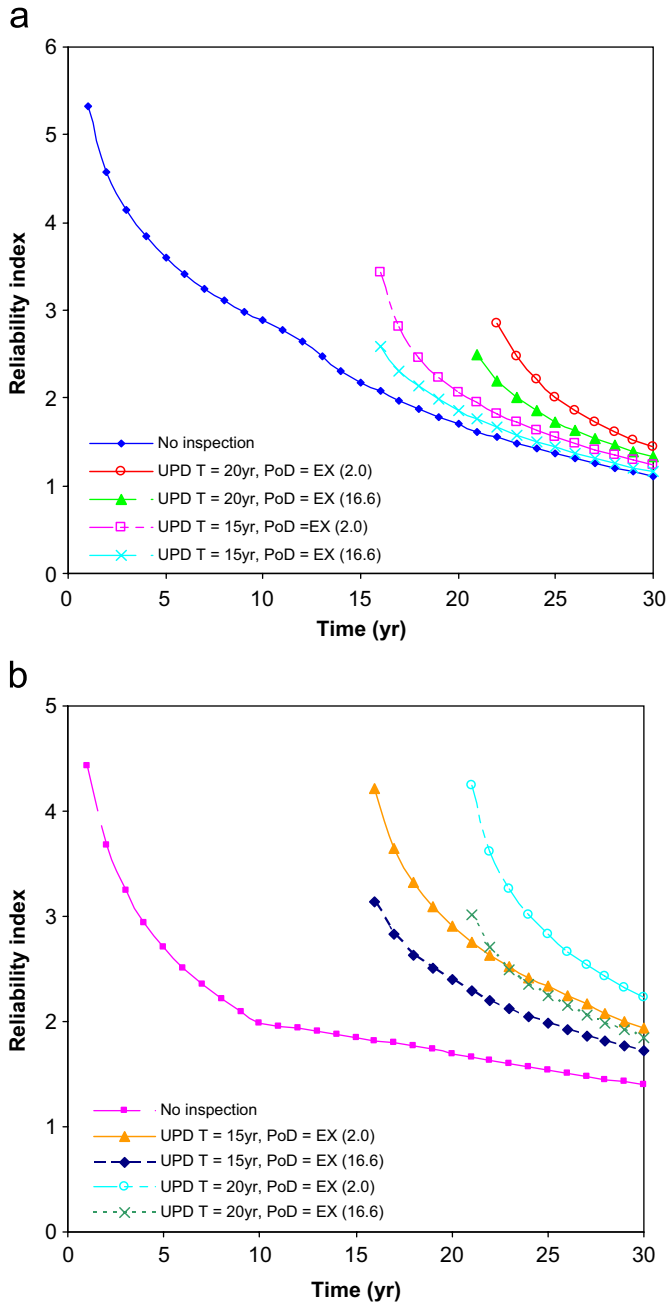

Fig. 11. Sensitivity of different POD curves in updating of fatigue reliability, no crack detection. Non-destructive technique, POD = EX(2.0 mm); close visual inspection, POD = EX(16.6 mm). (a) 10 years in *benign*, then *harsh*; (b) 10 years in *harsh*, then *benign*.

it is inspected in benign conditions with no crack found than the opposite case, i.e. 10 year in benign conditions and then inspected under harsh climate. This occurs because larger fatigue damage is expected during the first 10 years of service in *harsh* climate. The proposed model enables to explicitly quantify this effect in terms of failure probability.

The use of visual inspection in the particular case study showed that it could be used as a reliable means of updating in FPSOs operating originally under harsh conditions and moved to benign climates. However, effects of corrosion may lead to different conclusions.

Acknowledgments

The examples presented herein were partly adapted from an extensive case study carried out in the project "Reliability-based assessment of FPSOs for service life extension" for American Bureau of Shipping (ABS). The authors gratefully acknowledge the support received from ABS. The second author also acknowledges Instituto Mexicano del Petróleo for providing the opportunity to pursue Ph.D. studies at the Norwegian University of Science and Technology.

References

[1] Sucharski D. Crude oil tanker hull structure fracturing: an operator's perspective. In: Proceedings of the symposium and workshop on the prevention of fracture in ship structure, Ship Structure Committee, Washington, DC, 1997. p. 87–124.
[2] Melchers RE. Corrosion uncertainty modelling for steel structures. J Construct Steel Res 1999;52:3–19.
[3] Tanker Structure Co-operative Forum & IACS (TSCF). Guidance manual for tanker structures. London: Whitherby Publishers; 1997.
[4] Paik JK, Lee JM, Hwang JS, Park YI. A time-dependent corrosion wastage model for the structures of single- and double-hull tankers and FSOs and FPSOs. Mar Technol 2003;40(3):201–17.
[5] Yang YN. Application of reliability methods to fatigue, quality assurance and maintenance. In: Schuëller, Shinozuka, Yao, editors. Structural safety & reliability. Rotterdam: Balkema; 1994 [The Freudental Lecture].
[6] Madsen HO, Krenk S, Lind NC. Methods of structural safety. New Jersey: Prentice-Hall Inc.; 1986.
[7] Nordeström N. A method to predict long-term distributions of waves and wave-induced motions and loads on ships and other floating structures. Publication no. 81, Det norske Veritas, 1973.
[8] Guedes Soares C, Moan T. Model uncertainty in the long-term distribution of wave-induced bending moments for fatigue design of ship structures. Mar Struct 1991;4(4):295–315.
[9] Newman JC, Raju JS. An empirical stress-intensity factor equation for the surface crack. Eng Fract Mech 1981;15(1–2):185–92.
[10] Burns DJ, Lambert SB, Mohaupt UH. Crack growth behaviour and fracture mechanics approach. In: Noordhoek, Back, editors. Steel in marine structures. Amsterdam: Elsevier Science Publishers; 1987.
[11] Bowness D, Lee MMK. Weld toe magnification factors for semi-elliptical cracks in T-butt joints. Offshore Technology Report—OTO 1999 014. UK: Health Safety Executive; 1999.
[12] BS 7910. Guidance on methods for assessing the acceptability of flaws in fusion welded structures. BS 7910:1999, British Standards, London, UK.
[13] Guedes Soares C, Garbatov Y. Reliability of maintained ship hull girders subjected to corrosion and fatigue. Struct Saf 1998;20:201–19.
[14] Guedes Soares C, Garbatov Y. Reliability of maintained ship hulls subjected to corrosion and fatigue under combined loading. J Construct Steel Res 1999;52:93–115.
[15] Akpan UO, Koko TS, Ayyub B, Dumbar TE. Risk assessment of aging ship hull structures in the presence of corrosion and fatigue. Mar Struct 2002;15:211–31.
[16] Det Norske Veritas. Fatigue assessment of ship structures—DNV classification notes no. 30.7. Oslo: Det Norske Veritas; 2001.
[17] Almar-Næss A. Fatigue handbook—offshore steel structures. Trondheim, Norway: Tapir Publishers; 1985.
[18] Ayala-Uraga E, Moan T. System reliability issues of offshore structures considering fatigue failure and updating based on

inspection. In: Proceedings of the first international ASRANet Colloquium, Glasgow, UK, 2002.
[19] Mann NR, Schafer RE, Singpurwalla ND. Methods for statistical analysis of reliability and life data. New Jersey: Wiley; 1974.
[20] Melchers RE. Structural reliability analysis and prediction. 2nd ed. West Sussex, UK: Wiley; 1999.
[21] Visser W. POD/POS curves for non-destructive examination. Offshore Technology Report OTO 2000/018. UK: Health & Safety Executive; 2002.
[22] Kauppinen P, Sillanpää J. Reliability of surface inspection techniques. In: Proceedings of the 12th world Conference on non-destructive testing. Amsterdam: Elsevier Publishers; 1989.
[23] Visser W, Dover WL, Rudlin JR. Review of UCL underwater inspection trails. Report OTN 96 179. UK: Health & Safety Executive; 1996.
[24] Dover WJ, Rudlin JR. Defect characterisation and classification for the ICON inspection reliability trials. In: Proceedings of the conference on offshore mechanics and arctic engineering, USA: ASME; 1996.
[25] Rudlin JR, Austin J. Topside inspection project: phase I final report. Offshore Technology Report OTN 96 169. UK: Health & Safety Executive; 1996.
[26] Moan T, Wei Z, Vårdal OT. Initial crack depth and POD data based on underwater inspection of fixed steel platforms. In: Corotis RB, Schuëller GI, Shinozuka M, editors. Structural safety and reliability, Proceedings of the eighth ICOSSAR'01. Rotterdam: A.A. Balkema; 2002.
[27] Moan T, Vårdal OT, Hellevig NC, Skjoldli K. In-service observations of cracks in North Sea jackets—a study on initial crack depth and pod values. In: Proceedings of the 16th international Conference on offshore mechanics and Arctic engineers. Yokohama: ASME; 1997.
[28] Fujimoto Y, et al. Study on fatigue reliability and inspection of ship structures based on enquete information. J Soc Naval Arch Japan 1996;180:601–9.
[29] Fujimoto Y. Inspection planning of fatigue deteriorating structures using genetic algorithm. J Soc Naval Arch Japan 1997; 182.
[30] Moan T. Target levels for reliability-based assessment of offshore structures during design and operation. Offshore Technology report OTO 1999/060. UK: Health & Safety Executive; 2002.
[31] Moan T, Hovde GO, Blanker AM. Reliability-based fatigue design criteria for offshore structures considering the effect of inspection and repair. In: Proceedings of the 25th offshore technology conference. Houston: OTC; 1993. p. 591–600.
[32] Moan T, Vårdal OT. Reliability-based requalification of existing offshore platforms. In: Wu, Cui, Zhou, editors. Practical design of ships and other floating structures PRADS'2001, vol. II. Oxford: Elsevier Science; 2001. p. 939–45.
[33] Moan T, Ayala-Uraga E. Reliability-based assessment of FPSOs for service life extension. Technical Report OTD 2003-01. Houston: American Bureau of Shipping; 2003.
[34] Hohenbichler M, Rackwitz R. Improvement of second-order reliability estimation by importance sampling. J Eng Mech ASCE 1988;114(12):2195–9.
[35] Det norske Veritas. PROBAN—general purpose probabilistic analysis program. Høvik, Norway: DNV; 1996.

Article 3. Time-variant reliability assessment of FPSO hull girder with long cracks

Authors: **Ayala-Uraga, Efren** and **Moan, Torgeir**,

Published in: *Journal of Offshore Mechanics and Arctic Engineering*, Vol. **129** (2007), No. 2, pp. 81-89.

Refereed article

Preface

An efficient time-variant reliability formulation for the safety assessment of an aging Floating Production Storage and Offloading (FPSO) vessels with the presence of through-thickness cracks (i.e. long cracks), is presented in this paper. The probability of brittle fracture of an aging stiffened panel with the presence of a long crack is studied in this paper. The mean stress effect due to the continuously varying still-water loading as well as residual stresses is explicitly accounted for in the crack growth calculation procedure.

Is not included due to copyright

R A P P O R T E R

UTGITT VED

INSTITUTT FOR MARIN TEKNIKK

(tidligere: FAKULTET FOR MARIN TEKNIKK)

NORGES TEKNISK-NATURVITENSKAPELIGE UNIVERSITET

PhD Theses (not all) from the Department of Marine Technology, NTNU

Report No.	Author	Title
	Kavlie, Dag	Optimization of Plane Elastic Grillages, 1967
	Hansen, Hans R.	Man-Machine Communication and Data-Storage Methods in Ship Structural Design, 1971
	Gisvold, Kaare M.	A Method for non-linear mixed -integer programming and its Application to Design Problems, 1971
	Lund, Sverre	Tanker Frame Optimalization by means of SUMT-Transformation and Behaviour Models, 1971
	Vinje, Tor	On Vibration of Spherical Shells Interacting with Fluid, 1972
	Lorentz, Jan D.	Tank Arrangement for Crude Oil Carriers in Accordance with the new Anti-Pollution Regulations, 1975
	Carlsen, Carl A.	Computer-Aided Design of Tanker Structures, 1975
	Larsen, Carl M.	Static and Dynamic Analysis of Offshore Pipelines during Installation, 1976
UR-79-01	Brigt Hatlestad, MK	The finite element method used in a fatigue evaluation of fixed offshore platforms. (Dr.Ing. Thesis)
UR-79-02	Erik Pettersen, MK	Analysis and design of cellular structures. (Dr.Ing. Thesis)
UR-79-03	Sverre Valsgård, MK	Finite difference and finite element methods applied to nonlinear analysis of plated structures. (Dr.Ing. Thesis)
UR-79-04	Nils T. Nordsve, MK	Finite element collapse analysis of structural members considering imperfections and stresses due to fabrication. (Dr.Ing. Thesis)
UR-79-05	Ivar J. Fylling, MK	Analysis of towline forces in ocean towing systems. (Dr.Ing. Thesis)
UR-80-06	Nils Sandsmark, MM	Analysis of Stationary and Transient Heat Conduction by the Use of the Finite Element Method. (Dr.Ing. Thesis)
UR-80-09	Sverre Haver, MK	Analysis of uncertainties related to the stochastic modeling of ocean waves. (Dr.Ing. Thesis)
UR-81-15	Odland, Jonas	On the Strength of welded Ring stiffened cylindrical Shells primarily subjected to axial Compression
UR-82-17	Engesvik, Knut	Analysis of Uncertainties in the fatigue Capacity of Welded Joints

UR-82-18	Rye, Henrik	Ocean wave groups
UR-83-30	Eide, Oddvar Inge	On Cumulative Fatigue Damage in Steel Welded Joints
UR-83-33	Mo, Olav	Stochastic Time Domain Analysis of Slender Offshore Structures
UR-83-34	Amdahl, Jørgen	Energy absorption in Ship-platform impacts
UR-84-37	Mørch, Morten	Motions and mooring forces of semi submersibles as determined by full-scale measurements and theoretical analysis
UR-84-38	Soares, C. Guedes	Probabilistic models for load effects in ship structures
UR-84-39	Aarsnes, Jan V.	Current forces on ships
UR-84-40	Czujko, Jerzy	Collapse Analysis of Plates subjected to Biaxial Compression and Lateral Load
UR-85-46	Alf G. Engseth, MK	Finite element collapse analysis of tubular steel offshore structures. (Dr.Ing. Thesis)
UR-86-47	Dengody Sheshappa, MP	A Computer Design Model for Optimizing Fishing Vessel Designs Based on Techno-Economic Analysis. (Dr.Ing. Thesis)
UR-86-48	Vidar Aanesland, MH	A Theoretical and Numerical Study of Ship Wave Resistance. (Dr.Ing. Thesis)
UR-86-49	Heinz-Joachim Wessel, MK	Fracture Mechanics Analysis of Crack Growth in Plate Girders. (Dr.Ing. Thesis)
UR-86-50	Jon Taby, MK	Ultimate and Post-ultimate Strength of Dented Tubular Members. (Dr.Ing. Thesis)
UR-86-51	Walter Lian, MH	A Numerical Study of Two-Dimensional Separated Flow Past Bluff Bodies at Moderate KC-Numbers. (Dr.Ing. Thesis)
UR-86-52	Bjørn Sortland, MH	Force Measurements in Oscillating Flow on Ship Sections and Circular Cylinders in a U-Tube Water Tank. (Dr.Ing. Thesis)
UR-86-53	Kurt Strand, MM	A System Dynamic Approach to One-dimensional Fluid Flow. (Dr.Ing. Thesis)
UR-86-54	Arne Edvin Løken, MH	Three Dimensional Second Order Hydrodynamic Effects on Ocean Structures in Waves. (Dr.Ing. Thesis)
UR-86-55	Sigurd Falch, MH	A Numerical Study of Slamming of Two-Dimensional Bodies. (Dr.Ing. Thesis)
UR-87-56	Arne Braathen, MH	Application of a Vortex Tracking Method to the Prediction of Roll Damping of a Two-Dimension Floating Body. (Dr.Ing. Thesis)
UR-87-57	Bernt Leira, MK	Gaussian Vector Processes for Reliability Analysis involving Wave-Induced Load Effects. (Dr.Ing. Thesis)
UR-87-58	Magnus Småvik, MM	Thermal Load and Process Characteristics in a Two-Stroke Diesel Engine with Thermal Barriers (in Norwegian). (Dr.Ing. Thesis)
MTA-88-59	Bernt Arild Bremdal, MP	An Investigation of Marine Installation Processes – A Knowledge -

		Based Planning Approach. (Dr.Ing. Thesis)
MTA-88-60	Xu Jun, MK	Non-linear Dynamic Analysis of Space-framed Offshore Structures. (Dr.Ing. Thesis)
MTA-89-61	Gang Miao, MH	Hydrodynamic Forces and Dynamic Responses of Circular Cylinders in Wave Zones. (Dr.Ing. Thesis)
MTA-89-62	Martin Greenhow, MH	Linear and Non-Linear Studies of Waves and Floating Bodies. Part I and Part II. (Dr.Techn. Thesis)
MTA-89-63	Chang Li, MH	Force Coefficients of Spheres and Cubes in Oscillatory Flow with and without Current. (Dr.Ing. Thesis
MTA-89-64	Hu Ying, MP	A Study of Marketing and Design in Development of Marine Transport Systems. (Dr.Ing. Thesis)
MTA-89-65	Arild Jæger, MH	Seakeeping, Dynamic Stability and Performance of a Wedge Shaped Planing Hull. (Dr.Ing. Thesis)
MTA-89-66	Chan Siu Hung, MM	The dynamic characteristics of tilting-pad bearings
MTA-89-67	Kim Wikstrøm, MP	Analysis av projekteringen for ett offshore projekt. (Licenciat-avhandling)
MTA-89-68	Jiao Guoyang, MK	Reliability Analysis of Crack Growth under Random Loading, considering Model Updating. (Dr.Ing. Thesis)
MTA-89-69	Arnt Olufsen, MK	Uncertainty and Reliability Analysis of Fixed Offshore Structures. (Dr.Ing. Thesis)
MTA-89-70	Wu Yu-Lin, MR	System Reliability Analyses of Offshore Structures using improved Truss and Beam Models. (Dr.Ing. Thesis)
MTA-90-71	Jan Roger Hoff, MH	Three-dimensional Green function of a vessel with forward speed in waves. (Dr.Ing. Thesis)
MTA-90-72	Rong Zhao, MH	Slow-Drift Motions of a Moored Two-Dimensional Body in Irregular Waves. (Dr.Ing. Thesis)
MTA-90-73	Atle Minsaas, MP	Economical Risk Analysis. (Dr.Ing. Thesis)
MTA-90-74	Knut-Aril Farnes, MK	Long-term Statistics of Response in Non-linear Marine Structures. (Dr.Ing. Thesis)
MTA-90-75	Torbjørn Sotberg, MK	Application of Reliability Methods for Safety Assessment of Submarine Pipelines. (Dr.Ing. Thesis)
MTA-90-76	Zeuthen, Steffen, MP	SEAMAID. A computational model of the design process in a constraint-based logic programming environment. An example from the offshore domain. (Dr.Ing. Thesis)
MTA-91-77	Haagensen, Sven, MM	Fuel Dependant Cyclic Variability in a Spark Ignition Engine - An Optical Approach. (Dr.Ing. Thesis)
MTA-91-78	Løland, Geir, MH	Current forces on and flow through fish farms. (Dr.Ing. Thesis)
MTA-91-79	Hoen, Christopher, MK	System Identification of Structures Excited by Stochastic Load Processes. (Dr.Ing. Thesis)

MTA-91-80	Haugen, Stein, MK	Probabilistic Evaluation of Frequency of Collision between Ships and Offshore Platforms. (Dr.Ing. Thesis)
MTA-91-81	Sødahl, Nils, MK	Methods for Design and Analysis of Flexible Risers. (Dr.Ing. Thesis)
MTA-91-82	Ormberg, Harald, MK	Non-linear Response Analysis of Floating Fish Farm Systems. (Dr.Ing. Thesis)
MTA-91-83	Marley, Mark J., MK	Time Variant Reliability under Fatigue Degradation. (Dr.Ing. Thesis)
MTA-91-84	Krokstad, Jørgen R., MH	Second-order Loads in Multidirectional Seas. (Dr.Ing. Thesis)
MTA-91-85	Molteberg, Gunnar A., MM	The Application of System Identification Techniques to Performance Monitoring of Four Stroke Turbocharged Diesel Engines. (Dr.Ing. Thesis)
MTA-92-86	Mørch, Hans Jørgen Bjelke, MH	Aspects of Hydrofoil Design: with Emphasis on Hydrofoil Interaction in Calm Water. (Dr.Ing. Thesis)
MTA-92-87	Chan Siu Hung, MM	Nonlinear Analysis of Rotordynamic Instabilities in Highspeed Turbomachinery. (Dr.Ing. Thesis)
MTA-92-88	Bessason, Bjarni, MK	Assessment of Earthquake Loading and Response of Seismically Isolated Bridges. (Dr.Ing. Thesis)
MTA-92-89	Langli, Geir, MP	Improving Operational Safety through exploitation of Design Knowledge - an investigation of offshore platform safety. (Dr.Ing. Thesis)
MTA-92-90	Sævik, Svein, MK	On Stresses and Fatigue in Flexible Pipes. (Dr.Ing. Thesis)
MTA-92-91	Ask, Tor Ø., MM	Ignition and Flame Growth in Lean Gas-Air Mixtures. An Experimental Study with a Schlieren System. (Dr.Ing. Thesis)
MTA-86-92	Hessen, Gunnar, MK	Fracture Mechanics Analysis of Stiffened Tubular Members. (Dr.Ing. Thesis)
MTA-93-93	Steinebach, Christian, MM	Knowledge Based Systems for Diagnosis of Rotating Machinery. (Dr.Ing. Thesis)
MTA-93-94	Dalane, Jan Inge, MK	System Reliability in Design and Maintenance of Fixed Offshore Structures. (Dr.Ing. Thesis)
MTA-93-95	Steen, Sverre, MH	Cobblestone Effect on SES. (Dr.Ing. Thesis)
MTA-93-96	Karunakaran, Daniel, MK	Nonlinear Dynamic Response and Reliability Analysis of Drag-dominated Offshore Platforms. (Dr.Ing. Thesis)
MTA-93-97	Hagen, Arnulf, MP	The Framework of a Design Process Language. (Dr.Ing. Thesis)
MTA-93-98	Nordrik, Rune, MM	Investigation of Spark Ignition and Autoignition in Methane and Air Using Computational Fluid Dynamics and Chemical Reaction Kinetics. A Numerical Study of Ignition Processes in Internal Combustion Engines. (Dr.Ing. Thesis)
MTA-94-99	Passano, Elizabeth, MK	Efficient Analysis of Nonlinear Slender Marine Structures. (Dr.Ing. Thesis)
MTA-94-100	Kvålsvold, Jan, MH	Hydroelastic Modelling of Wetdeck Slamming on Multihull Vessels.

		(Dr.Ing. Thesis)
MTA-94-102	Bech, Sidsel M., MK	Experimental and Numerical Determination of Stiffness and Strength of GRP/PVC Sandwich Structures. (Dr.Ing. Thesis)
MTA-95-103	Paulsen, Hallvard, MM	A Study of Transient Jet and Spray using a Schlieren Method and Digital Image Processing. (Dr.Ing. Thesis)
MTA-95-104	Hovde, Geir Olav, MK	Fatigue and Overload Reliability of Offshore Structural Systems, Considering the Effect of Inspection and Repair. (Dr.Ing. Thesis)
MTA-95-105	Wang, Xiaozhi, MK	Reliability Analysis of Production Ships with Emphasis on Load Combination and Ultimate Strength. (Dr.Ing. Thesis)
MTA-95-106	Ulstein, Tore, MH	Nonlinear Effects of a Flexible Stern Seal Bag on Cobblestone Oscillations of an SES. (Dr.Ing. Thesis)
MTA-95-107	Solaas, Frøydis, MH	Analytical and Numerical Studies of Sloshing in Tanks. (Dr.Ing. Thesis)
MTA-95-108	Hellan, Øyvind, MK	Nonlinear Pushover and Cyclic Analyses in Ultimate Limit State Design and Reassessment of Tubular Steel Offshore Structures. (Dr.Ing. Thesis)
MTA-95-109	Hermundstad, Ole A., MK	Theoretical and Experimental Hydroelastic Analysis of High Speed Vessels. (Dr.Ing. Thesis)
MTA-96-110	Bratland, Anne K., MH	Wave-Current Interaction Effects on Large-Volume Bodies in Water of Finite Depth. (Dr.Ing. Thesis)
MTA-96-111	Herfjord, Kjell, MH	A Study of Two-dimensional Separated Flow by a Combination of the Finite Element Method and Navier-Stokes Equations. (Dr.Ing. Thesis)
MTA-96-112	Æsøy, Vilmar, MM	Hot Surface Assisted Compression Ignition in a Direct Injection Natural Gas Engine. (Dr.Ing. Thesis)
MTA-96-113	Eknes, Monika L., MK	Escalation Scenarios Initiated by Gas Explosions on Offshore Installations. (Dr.Ing. Thesis)
MTA-96-114	Erikstad, Stein O., MP	A Decision Support Model for Preliminary Ship Design. (Dr.Ing. Thesis)
MTA-96-115	Pedersen, Egil, MH	A Nautical Study of Towed Marine Seismic Streamer Cable Configurations. (Dr.Ing. Thesis)
MTA-97-116	Moksnes, Paul O., MM	Modelling Two-Phase Thermo-Fluid Systems Using Bond Graphs. (Dr.Ing. Thesis)
MTA-97-117	Halse, Karl H., MK	On Vortex Shedding and Prediction of Vortex-Induced Vibrations of Circular Cylinders. (Dr.Ing. Thesis)
MTA-97-118	Igland, Ragnar T., MK	Reliability Analysis of Pipelines during Laying, considering Ultimate Strength under Combined Loads. (Dr.Ing. Thesis)
MTA-97-119	Pedersen, Hans-P., MP	Levendefiskteknologi for fiskefartøy. (Dr.Ing. Thesis)
MTA-98-120	Vikestad, Kyrre, MK	Multi-Frequency Response of a Cylinder Subjected to Vortex Shedding and Support Motions. (Dr.Ing. Thesis)

MTA-98-121	Azadi, Mohammad R. E., MK	Analysis of Static and Dynamic Pile-Soil-Jacket Behaviour. (Dr.Ing. Thesis)
MTA-98-122	Ulltang, Terje, MP	A Communication Model for Product Information. (Dr.Ing. Thesis)
MTA-98-123	Torbergsen, Erik, MM	Impeller/Diffuser Interaction Forces in Centrifugal Pumps. (Dr.Ing. Thesis)
MTA-98-124	Hansen, Edmond, MH	A Discrete Element Model to Study Marginal Ice Zone Dynamics and the Behaviour of Vessels Moored in Broken Ice. (Dr.Ing. Thesis)
MTA-98-125	Videiro, Paulo M., MK	Reliability Based Design of Marine Structures. (Dr.Ing. Thesis)
MTA-99-126	Mainçon, Philippe, MK	Fatigue Reliability of Long Welds Application to Titanium Risers. (Dr.Ing. Thesis)
MTA-99-127	Haugen, Elin M., MH	Hydroelastic Analysis of Slamming on Stiffened Plates with Application to Catamaran Wetdecks. (Dr.Ing. Thesis)
MTA-99-128	Langhelle, Nina K., MK	Experimental Validation and Calibration of Nonlinear Finite Element Models for Use in Design of Aluminium Structures Exposed to Fire. (Dr.Ing. Thesis)
MTA-99-129	Berstad, Are J., MK	Calculation of Fatigue Damage in Ship Structures. (Dr.Ing. Thesis)
MTA-99-130	Andersen, Trond M., MM	Short Term Maintenance Planning. (Dr.Ing. Thesis)
MTA-99-131	Tveiten, Bård Wathne, MK	Fatigue Assessment of Welded Aluminium Ship Details. (Dr.Ing. Thesis)
MTA-99-132	Søreide, Fredrik, MP	Applications of underwater technology in deep water archaeology. Principles and practice. (Dr.Ing. Thesis)
MTA-99-133	Tønnessen, Rune, MH	A Finite Element Method Applied to Unsteady Viscous Flow Around 2D Blunt Bodies With Sharp Corners. (Dr.Ing. Thesis)
MTA-99-134	Elvekrok, Dag R., MP	Engineering Integration in Field Development Projects in the Norwegian Oil and Gas Industry. The Supplier Management of Norne. (Dr.Ing. Thesis)
MTA-99-135	Fagerholt, Kjetil, MP	Optimeringsbaserte Metoder for Ruteplanlegging innen skipsfart. (Dr.Ing. Thesis)
MTA-99-136	Bysveen, Marie, MM	Visualization in Two Directions on a Dynamic Combustion Rig for Studies of Fuel Quality. (Dr.Ing. Thesis)
MTA-2000-137	Storteig, Eskild, MM	Dynamic characteristics and leakage performance of liquid annular seals in centrifugal pumps. (Dr.Ing. Thesis)
MTA-2000-138	Sagli, Gro, MK	Model uncertainty and simplified estimates of long term extremes of hull girder loads in ships. (Dr.Ing. Thesis)
MTA-2000-139	Tronstad, Harald, MK	Nonlinear analysis and design of cable net structures like fishing gear based on the finite element method. (Dr.Ing. Thesis)
MTA-2000-140	Kroneberg, André, MP	Innovation in shipping by using scenarios. (Dr.Ing. Thesis)
MTA-2000-141	Haslum, Herbjørn Alf, MH	Simplified methods applied to nonlinear motion of spar platforms.

		(Dr.Ing. Thesis)
MTA-2001-142	Samdal, Ole Johan, MM	Modelling of Degradation Mechanisms and Stressor Interaction on Static Mechanical Equipment Residual Lifetime. (Dr.Ing. Thesis)
MTA-2001-143	Baarholm, Rolf Jarle, MH	Theoretical and experimental studies of wave impact underneath decks of offshore platforms. (Dr.Ing. Thesis)
MTA-2001-144	Wang, Lihua, MK	Probabilistic Analysis of Nonlinear Wave-induced Loads on Ships. (Dr.Ing. Thesis)
MTA-2001-145	Kristensen, Odd H. Holt, MK	Ultimate Capacity of Aluminium Plates under Multiple Loads, Considering HAZ Properties. (Dr.Ing. Thesis)
MTA-2001-146	Greco, Marilena, MH	A Two-Dimensional Study of Green-Water Loading. (Dr.Ing. Thesis)
MTA-2001-147	Heggelund, Svein E., MK	Calculation of Global Design Loads and Load Effects in Large High Speed Catamarans. (Dr.Ing. Thesis)
MTA-2001-148	Babalola, Olusegun T., MK	Fatigue Strength of Titanium Risers – Defect Sensitivity. (Dr.Ing. Thesis)
MTA-2001-149	Mohammed, Abuu K., MK	Nonlinear Shell Finite Elements for Ultimate Strength and Collapse Analysis of Ship Structures. (Dr.Ing. Thesis)
MTA-2002-150	Holmedal, Lars E., MH	Wave-current interactions in the vicinity of the sea bed. (Dr.Ing. Thesis)
MTA-2002-151	Rognebakke, Olav F., MH	Sloshing in rectangular tanks and interaction with ship motions. (Dr.Ing. Thesis)
MTA-2002-152	Lader, Pål Furset, MH	Geometry and Kinematics of Breaking Waves. (Dr.Ing. Thesis)
MTA-2002-153	Yang, Qinzheng, MH	Wash and wave resistance of ships in finite water depth. (Dr.Ing. Thesis)
MTA-2002-154	Melhus, Øyvin, MM	Utilization of VOC in Diesel Engines. Ignition and combustion of VOC released by crude oil tankers. (Dr.Ing. Thesis)
MTA-2002-155	Ronæss, Marit, MH	Wave Induced Motions of Two Ships Advancing on Parallel Course. (Dr.Ing. Thesis)
MTA-2002-156	Økland, Ole D., MK	Numerical and experimental investigation of whipping in twin hull vessels exposed to severe wet deck slamming. (Dr.Ing. Thesis)
MTA-2002-157	Ge, Chunhua, MK	Global Hydroelastic Response of Catamarans due to Wet Deck Slamming. (Dr.Ing. Thesis)
MTA-2002-158	Byklum, Eirik, MK	Nonlinear Shell Finite Elements for Ultimate Strength and Collapse Analysis of Ship Structures. (Dr.Ing. Thesis)
IMT-2003-1	Chen, Haibo, MK	Probabilistic Evaluation of FPSO-Tanker Collision in Tandem Offloading Operation. (Dr.Ing. Thesis)
IMT-2003-2	Skaugset, Kjetil Bjørn, MK	On the Suppression of Vortex Induced Vibrations of Circular Cylinders by Radial Water Jets. (Dr.Ing. Thesis)
IMT-2003-3	Chezhian, Muthu	Three-Dimensional Analysis of Slamming. (Dr.Ing. Thesis)

IMT-2003-4	Buhaug, Øyvind	Deposit Formation on Cylinder Liner Surfaces in Medium Speed Engines. (Dr.Ing. Thesis)
IMT-2003-5	Tregde, Vidar	Aspects of Ship Design: Optimization of Aft Hull with Inverse Geometry Design. (Dr.Ing. Thesis)
IMT-2003-6	Wist, Hanne Therese	Statistical Properties of Successive Ocean Wave Parameters. (Dr.Ing. Thesis)
IMT-2004-7	Ransau, Samuel	Numerical Methods for Flows with Evolving Interfaces. (Dr.Ing. Thesis)
IMT-2004-8	Soma, Torkel	Blue-Chip or Sub-Standard. A data interrogation approach of identity safety characteristics of shipping organization. (Dr.Ing. Thesis)
IMT-2004-9	Ersdal, Svein	An experimental study of hydrodynamic forces on cylinders and cables in near axial flow. (Dr.Ing. Thesis)
IMT-2005-10	Brodtkorb, Per Andreas	The Probability of Occurrence of Dangerous Wave Situations at Sea. (Dr.Ing. Thesis)
IMT-2005-11	Yttervik, Rune	Ocean current variability in relation to offshore engineering. (Dr.Ing. Thesis)
IMT-2005-12	Fredheim, Arne	Current Forces on Net-Structures. (Dr.Ing. Thesis)
IMT-2005-13	Heggernes, Kjetil	Flow around marine structures. (Dr.Ing. Thesis
IMT-2005-14	Fouques, Sebastien	Lagrangian Modelling of Ocean Surface Waves and Synthetic Aperture Radar Wave Measurements. (Dr.Ing. Thesis)
IMT-2006-15	Holm, Håvard	Numerical calculation of viscous free surface flow around marine structures. (Dr.Ing. Thesis)
IMT-2006-16	Bjørheim, Lars G.	Failure Assessment of Long Through Thickness Fatigue Cracks in Ship Hulls. (Dr.Ing. Thesis)
IMT-2006-17	Hansson, Lisbeth	Safety Management for Prevention of Occupational Accidents. (Dr.Ing. Thesis)
IMT-2006-18	Zhu, Xinying	Application of the CIP Method to Strongly Nonlinear Wave-Body Interaction Problems. (Dr.Ing. Thesis)
IMT-2006-19	Reite, Karl Johan	Modelling and Control of Trawl Systems. (Dr.Ing. Thesis)
IMT-2006-20	Smogeli, Øyvind Notland	Control of Marine Propellers. From Normal to Extreme Conditions. (Dr.Ing. Thesis)
IMT-2007-21	Storhaug, Gaute	Experimental Investigation of Wave Induced Vibrations and Their Effect on the Fatigue Loading of Ships. (Dr.Ing. Thesis)
IMT-2007-22	Sun, Hui	A Boundary Element Method Applied to Strongly Nonlinear Wave-Body Interaction Problems. (PhD Thesis, CeSOS)
IMT-2007-23	Rustad, Anne Marthine	Modelling and Control of Top Tensioned Risers. (PhD Thesis, CeSOS)
IMT-2007-24	Johansen, Vegar	Modelling flexible slender system for real-time simulations and

		control applications
IMT-2007-25	Wroldsen, Anders Sunde	Modelling and control of tensegrity structures. (PhD Thesis, CeSOS)
IMT-2007-26	Aronsen, Kristoffer Høye	An experimental investigation of in-line and combined inline and cross flow vortex induced vibrations. (Dr. avhandling, IMT)
IMT-2007-27	Gao, Zhen	Stochastic Response Analysis of Mooring Systems with Emphasis on Frequency-domain Analysis of Fatigue due to Wide-band Response Processes (PhD Thesis, CeSOS)
IMT-2007-28	Thorstensen, Tom Anders	Lifetime Profit Modelling of Ageing Systems Utilizing Information about Technical Condition. (Dr.ing. thesis, IMT)
IMT-2008-29	Berntsen, Per Ivar B.	Structural Reliability Based Position Mooring. (PhD-Thesis, IMT)
IMT-2008-30	Ye, Naiquan	Fatigue Assessment of Aluminium Welded Box-stiffener Joints in Ships (Dr.ing. thesis, IMT)
IMT-2008-31	Radan, Damir	Integrated Control of Marine Electrical Power Systems. (PhD-Thesis, IMT)
IMT-2008-32	Thomassen, Paul	Methods for Dynamic Response Analysis and Fatigue Life Estimation of Floating Fish Cages. (Dr.ing. thesis, IMT)
IMT-2008-33	Pákozdi, Csaba	A Smoothed Particle Hydrodynamics Study of Two-dimensional Nonlinear Sloshing in Rectangular Tanks. (Dr.ing.thesis, IMT)
IMT-2007-34	Grytøyr, Guttorm	A Higher-Order Boundary Element Method and Applications to Marine Hydrodynamics. (Dr.ing.thesis, IMT)
IMT-2008-35	Drummen, Ingo	Experimental and Numerical Investigation of Nonlinear Wave-Induced Load Effects in Containerships considering Hydroelasticity. (PhD thesis, CeSOS)
IMT-2008-36	Skejic, Renato	Maneuvering and Seakeeping of a Singel Ship and of Two Ships in Interaction. (PhD-Thesis, CeSOS)
IMT-2008-37	Harlem, Alf	An Age-Based Replacement Model for Repairable Systems with Attention to High-Speed Marine Diesel Engines. (PhD-Thesis, IMT)
IMT-2008-38	Alsos, Hagbart S.	Ship Grounding. Analysis of Ductile Fracture, Bottom Damage and Hull Girder Response. (PhD-thesis, IMT)
IMT-2008-39	Graczyk, Mateusz	Experimental Investigation of Sloshing Loading and Load Effects in Membrane LNG Tanks Subjected to Random Excitation. (PhD-thesis, CeSOS)
IMT-2008-40	Taghipour, Reza	Efficient Prediction of Dynamic Response for Flexible amd Multi-body Marine Structures. (PhD-thesis, CeSOS)
IMT-2008-41	Ruth, Eivind	Propulsion control and thrust allocation on marine vessels. (PhD thesis, CeSOS)
IMT-2008-42	Nystad, Bent Helge	Technical Condition Indexes and Remaining Useful Life of Aggregated Systems. PhD thesis, IMT
IMT-2008-43	Soni, Prashant Kumar	Hydrodynamic Coefficients for Vortex Induced Vibrations of Flexible Beams, PhD thesis, CeSOS

IMT-2009-43	Amlashi, Hadi K.K.	Ultimate Strength and Reliability-based Design of Ship Hulls with Emphasis on Combined Global and Local Loads. PhD Thesis, IMT
IMT-2009-44	Pedersen, Tom Arne	Bond Graph Modelling of Marine Power Systems. PhD Thesis, IMT
IMT-2009-45	Kristiansen, Trygve	Two-Dimensional Numerical and Experimental Studies of Piston-Mode Resonance. PhD-Thesis, CeSOS
IMT-2009-46	Ong, Muk Chen	Applications of a Standard High Reynolds Number Model and a Stochastic Scour Prediction Model for Marine Structures. PhD-thesis, IMT
IMT-2009-47	Hong, Lin	Simplified Analysis and Design of Ships subjected to Collision and Grounding. PhD-thesis, IMT
IMT-2009-48	Koushan, Kamran	Vortex Induced Vibrations of Free Span Pipelines, PhD thesis, IMT
IMT-2009-49	Korsvik, Jarl Eirik	Heuristic Methods for Ship Routing and Scheduling. PhD-thesis, IMT
IMT-2009-50	Lee, Ji Hoon	Experimental Investigation and Numerical Methods in Analyzing the Ocean Current Displacement Phenomena of Long Lines. PhD-thesis, IMT
IMT-2009-51	Ayala-Uraga, Efren	Reliability-based Assessment of Deteriorating Ship-shaped Offshore Structures. Dr. ing. Thesis, IMT